Master Thesis in Geosciences

Numerical and Analytical modelling of ground water flow in delta structures

Jane Blegen

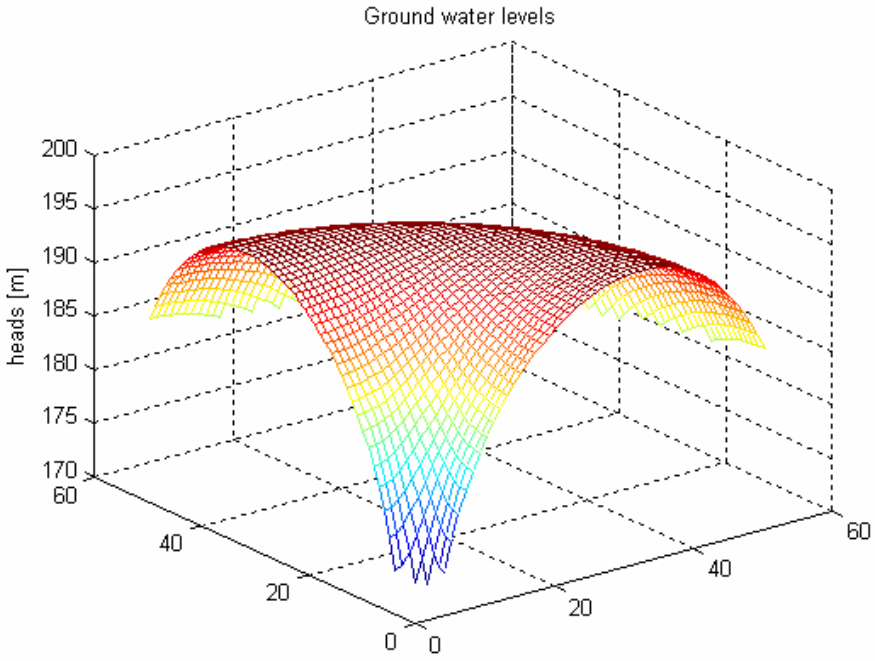

UNIVERSITY OF OSLO

FACULTY OF MATHEMATICS AND NATURAL SCIENCES

Numerical and Analytical modelling of ground water flow in delta structures

Jane Blegen

Master Thesis in Geosciences

Discipline: Environmental geology and Geohazards

Department of Geosciences

Faculty of Mathematics and Natural Sciences

UNIVERSITY OF OSLO

[03.06.05]

TABLE OF CONTENTS

CHAPTER 1

INTRODUCTION

1.1

Next to air, water is the most essential of Man's requirements for life. The amount of water necessary to society has increased as population and urbanisation have increased. Today, conflicting interest on water issues appear frequently. All people in the world compete for less than 1% of earth's water supply. This is enough fresh water to supply all the people on the earth, but the problem rise as both people and fresh water is unevenly distributed over the world. The access to water resources is of vital importance for a broad spectrum of human activities, and a careful management of the water resources is of great concern to society and the environment. It is of major importance that investigation and management of the water supply aim to optimise the utilisation of a common resource. Groundwater is defined as all the water contained in spaces within bedrock and regolith (Skinner and Porter 1995).

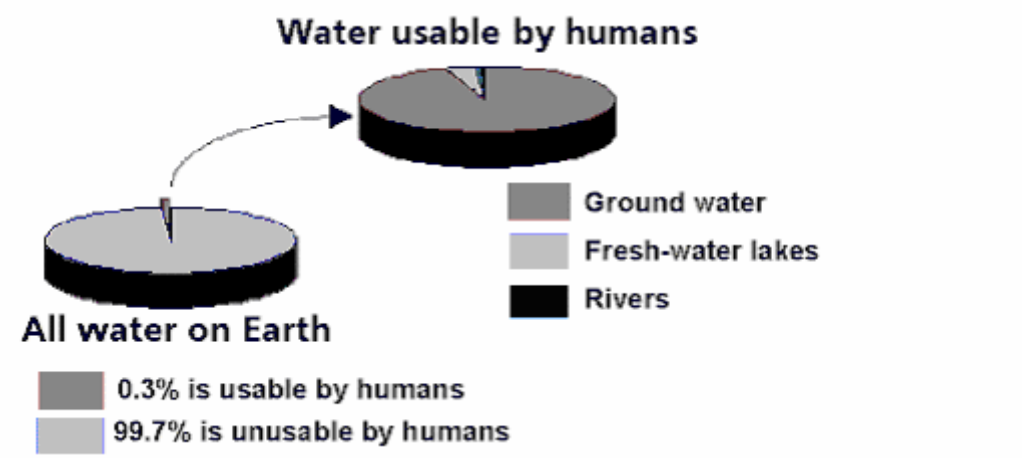

Figure 1.1: How much of the water on earth that is usable for humans (USGS).

Less than 1 % of the water on the Earth is groundwater, although the volume of groundwater sounds small, it is 40 times larger than the volume of all the water in freshwater lakes or flowing in streams and nearly a third as large as the water contained in all the world's glaciers and polar ice (Skinner and Porter 1995). In the work of mapping, managing and investigation

of the water resources in the different part of the world modelling is an important tool to understand and optimise the use of water resources that are available (Figure 1.1). The greatest part of the freshwater that is available is found as groundwater. The major part of the worlds population are dependent on the groundwater supply in the area they live in. Administration of the groundwater resources is therefore vital. Today groundwater modelling is a common practise in groundwater management. Modelling increase the value of observations and makes it easier to understand physical and geochemical responses. In the investigations of groundwater supply there has been used for instance finite mathematics and computer technology to make numerical modeling of these problems. These numerical solutions need a lot of data and a great deal of effort to get a simulation that is realistic enough. Analytical solutions of the same problems can be useful because they don't need the same amount of data and details as the numerical solutions, but can still give an understanding of the physical conditions in the area and how they affect the groundwater flow.

1.2 The Main Objective

The main objective of this thesis is to accomplish both analytical and numerical solutions for steady state piezometric head in confined and unconfined/phreatic aquifers in delta structures. I will carry out both analytical and numerical models over the same area, the Trandum delta that is a part of the Hauerseter-delta, in Øvre Romerike in eastern Norway, and compare these with each other and with observations from the field. This will give an indication of how good the different models are. The Hauerseter-delta is a delta formation that prograde into a sedimentation basin, and it has a radial structure. This structure may be simplified to a one-dimensional flow due to axial symmetry of the aquifer. This makes it possible to use Poisson's equation to do the calculations. I will use an extension of the Poisson'equation, the "Doughnut equation" compiled by Kitterød (2004a) to make the analytical models. The numerical models are carried out using MODFLOW with the PMWIN pre- and post processing (Chiang and Kinzelbach, 2001). Next I introduce a more realistic geology in form of the ravines that are to be found at the edges of the Trandum-delta. For the analytical model I read the different boundary conditions out of a hydrogeological map over the area (Østmo 1976a), and make different models for each. For the numerical models I will integrate the ravines into the model in PMWIN. In the last instance I will compare the different numerical models and analytical solutions with each other.

1.3 Mathematical Background

Due to the axial symmetry of the delta structures, earlier observations has indicated that the groundwater flow in such structures may be simplified to radial flow. A lot of prograding deltas have a radial structure, where the river mouth is situated on the axis of symmetry and this allow us to make a simplification of the geometry of the delta. The regional trend of groundwater heads and groundwater divide may be calculated by solving the Poisson's equation. Previous solutions are based on constant head boundary, superimposed on a solution that allowed constant discharge or recharge at the center of the aquifer (Kitterød 2004a). A constant Transmissivity is usually an over-simplification of nature. The Dupuit-Forchheimer assumption implies that the vertical head gradients are ignored; this does not have to be valid close to the flow boundaries. Kitterød (2004a) expanded the solutions of the Poisson's equation and introduced two constant head boundaries and let the hydraulic conductivity, for phreatic aquifers or the thickness, for confined aquifers to be a linear function of the radius. In this way the vertical flow is not limited to the boundaries.

1.4 Investigation area and geological background

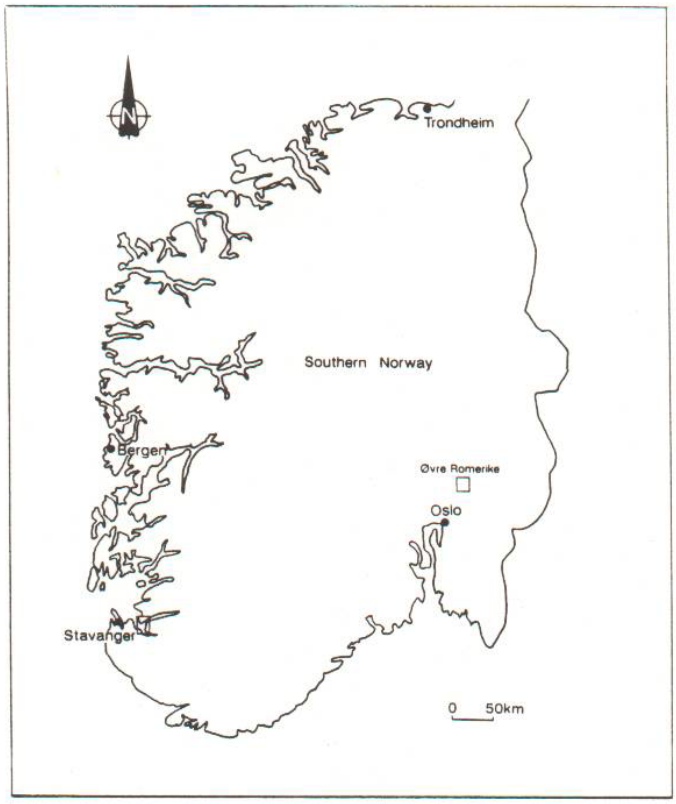

Figure 1.2: Location map of study area (Tuttle 1990).

I will use data from the Trandum-delta, which is one of two subdeltas at the Hauerseter delta complex in Øvre Romerike in Southeastern Norway. It is situated approximately 55 kilometers North of Oslo (Figure 1.2).

In this context the paleo-geology of the area that is to be investigated is important because it gives the physical conditions for groundwater movement in the area.

The bedrock geology in the Øvre Romerike area consists mainly of Precambrian gneiss-basement that is bordered in the west of the eruptives in the Oslo-region. The Precambrian basement consists of more than 95% gneisses while the remaining part includes granites and pegmatites (Østmo 1975). During the deglaciation of Scandinavia and the retreat of the Late Weichselian icecap in eastern Norway there were deposited glasiofluvial deposits that are important groundwater aquifers today. The Romerike substage deltas were deposited in the shallow marine, but brackish environment in the Romeriksfjord (Tuttle 1990). The deglaciation of Romerike area lasted for approximately 400 years (Jørgensen et al. 1997). The Hauerseter-delta was deposited and formed about 9500 years B.P, and is a marine ice-contact-delta built during a stop in the retreat of the ice (Jørgensen et al. 1997). By calculating the volume and the area of the delta the approximately duration for the deposition was found to be between 40-70 years (Tuttle 1990). In such a short time span, there must have been enormous amounts of glacial melt water and sediments that passed through the glacial portals to fill in the Romeriksfjord. There are several levels in the deglaciation of Romerike where the ice cap had marked pauses in the retreat and there have been deposited glasiofluvial deposits as ice-front deltas (Tuttle1990). From the south there are Asak-Berger, Jessheim, Hauerseter, Dal and Minnesund. The Hauerseter-delta consist of two ice-contact deltas (Jørgensen et al. 1997). Two different arms of the glacier build up the delta. This is reflected in the composition of the delta. Deposits from Hurdal containing Permian rocks dominate the Northwest part, the Trandum delta. The southern part of the deposition is dominated by precambrian and late-precambrian rocks from the area north of the delta towards Gudbrandsdalen and Mjøsa , the Li delta (Figure 1.3.)(Jørgensen et al.1997). The delta is composed of glasiofluvial sand and gravel and are partly underlain by silty glacio-marine sediments (Jørgensen and Østmo 1990). When the delta was built up, the sea level was approximately 205m higher than today. The proximal side of the delta (closest to the ice-cap) was built up to a maximum height of 222m above sea level, so the inner part of the delta were lying above the sea level and was a sanddurdelta. This is where you find the coarsest material

on the delta, where the sub glacial rivers came out under the glacier front. On the more distal parts of the delta the materials gets finer and turns into sand on the outer part of the delta. Underneath the sandy layers in the distal part of the delta there are clay. (Jørgensen et al.1997). When the ice retreated it left behind big blocks of ice north of the delta and when the ice were laying at Dal, the deadice were buried by sediments. When the ice finally melted, kettle holes were the result, for example Hersjøen (Jørgensen et al. 1997).
When the sea level sank and the delta became dry land, the (catabatic) wind made the sand migrates and it resulted in sand dunes at Nordmoen (Figure 1.3). The delta is nearly intact as it was made for almost 10 000 years ago, except from the ravines at the edge of the delta. (Worsley et al. 2003)

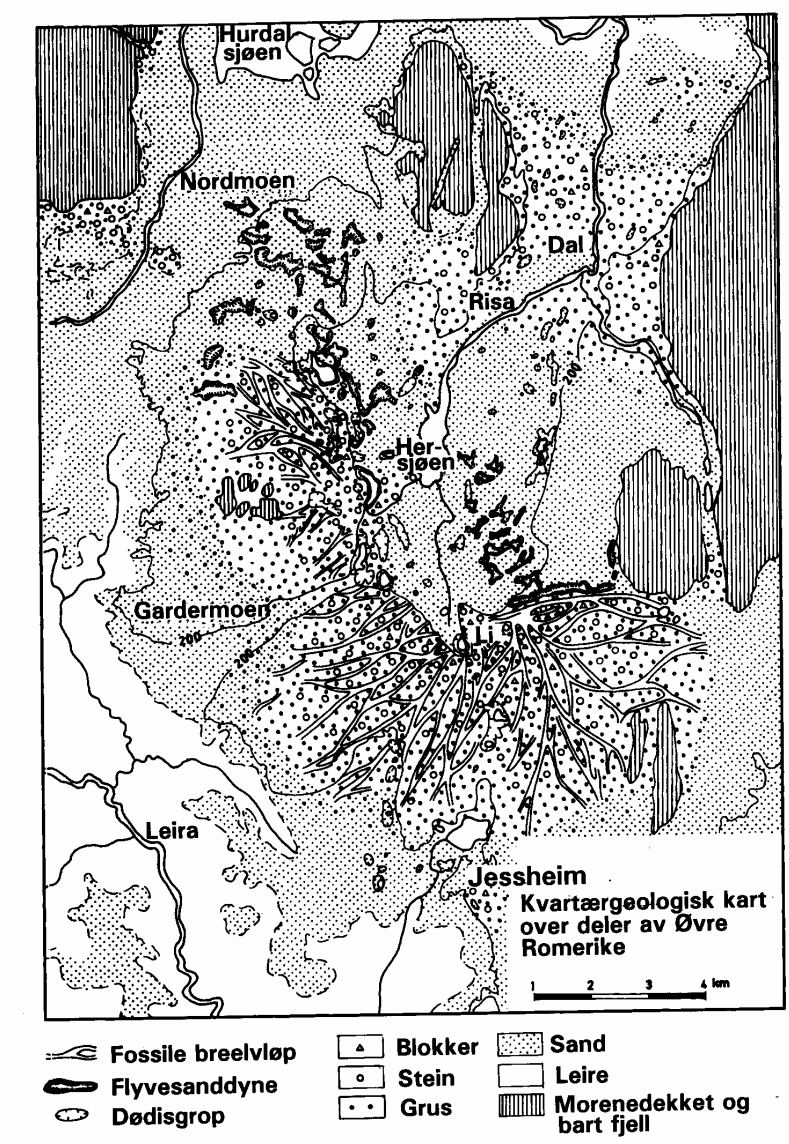

Figure 1.3: The Hauerseter-delta with the surrounding sediments after Jørgensen and Østmo (1990)

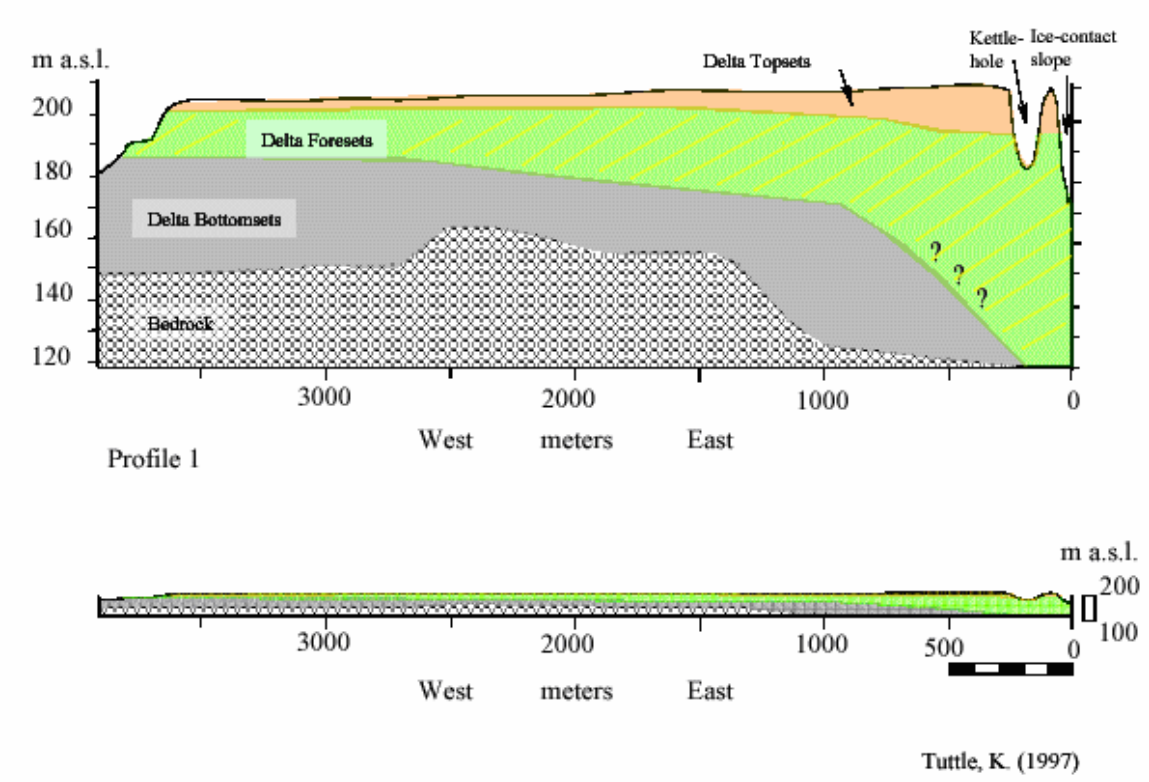

Figure 1.4: Cross section of the Trandum-delta.

The stratigraphy of a glacial-contact delta is very similar to the classical Gilbert type delta, and delta deposits close to a melting glacier are classified as a special class of Gilbert deltas (Reading 2002), and the Trandum-delta can be characterised as a Gilbert-type delta. Gilbert-type deltas form where coarse-grained-debris is supplied under relatively high-energy conditions to a lake margin (Reading 2002). A Gilbert-type delta display is generated where sediments are deposited in a stable water body where topset, foreset and bottomset beds are created. Topset and foreset developes on top of the bottomsets, as sediment deposition prograde basinward (Boggs 1995). When the density of the water entering the basin water, the flow is called homopycnal flow (Bates 1932), it leads to rapid mixing and sudden deposition of most of the sediment load (Figure 1.5.). In an ice-contact delta the amount of material and the coarseness of it, is dependent on the availability of the material, how much coarse material is available, and the energy in the melt-water from the ice. The ground water resources in Gilbert type deltas constitute valuable resources. The Hauerseter-delta is built up by relatively coarse material and the topset-beds frequently consist of boulders, stones, gravel, and sand, which show gradual distally fining. The foreset-beds are composed of sand and gravel, but

often with stone in it, and the bottomset layers are made up of fine sand to silty clay (Tuttle 1990).

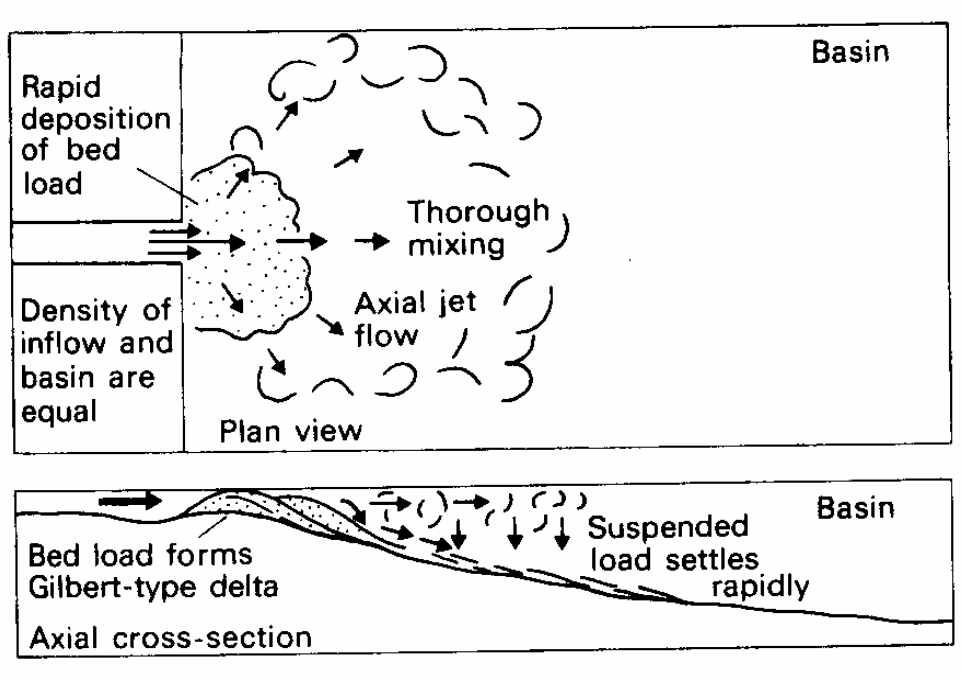

Figure 1.5: Homopycnal flow: The figure shows the principle of homopycnal flow and the interactions of sediment-laden river water and basin water, when the water bodies are of almost equal density. This phenomena leads to almost complete mixing and abrupt deposition of much of the sediment load. (Boggs 1995) This kind of outflow most likely leads to the formation of Gilbert-type deltas. As the sediment deposition progrades basinward there are deposited a topset, a foreset and a bottomset arrangements of beds.

1.5 Hydrogeological background

The Øvre Romerike groundwater magazine which the Trandum delta is a part of, is a phreatic aquifer fed by precipitation, and the groundwater-level changes with respect to the quantity of the precipitation (Tuttle1990). In the delta front, the distal part of the delta, the small and fine particles were deposited and made up a deposition of silt and clay. Today these layers make impermeable layers that limit the groundwater magazine toward south and west. The ground water divide is located nearest to the distal boundary of the delta, hence 80%, drains toward north and east, and merge in Hersjøen and runs out in the river Risa. The rest, about 20% drains out in the distal part of the delta and creates the characteristic ravines (Worsley et al. 2003). This is illustrated in Figure 1.6.

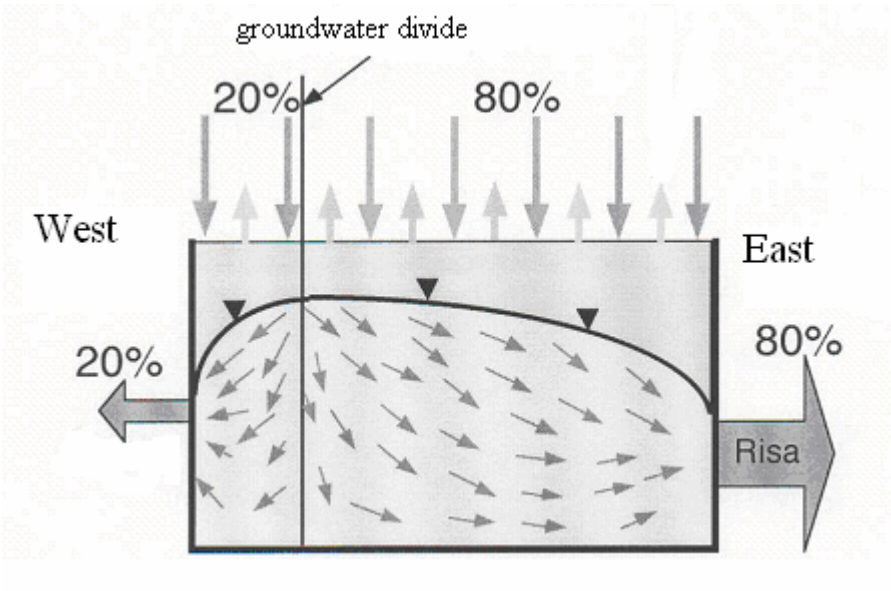

Figure 1.6:Principal sketch showing how the groundwater divide position is defined of how much water that flow out of the groundwater magazine on each side of the groundwater divide (after Worsley et al. 2003).

This may indicate decreasing transmissivity towards the distal parts of the delta (Kitterød 2004a). The fine grained deposits at the bottom of the aquifer may be considered as an aquitard or an aquiclude (Tuttle 1990).The ground water magazine consists of glasiofluvial, glasiolacustrine, eolian, bogg and marine clay deposits(Østmo 1976b). These sediments will influence the groundwater flow, due to their varying porosity and permeability. Since the delta deposits become finer grained in the distal direction it is expected that the transmissivity will decrease toward the distal parts. The marine-clay may once have functioned as a barrier for groundwater flow out of the distal part of the delta (Figure 1.7.). Before the ravine incision, the groundwater flux must have flowed mainly to the Hersjøen and Risa drainage system, where the groundwater had a much easier path through the porous glasiofluvial deposits (Tuttle 1990).

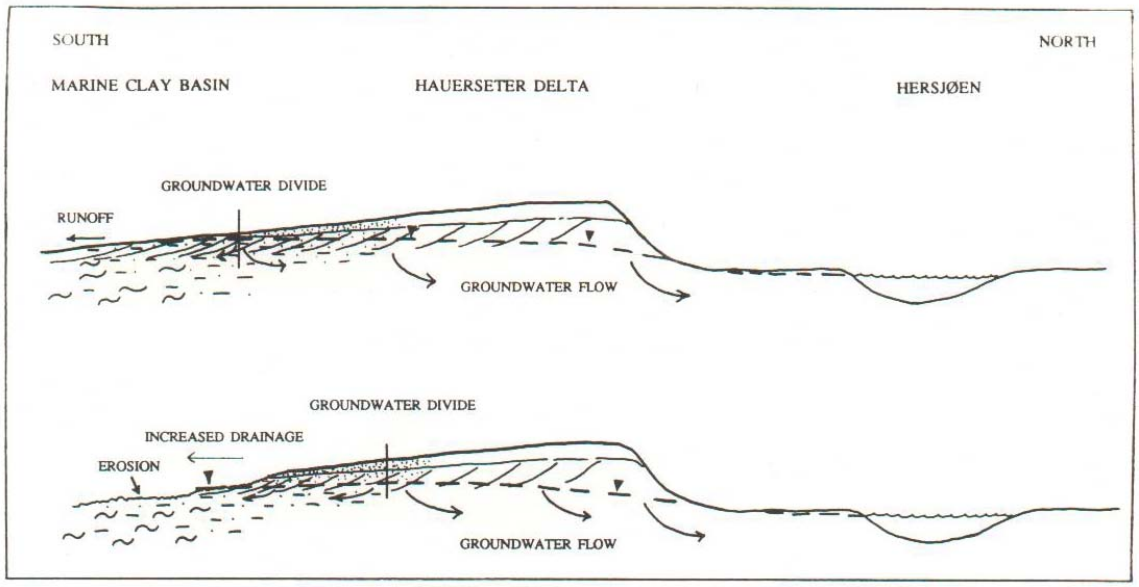

Figure 1.7: The illustration show the groundwater flow and drainage system both before and after erosion of the marine clays with incision of the delta boundary. After erosion of the marine clays and the delta boundary, an increased groundwater flow has been directed toward the marine-clay basin, and the groundwater divide has been displaced toward the Hersjøen drainage system.

Due to this portion of drainage to Hersjøen and the river Risa, the groundwater divide would be displaced in the opposite direction. At present there is well-developed ravine topography along the distal edge of the delta caused by fluvial erosion. The ravines have incised the majority of the perimeter of the aquifer. Tuttles (1990) field study results revealed that the main factors controlling the groundwater flow are the boundary conditions and the level of the groundwater table. The erosion of undisturbed clay and further development of the ravines will most likely increase the drainage towards the distal part of the delta, and it may increase a displacement of the groundwater divide closer to Hersjøen.

The groundwater table has risen and fallen with variation of precipitation quantity over the years (Jørgensen et al. 1990). It is important to notice that the groundwater map of Østmo (1976a) was made during a period when the groundwater table was very low.

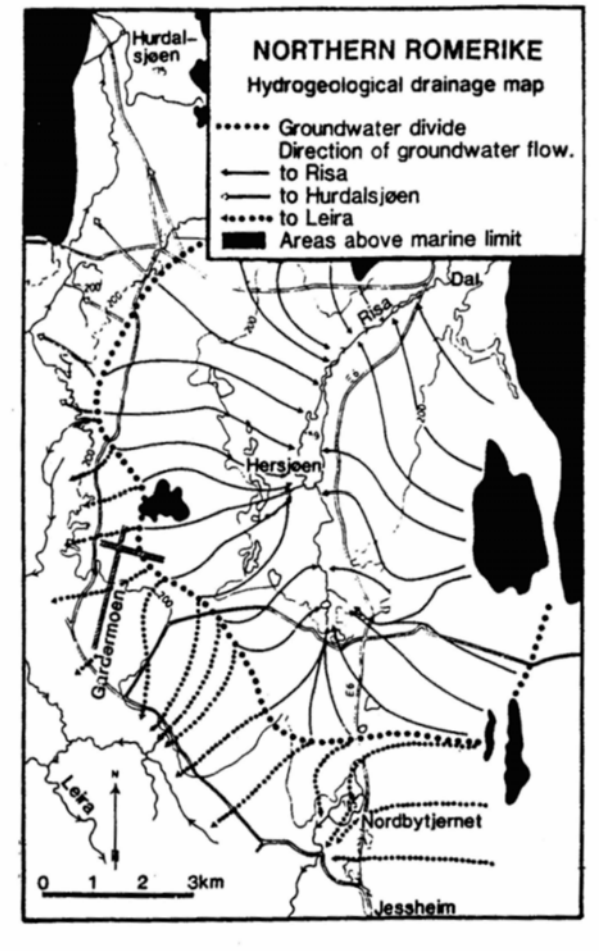

Figure 1.8: An illustration of the groundwater drainage in Øvre Romerike (Østmo1976c).

CHAPTER 2

THEORETICAL BACKGROUND

2.1

Groundwater is present in almost all geological formations. The movement of the groundwater is dependent on the media it's in. Groundwater must move through small, constricted passages, often along a tortuous route, and the movement and flow of groundwater is on a large degree dependent on the nature of the rock or sediment through which the water moves (Skinner and Porter 1995). In marine clay or rock, the motion is slow compared to sand and gravel formations.

An aquifer is a permeable formation that stores and transmits groundwater in sufficient quantity to supply wells (Domenico and Schwartz 1990). An unconfined / phreatic aquifer has an upper surface that is in contact with the atmosphere and the upper limit of the aquifer coincides with the water table. A confined aquifer on the other hand is bounded by aquicludes, a body of impermeable or distinctly less permeable layers adjacent to the permeable aquifer. (Skinner and Porter 1995). In a confined aquifer the head is above the top of the aquifer.

Mathematical descriptions of movement of groundwater are based on two principles: Darcy's law and conservation of mass (Haitjema 1995).

2.2 Hydraulic head/Piezometric head/head

Darcy's law is formulated in terms of piezometric heads, not water pressure. This is because the hydrostatic pressure distribution caused by gravity is not a driving force for flow. For

instance, there can be a difference in pore pressure at the same points as there is no difference in heads (Haitjema 1995). A piezometer is a tube or pipe used to measure water-level elevation in field situations. It is open in both ends (Figure 2.1). Bernoulli's equation states that under conditions of steady flow, the total energy of an incompressible fluid is constant at all positions along a flow path in a closed system (Domenico and Schwartz 1990). This may be written as:

$$gz + \frac{P}{\rho_w} + \frac{v^2}{2} = \text{constant} \qquad (2.1)$$

where: g is the acceleration due to gravity, z is the elevation of the base of the piezometer, P is the pressure exerted by the water column, ρ_w is the fluid density and v is the velocity.

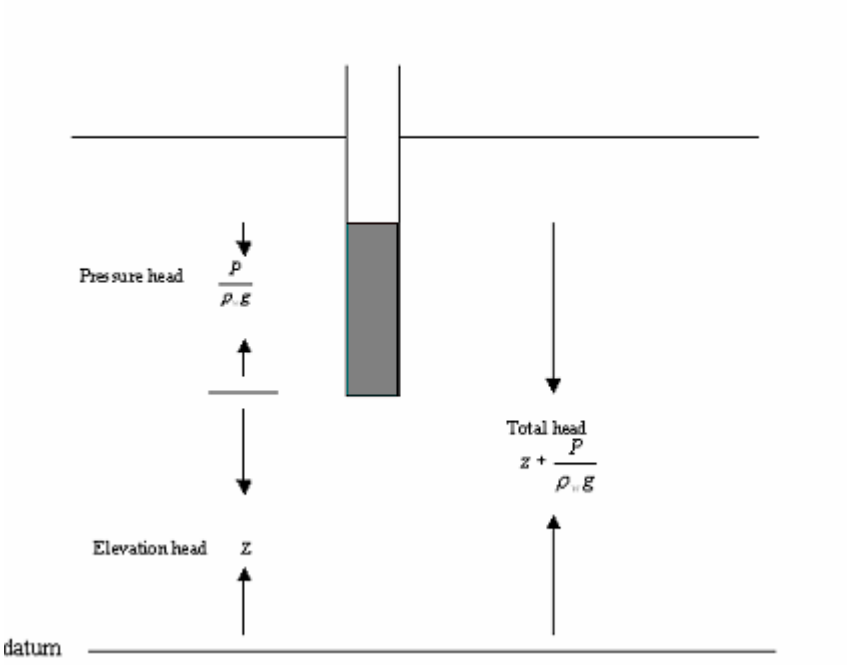

Figure 2.1: Simplified modified model from Domenico and Schwartz 1990, showing the principle of piezometer, elevation, pressure and hydraulic head/piezometric head/head for a point in the flow field.

If we divide by g we get:

$$z + \frac{P}{\rho_w g} + \frac{v^2}{2g} = \text{constant} \qquad (2.2)$$

Where z represents the base of the piezometer, it is the energy of the position and it is called elevation-head. The second component of the equation; $\frac{P}{\rho_w g}$ is the energy due to sustained fluid pressure and it is called the pressure-head. It represents the length of the water column in the piezometer, the potential energy of the fluid. $\rho_w g$ is the unit weight of water. The third and last component is the energy due to fluid movement, and represent the kinetic energy, and it is called the velocity-head. Since the velocity of groundwater is slow the term is neglected and we get:

$$\varphi = z + \frac{P}{\rho_w g} \tag{2.3}$$

Where φ is called hydraulic head or piezometric head or just head (Domenico and Schwartz 1990). In the rest of the thesis I will use the term head.

2.3 Differential equations and Boundary conditions

Differential equations

In the mathematical descriptions of movement of groundwater in the ground you have to deal with differential equations. A differential equation is an equation that contains a derivative. A differential equation tells you about the relationship between two (or more) variables. Often there is just one expression for the alteration rate in the equation itself, that's why a differential equation may have an unlimited number of solutions. In reality there is just one of these solutions that describes the situation. This is why you have to put up some boundary conditions to isolate the proper solution from all of the other solutions. This means that you have to define the boundary conditions along the boarders to the area that the equation is valid for, and it is of great concern to find the correct boundary conditions.

Boundary conditions of the first kind; Dirichlet condition, is formulated entirely in terms of specific heads. It is used when the head along the boarder is a known function of time: φ = f(t). This variant of boundary condition is often used when the head at a given point is

constant: $\varphi = c$. In such cases it is in form of natural systems as a river, a lake or a spring that is in direct contact with the aquifer. It leads to a solution independent of any aquifer parameter, such as hydraulic conductivity or aquifer thickness. The head distribution is simply a straight line from φ_1 at $x = 0$ to φ_2 at $x = L$. Solutions to Laplace's equation, subjected to Dirichlet conditions are fully determined by these boundary conditions (Haitjema 1995).

Boundary conditions of the second kind; Neumann condition, is a flux specific boundary which means that a known amount of water is withdrawn from or infiltrated into the aquifer (Haitjema 1995). When the flux over a boarder is known, the gradient is too, because the flux is proportional with the gradient. This kind of boundary condition is used when the "normal component" to the gradient over the boarder is a known function of time. The "normal component" is the projection of the gradient vector to a line perpendicular to the boarder: $\partial h/\partial n = f(t)$. This is used when the gradients "normal component" over a boarder is equal to zero, this means that the boarder is almost or total impermeable. All the eqvipotential lines will occur perpendicular on the place, usually where there is a changeover to hard rock, clay or till.
Most real world problems have mixed boundary conditions, a combination of Dirichlet and Neuman conditions. It is called the boundary condition of the third kind.

2.4 Darcy's law

Darcy did several experiments on the flow of water through columns of sand and the result of his work was published in 1856. Figure 2.2 shows the equipment similar to that used by Darcy in his experiments. It consists of a cylinder that contains a porous medium (sand). The cylinder contains two manometers. A *Manometer* is a device to measure pressures. The elevation to which the water level rises in a manometer is a measure of the energy that the ground water possesses at the inlet of the manometer (Domenico et al 1990). This is called the hydraulic head or the head.In an experiment water flows into and out of the cylinder at a known volumetric flow rate: Q $[L^3/T]$ (L and T stands for length and time respectively). The cross-section area A $[^{L\ 2}]$ is also known.

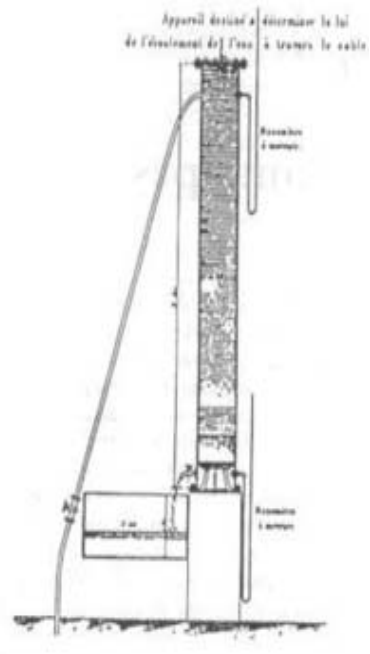

Figure 2.2: From Darcy's original experiment shown in his paper from 1856.

The elevation of the water in the manometers is measured relative to a local datum. The specific discharge q [L/T] represents the volumetric flow rate per unit surface area of the cylinder. It is determined by the volumetric flow rate Q, and the cross-section area A: q = Q/A.

A one-dimensional flow column is shown in Figure 2.3 The hydraulic gradient is dimensionless; $\frac{\varphi_2 - \varphi_1}{z_2 - z_1}$ and represents the change in water level elevation in the manometers, which is separated by the length $z_2 - z_1$.
Darcy's law is expressed:

$$\frac{Q}{A} = q = -k\frac{\varphi_2 - \varphi_1}{z_2 - z_1} \tag{2.4}$$

Where the parameter k [L/T] is a proportionality constant dependent on the medium. It is called the hydraulic conductivity and it is defined as the water flow per unit of time through a specific area of the aquifer when the hydraulic gradient is similar to one (Henriksen and

Nielsen 1996). It describes the interaction between the water and the soil/bedrock. Because the gradient is a dimensionless quantity, k has the unit of velocity.

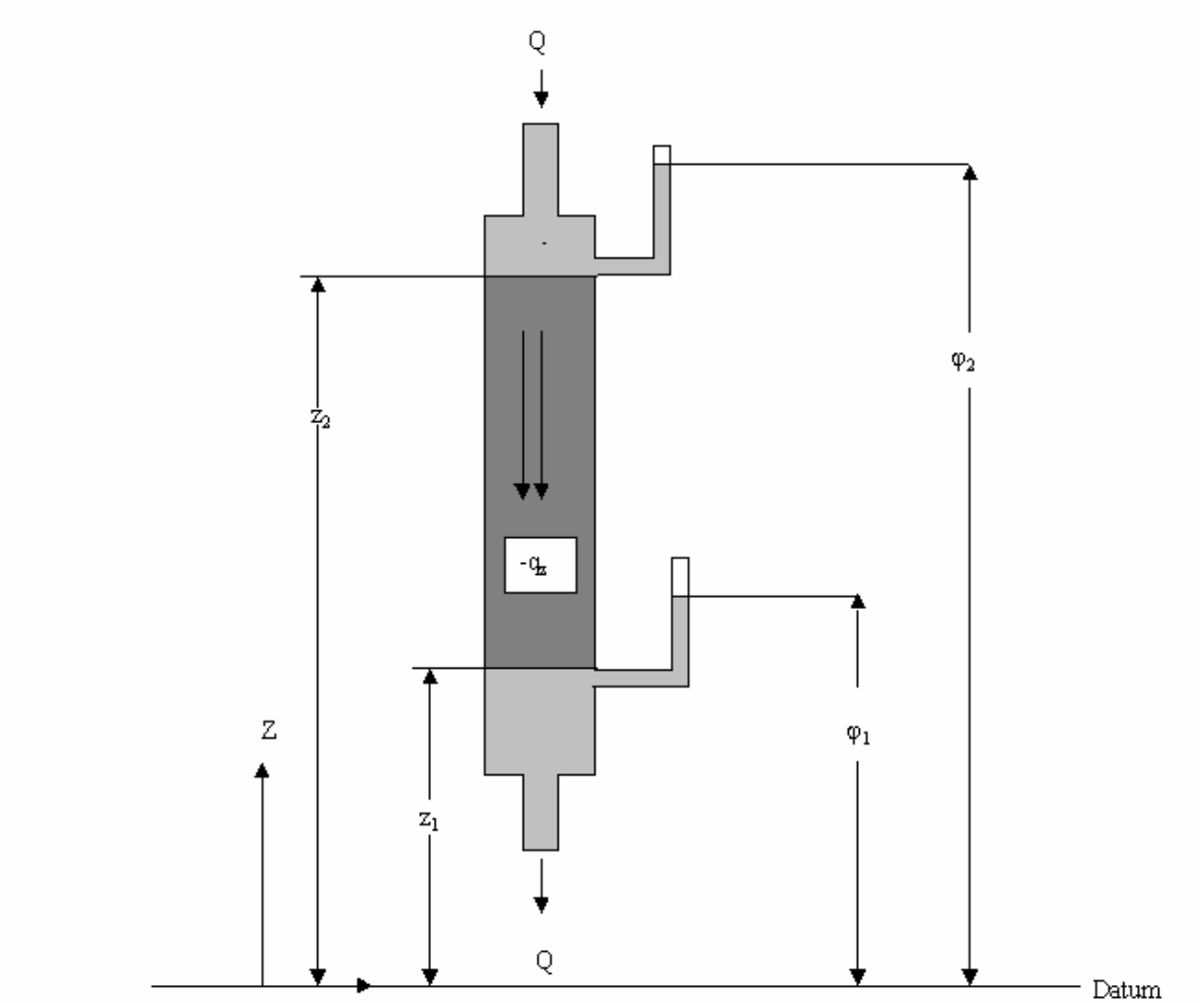

Figure 2.3: Demonstration of Darcy's law modified after Haitjema1995.

The minus sign is used because flow is in the direction of decreasing water levels, from where φ is high to where φ is low (Domenico et al 1990). Four of the parts in Darcy's law need to be clarified with field observations: The specific discharge q, the water level measurements and the gradient and proportionality constant k (Haitjema 1995). Darcy's law suggests that there is a linear relationship between the specific discharge and the hydraulic gradient. This is valid as long as the flow is laminar. Flow through large pore space, as in large fractures in rocks or for instance in coarse gravel formations close to high-capacity wells, can be turbulent. In such cases Darcy's law can't describe the flow (Haitjema 1995). If there is a linear relationship between the specific discharge and the hydraulic gradient the hydraulic head can be written as a function of z:

$$\varphi(z) = \frac{\varphi_2 - \varphi_1}{z_2 - z_1} z + \frac{\varphi_1 z_2 - \varphi_2 z_1}{z_2 - z_1} \tag{2.5}$$

The term: $\frac{\varphi_2 - \varphi_1}{z_2 - z_1}$ from equation (2.4) is the derivative of φ(z):

$$\frac{d\varphi}{dz} = \frac{\phi_2 - \varphi_1}{z_2 - z_1} \tag{2.6}$$

Darcy's law can then be written as:

$$q_z = -k \frac{d\varphi}{dz} \tag{2.7}$$

The index z means that the specific discharge is parallel to the z-direction, and the minus sign that, the flow is going in the negative direction of z. This new equation states that if the derivative of the head in the z-direction is known, the specific discharge in the z-direction follows from (2.7). The result in (2.7) holds in any direction including the x- and y- direction. The partial derivatives of φ(x,y,z) represent the three components of the hydraulic gradient (Haitjema 1995).

$$q_x = -k \frac{\partial \varphi}{\partial x}$$

$$q_y = -k \frac{\partial \varphi}{\partial y} \tag{2.8}$$

$$q_z = -k \frac{\partial \varphi}{\partial z}$$

Darcy's law expressed as (2.8) describes the fluid flow along x, y, and z direction where the material properties and thus the hydraulic conductivities are different.

2.5 The continuity equation

Because the head φ(x,y,z) usually is not know throughout an entire aquifer an additional equation is required to calculate the groundwater flow. This equation is given by the realization that no water can spontaneously disappear or appear at a particular point in the aquifer: *Conservation of mass* (Haitjema 1995).

The sides of the block n figure X are parallel to the coordinate directions x,y,z, and measure Δx, Δy, Δz. The specific discharge vectors are at the centers of all the six sides of the block. It is assumed that the discharge at the center of a side represents the average for the entire side. The water balance for the block is: Total inflow is equal to total outflow:

Total outflow-Total inflow = 0

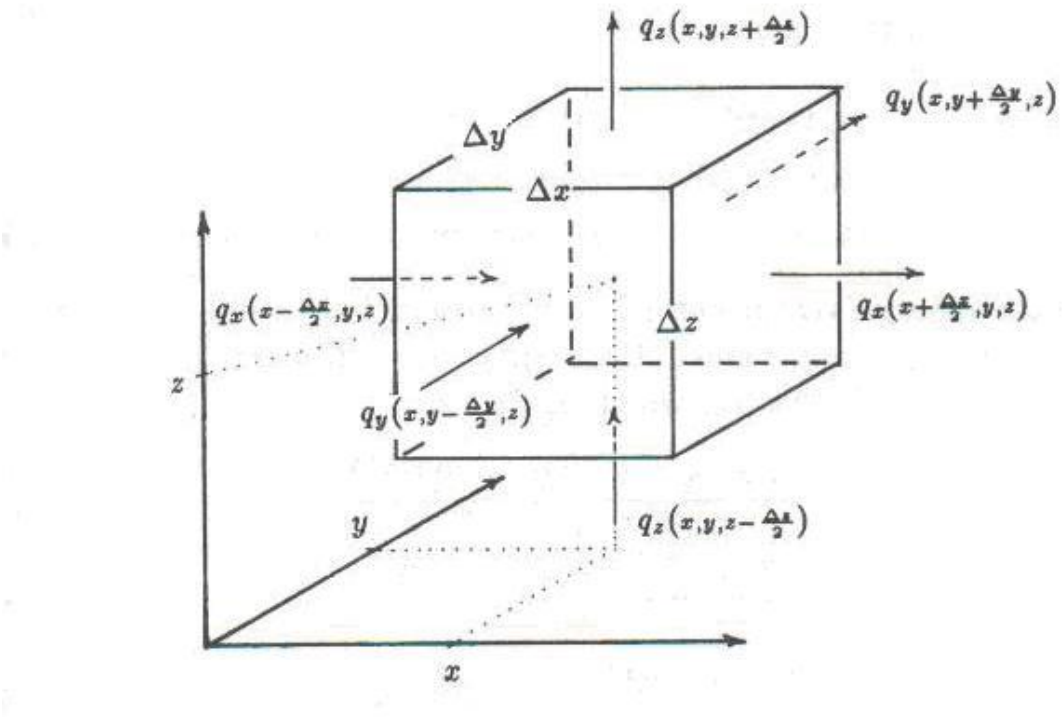

Figure 2.4: Model of a small block of soil and water in an aquifer and the continuity of flow (Haitjema 1995).

From figure 2.4 you can see that this leads to:

$$\left(q_x\left(x+\frac{\Delta x}{2},y,z\right)-q_x\left(x-\frac{\Delta x}{2},y,z\right)\right)\Delta y\Delta z$$
$$+\left(q_y\left(x,y+\frac{\Delta y}{2},z\right)-q_y\left(x,y-\frac{\Delta y}{2},z\right)\right)\Delta x\Delta z \qquad (2.9)$$
$$+\left(q_z\left(x,y,z+\frac{\Delta z}{2}\right)-q_z\left(x,y,z-\frac{\Delta z}{2}\right)\right)\Delta x\Delta y=0$$

Both sides of equation (2.9) are divided by the volume of the block: ΔxΔyΔz, which gives:

$$\frac{\left(q_x\left(x+\frac{\Delta x}{2},y,z\right)-q_x\left(x-\frac{\Delta x}{2},y,z\right)\right)\Delta y\Delta z}{\Delta x}$$
$$+\frac{\left(q_y\left(x,y+\frac{\Delta y}{2},z\right)-q_y\left(x,y-\frac{\Delta y}{2},z\right)\right)\Delta x\Delta z}{\Delta y} \qquad (2.10)$$
$$+\frac{\left(q_z\left(x,y,z+\frac{\Delta z}{2}\right)-q_z\left(x,y,z-\frac{\Delta z}{2}\right)\right)\Delta x\Delta y}{\Delta z}=0$$

If $\Delta x \to 0$, $\Delta y \to 0$ and $\Delta z \to 0$, the quotients in equation (2.10) become partial derivatives:

$$\frac{\partial q_x}{\partial x}+\frac{\partial q_y}{\partial y}+\frac{\partial q_z}{\partial z}=0 \qquad (2.11)$$

2.6 Laplace's Equation

If you combine Darcy's law (2.8) with the continuity equation (2.11) it forms the basic principal differential equation for steady state groundwater flow:

$$\frac{\partial}{\partial x}\left[-k\frac{\partial \varphi}{\partial x}\right]+\frac{\partial}{\partial y}\left[-k\frac{\partial \varphi}{\partial y}\right]+\frac{\partial}{\partial z}\left[-k\frac{\partial \varphi}{\partial z}\right]=0 \qquad (2.12)$$

or

$$\frac{\partial^2 \varphi}{\partial x^2}+\frac{\partial^2 \varphi}{\partial y^2}+\frac{\partial^2 \varphi}{\partial z^2}=0 \qquad (2.13)$$

This last equation is called the *equation of Laplace*. This equation is universally used in physics. To apply this equation to real world ground water flow problems you have to apply a set of boundary conditions formed by for instance streams, lakes, wells etc, by making simplified assumptions(Haitjema 1995).

2.7 Dupuit Forcheimer flow

Both Dupuit(1863) and Forcheimer (1886) came with the same suggestion, that when following a fictive water particle from entry to exit, most of it movement in the medium will be horizontal. Even though groundwater flow is three-dimensional, the flow is predominantly horizontal (Haitjema 1995). If the flow is assumed to be only flowing in the horizontal direction will:

$$q_z = 0 \qquad (2.14)$$

and Darcy's law will be:

$$\frac{d\varphi}{dz} = 0 \qquad (2.15)$$

Equation (2.15) is the most important since the heads do not vary with depth. These two equations reduce the three-dimensional flow problem to a two-dimensional flow problem. This approximation is based on the assumption that the ratios between vertical and horizontal dimension are very small: *The Dupuit-Forchheimer assumption* (Kitterød 2004a).

2.8 Confined flow, discharge potential

When using the Dupuit-Forchheimer assumption in calculating ground water flow there are convenient to use the discharges integrated over the aquifers height rather than specific discharges (Haitjema 1995).This means that you for the x and y direction with components Q_x, Q_y you get:

$$Q_x = Hq_x \qquad (2.16)$$

$$Q_y = Hq_y$$

When applying Darcy's law to this we can express Q_x and Q_y in terms of φ:

$$Q_x = Hq_x = H\left[-k\frac{\partial\varphi}{\partial x}\right]$$

$$Q_y = Hq_y = H\left[-k\frac{\partial\varphi}{\partial y}\right] \tag{2.17}$$

Both k and H are independent of x and y. Equation (2.17) can then be written as

$$Q_x = -\frac{\partial[Hk\varphi]}{\partial x}$$

$$Q_y = -\frac{\partial[Hk\varphi]}{\partial y} \tag{2.18}$$

Then we introduce a new variable $\Phi = Hk\varphi$, called the discharge potential. Equation (2.18) can now be written as:

$$Q_x = -\frac{\partial\Phi}{\partial x}$$

$$Q_y = -\frac{\partial\Phi}{\partial y} \tag{2.19}$$

When writing Laplae's equation (2.13) in terms of Φ you have to set $\frac{\partial^2\varphi}{\partial z^2}$ equal to zero:

$$\frac{\partial^2\varphi}{\partial x^2} + \frac{\partial^2\varphi}{\partial y^2} = 0 \tag{2.20}$$

Then you multiply both sides in the equation with H and k(the product of hydraulic conductivity and aquifer thickness is often referred to as aquifer transmissivity T):

$$\frac{\partial^2\Phi}{\partial x^2} + \frac{\partial^2\Phi}{\partial y^2} = 0 \tag{2.21}$$

When (2.19) is substituted into (2.21), the continuity equation in terms of discharges is obtained:

$$\frac{\partial Q_X}{\partial_X} + \frac{\partial Q_Y}{\partial_Y} = 0 \tag{2.22}$$

For one-dimensional flow, Laplace's equation (2.21) reduces to:

$$\frac{\partial^2 \Phi}{\partial x^2} = 0 \tag{2.23}$$

2.9 Phreatic flow, discharge potential

In an unconfined aquifer where the saturated aquifer thickness are the same as the head measured with respect to the aquifer bottom the total discharge is:

$$Q_x = hq_x \tag{2.24}$$

or:

$$Q_x = \varphi q_x \tag{2.25}$$

or; with Darcy's law;

$$Q_x = \varphi\left[-k\frac{d\varphi}{dx}\right] \tag{2.26}$$

Q_x can be written as the negative derivative of a discharge potential Φ, as in equation (2.19) for confined aquifers:

$$Q_x = -\frac{d\Phi}{dx} \tag{2.27}$$

Equations (2.26) and (2.27) are identical when Φ is chosen as:

$$\Phi = \frac{1}{2}k\varphi^2 \tag{2.28}$$

The discharge vector Q_i, in terms of potentials and Darcy's law in terms of Φ are defined in the same way for confined and unconfined flow. The potential Φ, is defined different. The continuity equation for unconfined flow in terms of discharges is the same as for confined flow; equation (2.22):

$$\frac{\partial Q_X}{\partial_X} + \frac{\partial Q_Y}{\partial_Y} = 0 \tag{2.29}$$

Writing the differential equation for unconfined flow in terms of head gives substituting equation (2.28) into (2.21) yields:

$$\frac{\partial^2\left[\frac{1}{2}k\varphi^2\right]}{\partial x^2}+\frac{\partial^2\left[\frac{1}{2}k\varphi^2\right]}{\partial y^2}=0 \qquad (2.30)$$

which reduces to:

$$\frac{\partial^2\varphi^2}{\partial x^2}+\frac{\partial^2\varphi^2}{\partial y^2}=0 \qquad (2.31)$$

2.10 Poisson's Equation

The Dupuit-Forchheimer assumption ignores the vertical flow. Areal recharge causes a vertical downward flow into the aquifer. This flow is equal to the areal recharge rate. To include this recharge it is put into the continuity equation (2.11). Combining this again with Darcy's law will give a new differential equation for Dupuit-Forchheimer flow: Poisson's equation (Haitjema 1995).

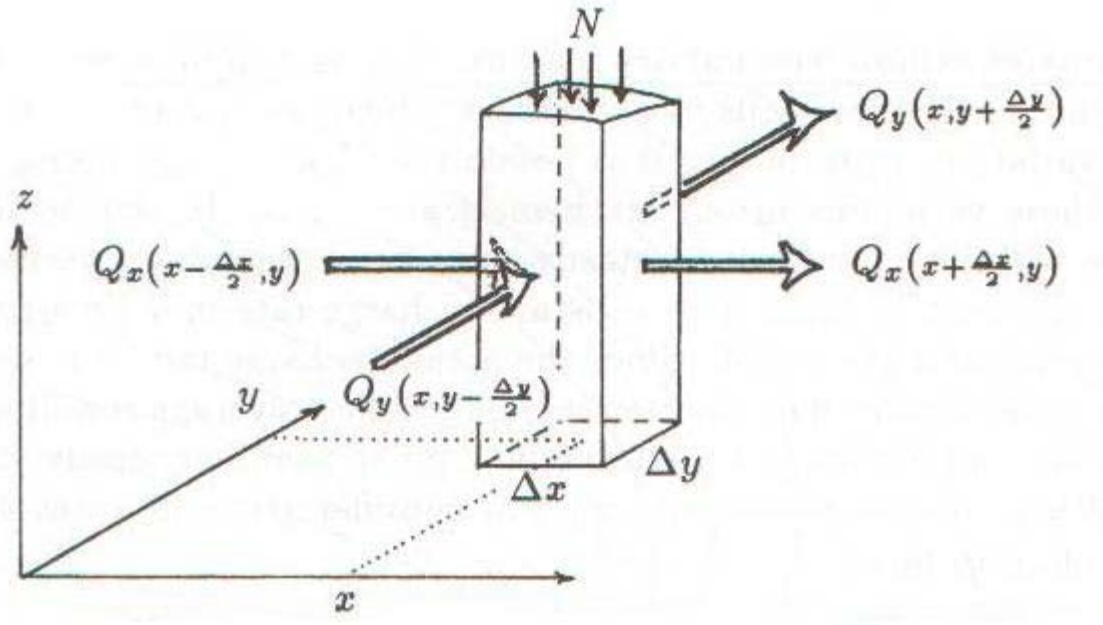

Figure 2.5: Continuity of flow in a Dupuit-Forchheimer model with areal recharge, from Haitjema 1995.

The inflows and outflows of a Dupuit-Forchheimer model is shown in Figure 2.5. The model shows a column of soil fully saturated by water in the aquifer height. The cross section measure Δx times Δy. The center of the column is at (x,y). The areal recharge is N [L/T], volume of water per unit time. We have the continuity of flow equation:

Total outflow-Total inflow = 0

$$\left(Q_x\left(x+\frac{\Delta x}{2},y\right)-Q_x\left(x-\frac{\Delta x}{2},y\right)\right)\Delta y + \left(Q_y\left(x,y+\frac{\Delta y}{2}\right)-Q_y\left(x-\frac{\Delta y}{2}\right)\right)\Delta x + -N\Delta x\Delta y = 0 \quad (2.32)$$

We divide both sides by ΔxΔy, let Δx→0 and Δy→0 and bring the term of N to the right hand side. This gives:

$$\frac{\partial Q_x}{\partial x}+\frac{\partial Q_y}{\partial y}=N \quad (2.33)$$

When we combine this equation with Darcy's law (2.19) we get Poisson's equation:

$$\frac{\partial^2 \Phi}{\partial x^2}+\frac{\partial^2 \Phi}{\partial y^2}=-N \quad (2.34)$$

The only difference between Laplace's equation and Poissons equation is the term –N. this is called the source term. This is the term that recharges the aquifer in the Dupuit-Forchheimer model.

2.11 Radial flow with recharge

In problems with areal recharge on a circular formation you can solve them by using Poisson's equation (Haitjema 1995). From Figure 2.6 we can see that the total amount of water per unit time that enters the circle with the radius r, is equal to the recharge rate N times the surface area of the circle. Across the circle you have a discharge vector called Q_r. Q_r is defined as the amount of water per unit time per unit length of the circle. This means that Q_r is equal to the total flow across the circle divided by the circumference of the circle:

$$Q_r = \frac{N\pi r^2}{2\pi r} = \frac{Nr}{2} \tag{2.35}$$

Because of the radial symmetry the potential depends only on the radial distance r. This means that Darcy's law can be written as:

$$Q_r = -\frac{d\Phi}{dr} \tag{2.36}$$

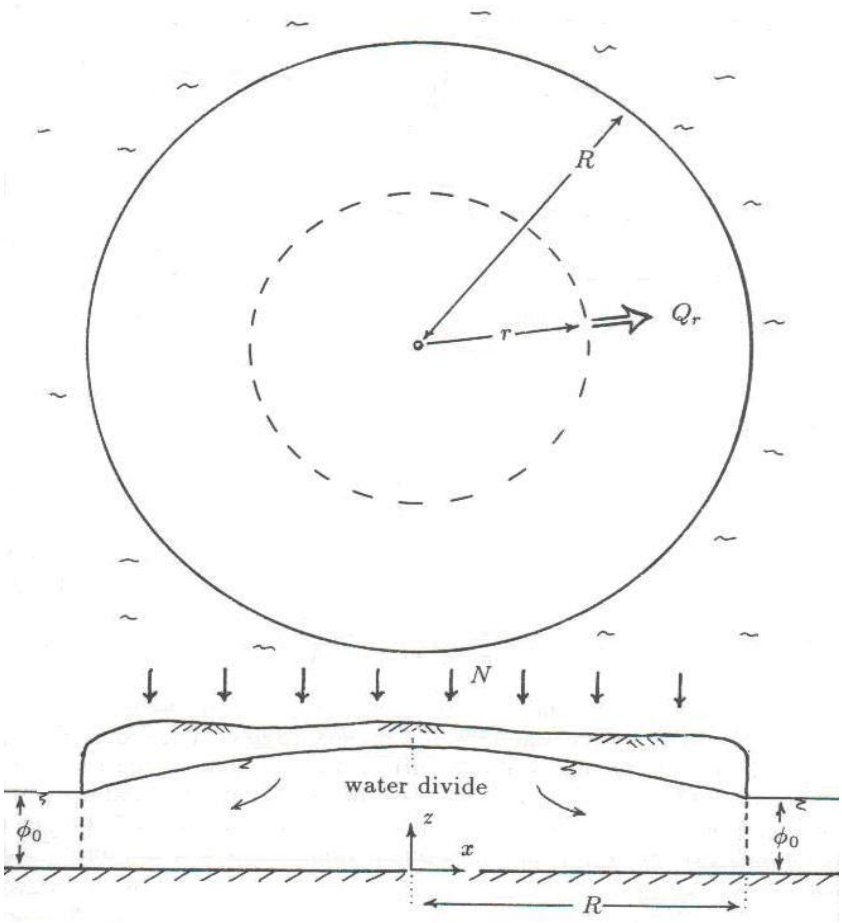

Figure 2.6: Principle sketch of areal recharge on a circular island from Haitjema 1995.

From the equations (2.35) and (2.36) it follows that the potential Φ, can be obtained by integrating equation (2.35) with respect to r:

$$\Phi = -\frac{N}{4}r^2 + C \tag{2.37}$$

At the boundary, see figure X, where r = R, the head is given: $\varphi = \varphi_0$. When we put this boundary condition into equation (2.37), it becomes:

$$\Phi = -\frac{N}{4}\left(r^2 - R^2\right) + \Phi_0 \qquad (2.38)$$

In this equation there are one constant head boundary; φ_0 at r = R, and N is the net infiltration to the groundwater. Equation (2.38) is the solution for both confined aquifer ($\Phi = kH\varphi$) and an unconfined aquifer (($\Phi = (1/2k\varphi^2)$). Where k is the hydraulic conductivity, H is the thickness of the aquifer, and φ is the head. In a saturated open aquifer φ is equal to the aquifer thickness (Kitterød 2004a).

2.12 "Doughnut" equation

The following deduction of radial groundwater flow is taken from Kitterød (2004a).

In Figure 2.7 there are two boundaries: R_1 and R_2. If we put the boundary R_2 into equation (2.38) it will be:

$$\Phi = -\frac{N}{4}\left(r^2 - R_2^2\right) + \Phi_2 \qquad (2.39)$$

The inner boundary R_1 can be introduced and we get two constant head boundaries, and a more geological correct expression due to solve the discharge potential for a circular structure as for instance a delta.

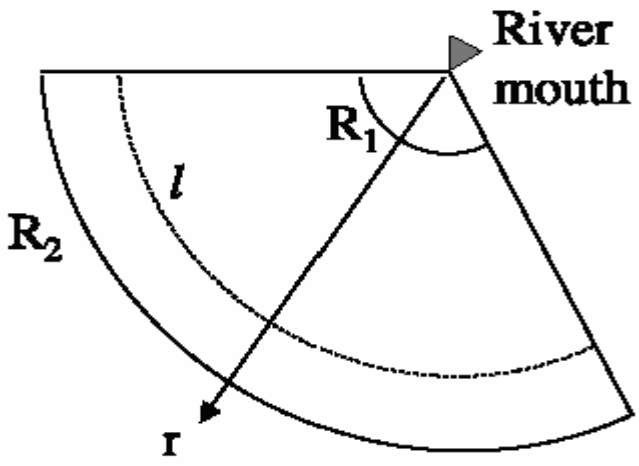

Figure 2.7: Principal sketch of delta geometry modified after Kitterød 2004a. Shows the relationship between the radius r and the inner and outer delta boundaries R_1 and R_2, and the location of the groundwater divide l.

The area between the inner boundary R_1 and the groundwater divide, where $R_1 \le r \le l$ can be expressed as:

$$Q = N\pi(l^2 - r^2) \tag{2.40}$$

The water balance Q implies that the net recharge (precipitation) N, on the inner area of the cylinder expressed by equation (2.40) is equal to the discharge vector Q_r across the cylinder with radius r:

$$-Q_r = \frac{Q}{2\pi r} \tag{2.41}$$

Since the flow direction is the opposite of r Q_r has to be negative.
If we combine Darcy's law, equation (2.36) with the two equations (2.40) and (2.41) it yield:

$$\Phi_a = \frac{Nl^2}{2}\ln r - \frac{N}{4}r^2 + C_a \tag{2.42}$$

If we then put the boundary values $\Phi = \Phi_1$ at $r = R_1$ into equation (2.42) we get:

$$\Phi_a = -\frac{N}{4}\left(r^2 - R_1^2\right) + \frac{Nl^2}{2}\ln\left(\frac{r}{R_1}\right) + \Phi_1 \tag{2.43}$$

Equation (2.43) is the discharge potential for radial flow with head boundary value at $r = R_1$ and impermeable boundary at $r = l$.
To found the discharge potential for the outer cylindrical area where $l \le r \le R_2$, we can do the same application. Here the boundary value are Φ_2 at $r = R_2$. Then the discharge potential for the outer cylindrical area is equal to:

$$\Phi_b = -\frac{N}{4}\left(r^2 - R_2^2\right) + \frac{Nl^2}{2}\ln\left(\frac{r}{R_2}\right) + \Phi_2 \tag{2.44}$$

At the groundwater divide where $r = l$, see equation (2.43) and (2.44), there is no radial flow. This means that: $\frac{d\Phi_a}{dr} = \frac{d\Phi_b}{dr} = 0$. The discharge potential is: $\Phi = \Phi_a = \Phi_b$. This is used to eliminate l from equations (2.43) and (2.44) and to form a closed equation:

$$\Phi = \left(\frac{N}{4}\left(r^2 - R_1^2\right) - \Phi_1\right)\left(\frac{\ln r - \ln R_2}{\ln R_2 - \ln R_1}\right) - \left(\frac{N}{4}\left(r^2 - R_2^2\right) - \Phi_2\right)\left(\frac{\ln r - \ln R_1}{\ln R_2 - \ln R_1}\right) \qquad (2.45)$$

This equation is referred to as the simple "doughnut" equation.

2.13 Head in a Confined Aquifer

To make the doughnut equation more geological correct we let the thickness of the confined aquifer *H,* be a linear function of the radius r:

$$H(r) = H_{1,2} - a\left(r - R_{1,2}\right) \qquad (2.46)$$

Where a is the gradient: $a = \frac{\left(H_1 - H_2\right)}{\left(R_2 - R_1\right)}$, see Figure 2.8.

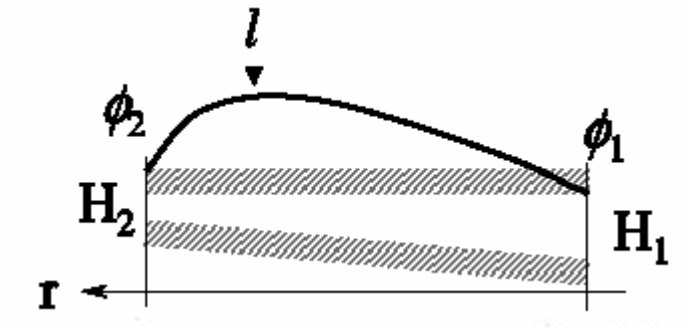

Figure 2.8: A radial cross section through a delta indicating a confined aquifer, with linearly decreasing aquifer thickness. ϕ_1 and ϕ_2 is the head at R_1 and R_2 (Kitterød 2004a).

If a is small, $H_1 - H_2 << R_2 - R_1$, it means that the ratio between the vertical and the horizontal dimension are very small. Then we can ignore the vertical part and the approximate head as a one-dimensional ordinary partial differential equation (Kitterød 2004).
We divide the flow equation into two parts as we did earlier, where the groundwater divide *l* is a no-flow boundary. Balance of mass for steady state flow where $R_1 \le r \le l$ gives the expression:

$$-q_r H = \frac{N}{2}\left(\frac{l^2 - r^2}{r}\right) \qquad (2.47)$$

Then we insert Darcy's law: $-k\left(\frac{\Phi_a}{dr}\right)$ into equation (2.47) and get:

$$d\Phi_a = \frac{N}{2k}\left(\frac{l^2 - r^2}{rH}\right)dr \tag{2.48}$$

Since H = H(r) is a linear function of r as given in equation (2.46), we have to solve two integrals, that is:

$$\int \frac{1}{r(H_0 - ar)}dr = -\frac{1}{H_0}\left(\ln\left(\frac{H_0 - ar}{r}\right)\right) + c, \tag{2.49}$$

$$\int \frac{r}{H_0 - ar}dr = -\frac{1}{a^2}(ar - H_0 + H_0 \ln(H_{0-ar})) + c, \tag{2.50}$$

where $H_0 = H_{1,2} + aR_{1,2}$, and c is the integral constant. H_0 is the theoretical aquifer thickness at r = 0. For the boundary condition $\varphi = \varphi_1$ at r =R_1, the solution of equation (2.48) is:

$$\varphi_a = \frac{N}{2ka}(r - R_1) - \frac{Nl^2}{2k}A_1 + \frac{N}{2k}B_1 + \varphi_1 \tag{2.51}$$

Where: $A_1 = \left(\frac{1}{H_0}\right)\ln\left(\frac{R_1 H}{H_1 r}\right)$ and $B_1 = \left(\frac{H_0}{a^2}\right)\ln\left(\frac{H}{H_1}\right)$, where H is given in the equation (x.36) for index 1. In the same way we find the head for the outer area where $l \le r \le R_2$:

$$\varphi_b = \frac{N}{2ka}(r - R_2) - \frac{Nl^2}{2k}A_2 + \frac{N}{2k}B_2 + \varphi_2 \tag{2.52}$$

Where: $A_1 = \left(\frac{1}{H_0}\right)\ln\left(\frac{R_2 H}{H_2 r}\right)$ and $B_1 = \left(\frac{H_0}{a^2}\right)\ln\left(\frac{H}{H_2}\right)$, where H is given in the equation (2.46) for index 2.

Then we eliminate the groundwater divide l in equation (2.51) and (2.52) and get one expression for the head:

$$\varphi = \frac{A_1 L_{2-} A_2 L_1}{A_1 - A_2} \tag{2.53}$$

Where: $L_1 = \left(\frac{N}{2ka}\right)(r - R_1) + \left(\frac{N}{2k}\right)B_1 + \varphi_1$, and

$$L_2 = \left(\frac{N}{2ka}\right)(r - R_2) + \left(\frac{N}{2k}\right)B_2 + \varphi_2$$

A_1, A_2, B_1 and B_2 is defined in equation (2.51) and (2.52) (Kitterød 2004).

2.14 Head in a Phreatic Aquifer

In the phreatic aquifer, to develop a more geological correct equation, the hydraulic conductivity k *is set as linear function of the radius r. It is then given as:*

$$k(r) = k_1 - b(r - R_1) \tag{2.54}$$

where; $b = \frac{(k_1 - k_2)}{(R_2 - R_1)}$,

similar to the linear equation used for a confined aquifer. Further on the law for balance of mass and Darcy's law gives:

$$d\varphi^2 = N\left(\frac{l^2 - r^2}{rk}\right)dr \ , \tag{2.55}$$

k is given in equation (2.54), and h is the head for a phreatic aquifer This together with the boundary conditions $h = h_1$ at r =R_1, and $h = h_2$ at r =R_2, will the solution of equation (2.55**)** be:

$$\varphi^2 = \frac{(\alpha_1 P_2 - \alpha_2 P_1)}{(\alpha_1 - \alpha_2)}, \tag{2.56}$$

where: $P_1 = \frac{N}{b}(r - R_1) + N\beta_1 + h_1^2$,

$P_2 = \frac{N}{b}(r - R_2) + N\beta_2 + h_2^2$,

$$\alpha_1 = \frac{1}{k_0}\ln\left(\frac{R_1 k}{k_1 r}\right),$$

$$\alpha_2 = \frac{1}{k_0}\ln\left(\frac{R_2 k}{k_2 r}\right),$$

$$\beta_1 = \frac{k_0}{b^2}\ln\left(\frac{k}{k_1}\right),$$

$$\beta_2 = \frac{k_0}{b^2}\ln\left(\frac{k}{k_2}\right),$$

and where: $k_0 = k_{1,2} + bR_{1,2}$, and k is given in equation (2.44) with the corresponding indexes.

2.15 Ground water divide

The ground water divide for a confined aquifer, for $R_1 \leq l \leq R_2$*, are to be find where the derivative of equation (2.53) is* $d\varphi/dr = 0$*:*

$$\frac{d\varphi}{dr} = \frac{d}{dr}\left(\frac{A_1 L_2 - A_2 L_1}{A_1 - A_2}\right) = 0 \qquad (2.57)$$

which is equal to:

$$l^2 = H_0\left(\frac{\frac{R_2 - R_1}{a} + \frac{H_0}{a^2}\ln\frac{H_2}{H_1} + \frac{2k}{N}(\varphi_1 - \varphi_2)}{\ln\frac{H_2}{H_1} + \ln\frac{R_1}{R_2}}\right) \qquad (2.58)$$

The ground water divide for a phreatic aquifer, for $R_1 \leq l \leq R_2$*, are to be find where the derivative of equation (2.56) is* $d\varphi^2/dr = 0$*:*

$$\frac{d\varphi^2}{dr} = \frac{d}{dr}\left(\frac{\alpha_1 P_2 - \alpha_2 P_1}{\alpha_1 - \alpha_2}\right) = 0 \tag{2.59}$$

wich is equal to:

$$l^2 = k_0\left(\frac{\frac{R_2 - R_1}{b} + \frac{k_0}{b^2}\ln\frac{k_2}{k_1} + \frac{1}{N}\left(\varphi_1^2 - \varphi_2^2\right)}{\ln\frac{k_2}{k_1} + \ln\frac{R_1}{R_2}}\right) \tag{2.60}$$

CHAPTER 3

Parameters and Boundary conditions

Chapter three will describe the parameters that I have used to calculate the analytical models, and a description of the models.

3.1 Analytical models

3.1.1 Equations

In my modelling of the Trandum delta I used equation (2.53) and equation (2.56) that is the analytical solutions for ground water heads in a confined and a phreatic aquifer where the geometry is simplified to a "doughnut"-structure, and the aquifer thickness or the hydraulic conductivity can be expressed as a linear function of radius..

3.1.2 Optimal parameters

A large number of groundwater levels were monitored at the Trandum delta, Figure 3.2 (Faneprosjekt Gardermoen, UiO). These observations was used to find the optimal parameters p = [k_1,k_2] of equation(2.56) and p = [H_1, H_2] of equation (2.53), by minimizing the root mean square deviation D, equation(3.1), between the observations y_i and the calculated groundwater heads $y(x_i;p)$:

$$D = \frac{1}{n}\sum_i^n \left(y_i^2 - y^2(x_i; p)\right)^{\frac{1}{2}}, \qquad (3.1)$$

where x is the location of the observation tubes, i= 1,….,n and n is the number of observations.

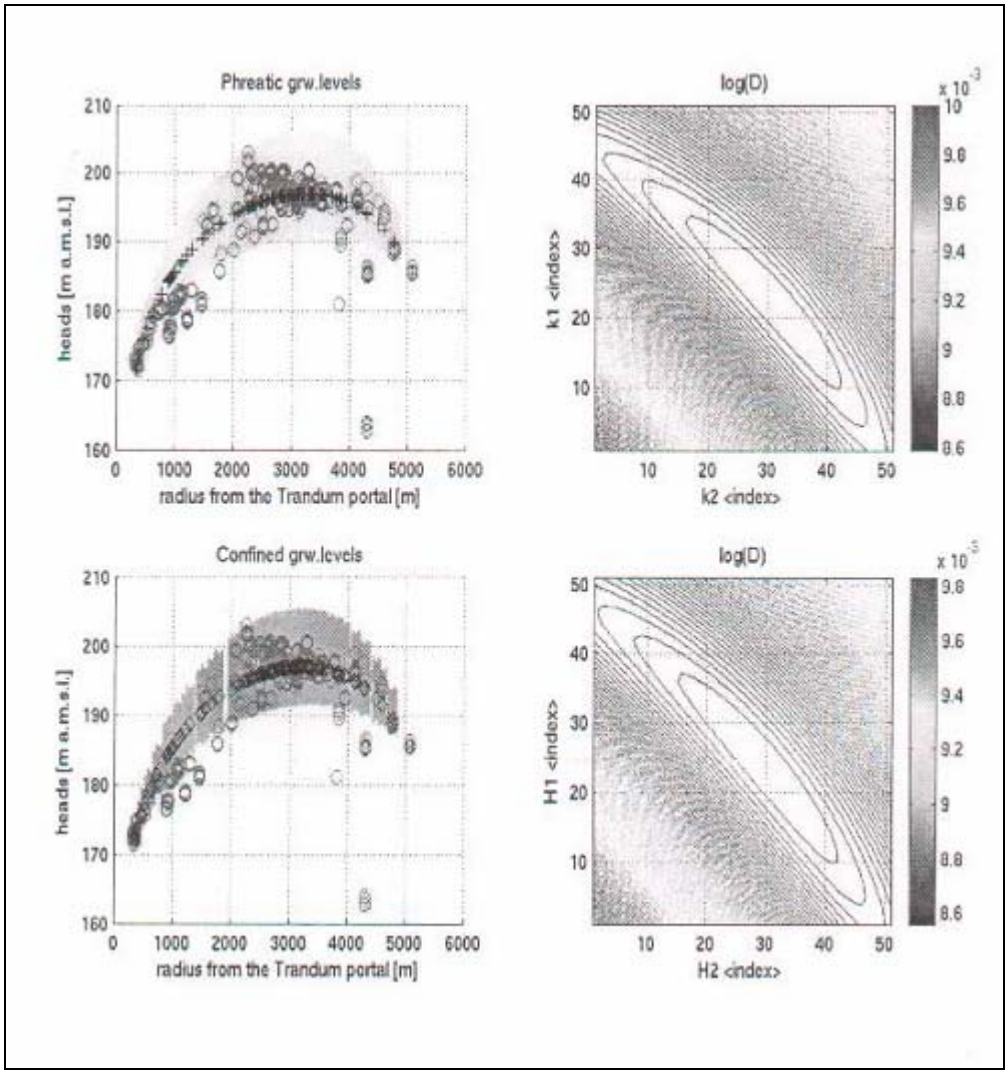

Figure 3.1: Optimal parameters for p = [k_1,k_2] of equation (2.56) and p = [H_1,H_2] of equation (2.53) estimated by minimizing the root-mean –square deviation D given in equation (3.1). The groundwater heads corresponding to optimal p are indicated as crosses for the phreatic aquifer and diamonds for confined aquifer. Observed heads are indicated as circles. The shaded areas that envelopes the observations are the perturbation range of p: 2,2 $\times 10^{-5}$ m/s $\leq k_1 \leq$ 4,1 $\times 10^{-5}$ m/s, 2,6 $\times 10^{-6}$ m/s $\leq k_2 \leq$ 9,4 $\times 10^{-6}$ m/s; 235m $\leq H_1 \leq$ 401m, 35m $\leq H_2 \leq$ 103m (Kitterød 2004b).

Measured and calculated heads are shown in Figure 3.1 together with the D function. Estimation results are given in Table 3.1.

The parameters found are the ones that give the minimum difference between the observed heads and the calculated heads.

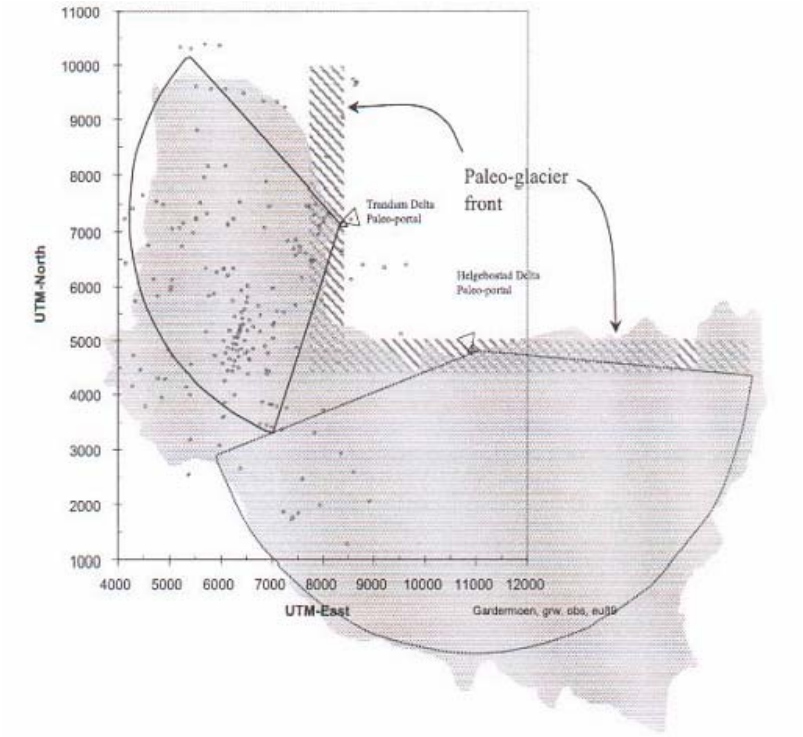

Figure 3.2: The Gardermoen aquifer at the Hauerseter delta complex is a superposition of two deltas with paleoportals at Trandum and Helgebostad. The observation wells at the Trandum delta are used for the estimation of aquifer parameters as shown in Figure 3.1.

Table 3.1. Results of the estimation based on observations from the Trandum-delta of confined- and phreatic aquifer conditions.
The boundary conditions used are: Net infiltration N: 1,266730e-08 m/s; R_1: 336.00m; constant head at R_1:171,50m; R_2: 5100,00m; constant head at R_2: 185,00m. At equation (2.56): $k = ½(k_1+k_2)$ = 1.727901e-05 m/s.

Confined (eq. (2.53))		Phreatic (eq.(2.56))	
parameter	values	parameter	values
H_1	301,86m	k_1	2,886e-05 m/s
H_2	66,19m	k_2	5693e-06 m/s

3.1.3 Origin

Since the equations used to make the analytical models is established on the circular geometry of the delta, an origin has to be set. This origin is set in Hersjøen. The location of origin for the analytical models at the Trandum-delta is set to (UTM-East, UTM-North): 8400,00 m 7150,00 m in UTM-zone: 32 V, EU89 datum. This origin is the same in all the analytical models

3.1.4 Radius

The different radiuses that I have used in the analytical part of the thesis have their origin in the positions of the observation wells at Trandum. The different radiuses are calculated on the basis of the origin that is set for the models and the location of the observation wells and Pythagoras ($r = (x^2 + y^2)^{½}$). This means that every model will find a head at the same radiuses as the observation wells are situated from the common origin. This makes it more convenient to compare the heads compiled from the analytical models and the observations done in the field. The same radiuses were used in the eleven different models with varying boundary conditions. Where the analytical models are compared with the numerical models, the radiuses are fit to suit the numerical ones.

3.1.5 Net infiltration

At Gardermoen the average net infiltration is about 1mm/d, equivalent to: 1,1574e-08m/s (Norwegian Meteorological Institute). The infiltration into the phreatic, precipitation fed aquifer in the Trandum-delta is dependent on the amount of precipitation and the snowmelt, and it fluctuates from year to year and through the year. Because the river Risa is greatly fed by groundwater, the response of precipitation and snowmelt is damped and the river discharge is fairly constant through the year. The specific discharge to the river Risa has been monitored to 1,095 mm/d, which correspond well with average values of precipitation and estimated evapotranspiration Norwegian Water and Energy Directorate). Thus a steady state recharge of N = 1,095mm/d = 1,26673e-08 m/s, was used to calculate the groundwater heads for all the analytical solutions.

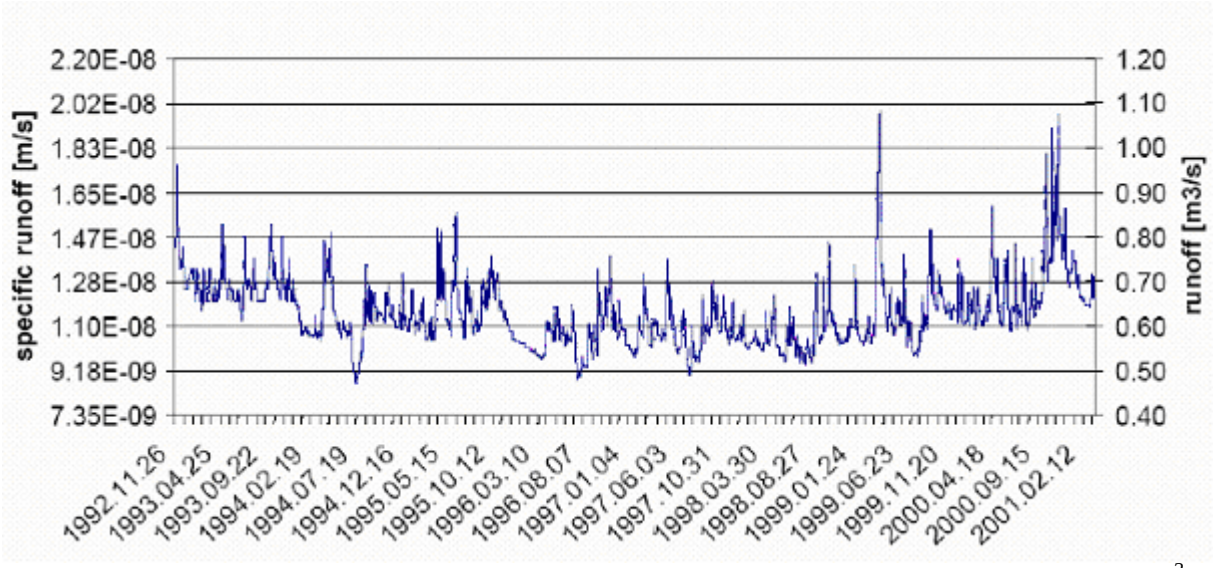

Figure 3.2: Runoff from the river Risa from 1992 to 2001 with a catchment area of 54.4 km^2 (Kitterød 2004b)

3.1.6 Parameters

Table 3.2: Parameters used in the analytical modelling of piezometric head distribution in the Trandum-delta. Where H_1 and H_2 is the aquifer thickness at R_1 and R_2 , k_1 and k_2 is the hydraulic conductivity at R_1 and R_2, k is the average between k_1 and k_2, φ_1 and φ_2 are the piezometric heads R_1 and R_2 for the confined aquifer, h_1 and h_2 are the piezometric head at R_1 and R_2 for the phreatic aquifer, and N is the net infiltration.

	CONFINED		PHREATIC
H_1	301,86 m	**k_1**	2,886e-05 m/s
H_2	66,19 m	**k_2**	5,693e-06 m/s
k	1,727901e-05 m/s		
φ_1	171,50 m	**h_1**	171,50 m
φ_2	185,00 m	**h_2**	185,00 m
R_1	336 m	**R_1**	336 m
R_2	5100 m	**R_2**	5100 m
N	1,266730e-08 m/s	**N**	1,266730e-08 m/s

In all the analytical models I used the optimal parameters from Table 3.1. and the net infiltration N, deduced from the specific discharge of the river Risa.
Tabell 3.2 show the parameters used in the analytical equations.

3.1.7 Three dimensional (3d) presentation

To present the analytical models in 3d, I made a script in MATLAB that transferred the analytical solutions of the heads into the forms of matrices (n*m = 50*50). In this way the diagonal solutions, by calculating new radiuses using Pythagoras ($r = (x^2 + y^2)^{½}$), are transferred into a three dimensional grid, and for this analytical solution you will always have the same ground water levels at the same radius from the origin.

3.1.8 Different boundary conditions from hydrogeological map.

To see how the ravines and the variations in the boundary conditions along the inner circumference and the outer circumference of the Trandum-delta are inflicting the head distribution, I used the Hydrogeological map by Østmo (1976a), and read out eleven new boundary conditions. The new boundaries were read out of the map as the ravines in the area. This means that I found the horizon for the springs that is marked on the map. I made a line from origin towards the outer horizon and read off the coordinates for R_1, the inner horizon and R_2, the outer horizon, at that particular line, together with the heads read out of the ground water counters on the map, at R_1 and R_2. The different coordinates were then transferred to meters using Pythagoras ($r = (x^2 + y^2)^{½}$, to represent the length of the radius out to the boundary of the delta. I read out the most extremes, so that the difference between the boundary condition should be at the most. In this way the greatest differences in boundary conditions from the area will be shown in the models.
I located the horizons that located far away from the origin and the horizon located close to the origin for both the inner and the outer boundary. The area where the different boundary conditions were red out of the hydrogeological map is indicated on the hydrogeological drainage map in Figure 3.3 as the area within the two black lines marked on the map.
The eleven different boundary conditions are listed in Table 3.3. The coordinates and the heads red out of the map are listed in Table 1 and Table 2 in the appendix.
Later on I will refer to the different boundary conditions that I have used by the number used in Table 3.3.

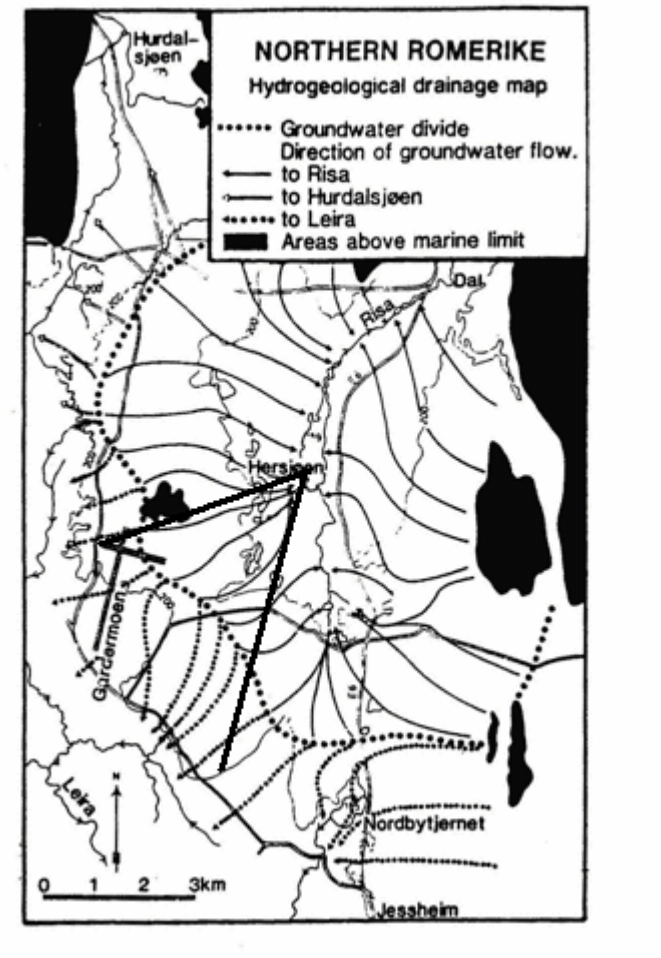

Figure 3.3: The two black lines which have theres origin in Hersjøen on the hydrogeological drainage map (Østmo 1976c) indicates the area where the eleven different boundary conditions where red out of the hydrogeological map (Østmo 1976a).

3.1.9 Analytical models using the eleven different boundary conditions.

For every one of the eleven different cases of boundary condition I made an analytical model. This means that each of the eleven models have different boundary condition. For the confined part they have the same thickness that is a linear function of radius and the same hydraulic conductivity and recharge. See Table3.2. For the phreatic aquifer, the eleven different models have different boundary condition as for the confined models, and the same recharge. The hydraulic conductivity however is a function of the radius. I used equation (2.53) to solve the confined models and equation (2.56) to solve the phreatic models.

Table 3.3: The eleven different boundary conditions read out of the Hyrdogeological map by Østmo(1976a). All of the values are in meters.

	R_1	φ_1	R_2	φ_2
1	291,2	160	5372,3	186
2	787,1	162	5298,3	188
3	761,6	162	6603,7	172
4	596,7	160	6216,6	178
5	466,9	160	6437,3	178
6	961,2	163	5937,9	176
7	869,3	163	6218,2	174
8	1156,0	166	6095,4	174
9	1084,1	166	6110,0	174
10	688,8	162	6762,9	172
11	672,3	162	7000,7	172

The eleven different models may show us how the ravines might affect the level of the heads in the aquifer, but they will not be representative for the whole aquifer. They will represent the diagonal of the aquifer where the boundary conditions are red out.

3.2 Numerical models

3.2.1 MODFLOW

The numerical models are carried out using MODFLOW with the PMWIN (Chiang and Kinzelbach, 2001). The principles for numerical solutions of groundwater problema are:

- The area is classificated into an appropriate number of cell, a grid, where you will find an expression for the piezometric head.
- Then you define the boundary conditions and initial condition in the area and apply this to the model.

- The unknown piezometric heads is expressed with consideration to the grids dimensions and the adjacent piezometric heads by Darcy's law. This means that we get a set of equations with the same amount of equations as there are unknown.
- The equations are solved by starting with a "qualified guess", and then step by step improve it to the solutions converge.

It is important to have in mind that the result from the models never get better than the data you put in it.

3.2.2 Origin

This origin is set in Hersjøen in the same place as for the analytical solutions: (UTM-East, UTM-North): 8400,00 m 7150,00 m in UTM-zone: 32 V, EU89 datum. This origin is the same in all the numerical models models.

3.2.3 Grid

The grid in the numerical models are set to 50 times 50 cells which each are 100 meters times 100 meters.

3.2.4 Boundary conditions

I made models for both confined and phreatic aquifers. In the first hand I made models where the boundaries followed the circular "doughnut"-form. In these models I used the same boundary conditions as in the analytical models, Figure 3.3 and Table 3.2. In the second hand I made models where the inner and outer radius were to follow the ravines in the area, Figure 3.3. Integrating the different boundary conditions for R_1 and R_2, from the analytical solution manually into the model made this possible. The areas in between the boundary conditions from Table 3.3 were adapted to fit the known boundary conditions. For the inner boundary I used the eleven boundary conditions, but for the outer boundary I used the boundary

conditions 2 to 7 from Table 3.3. The reason for not using boundary condition 8 to 11 at the outer boundary is that they are situated outside the limits of the models. The constant heads at the boundaries are also picked out from Table 3.3. The constant heads in between were adapted to fit the constant heads from Table 3.3. The coordinates of the boundaries and the constant heads are listed in Table 3 in appendix. To let the models represent exclusively the area where the boundary conditions are valid, inactive cells exclude the areas outside. In such way, the heads compiled in the models are from the area where the boundary conditions are valid (Figure 3.3).

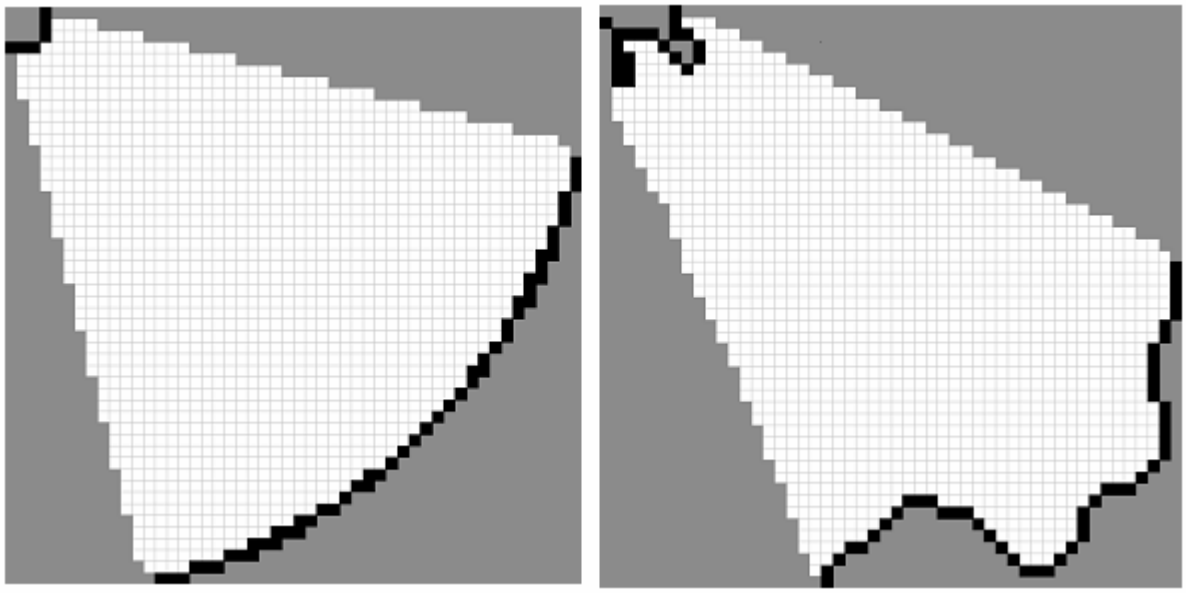

Figure 3.3: Illustrations of the boundary conditions: Black: fixed head cells, White: active cells and Grey: inactive cells. The figure at the left illustrates the boundary conditions in black where the circular "doughnut"-form is used. The figure at the right hand side illustrates the model where the boundary conditions in black follows the ravines.

This means that I have four different models, two which are confined, one with the circular "doughnut"-form and one with integrated ravines, and two which are phreatic, one with the circular "doughnut"-form and one with integrated ravines.

3.2.5 Hydraulic conductivity, Thickness and Transmissivity

Confined models

In the confined models the hydraulic conductivity is set to be constant all through the aquifer, and the average k of k_1 and k_2 from Table 3.1 is the k which is used in the two models. The thickness H is a linear function of the radius. For the inner boundary R_1; the thickness is set to H_1 and for the outer boundary R_2; the thickness is set to H_2 (Table 3.2). This means that there are two constant transmissivities, T_1 at the inner boundary R_1 and T_2 at the outer boundary R_2.Since the thickness varies linearly through the aquifer, the transmissivity do as well.

Phreatic models

In the phreatic models, the hydraulic conductivity is set as a linear function of the radius r through the aquifer, as it is in the analytical models, with hydraulic conductivity k_1 at boundary R_1 and k_2 at boundary R_1 (Table 3.2). The thickness of the aquifer are set to one meter, so there are one transmissivity T_1 at the inner boundary R_1 and one transmissivity T_2 at the outer boundary R_2. The transmissivity then varies as a function of radius through the aquifer.

3.2.6 Recharge

The recharge used in the numerical models is the same as for the analytical models from Table 3.2.

3.3 MATLAB

All of the numerical models and equations are carried out using MATLAB. For the numerical models I have made input files to PMWIN in MATLAB, and all of the output files from PMWIN are generated into MATLAB for further treatment. All of the MATLAB scripts that I have used are to be found in the appendix.

Chapter 4

Analytical and Numerical models

In chapter four, the results from both the analytical and the numerical models will be displayed and finally compared with each other.

4.1 Analytical models

4.1.1 Analytical solutions.

The analytical models, using the "dougnut"-equations, (2.53) for confined- and (2.56) for phreatic aquifer, using the boundary conditions in Table 3.2 gave the results illustrated in Figure 4.1.1. With optimal $H_{1,2}$ in equation (2.53) and $k_{1,2}$ in equation (2.56), that minimize the average difference between calculated and observed groundwater heads, there are only minor differences between these two solutions (Figure 4.1.1 A, and Table 4.1.1). The difference in the two models are so small that it constitute less than one percent of an head of 171.5 m, that is the constant head used at boundary R_1 (Table 3.2). Further on comparing the calculated heads, both the confined- and the phreatic solution, with the observed heads, you can see from Figure 4.1.1 B and C, that the calculated heads fits well into the observed ones as expected when using the optimal parameters. The mean, maximum, minimum and the standard deviation of the differences are listed in Table 4.1.2. This shows that the mean differences are small even though, especially the maximum but also the minimum differences are large. This may be due to some observation stations that have low groundwater levels, or high in the latter case, compared to the majority of the observation stations. This is also illustrated in Figure 4.1.1, where it is clear that some of the observed heads are very low compared to the others at the same radius from the origin in Hersjøen.

Table 4.1.1 Differences in heads between confined and phreatic analytical solution.

Difference between confined and phreatic solution			
mean(d) m	**max(d) m**	**min(d) m**	**std(d) m**
-0,0752	0,0059	-0,3559	0,1145

d = heads confined – heads phreatic

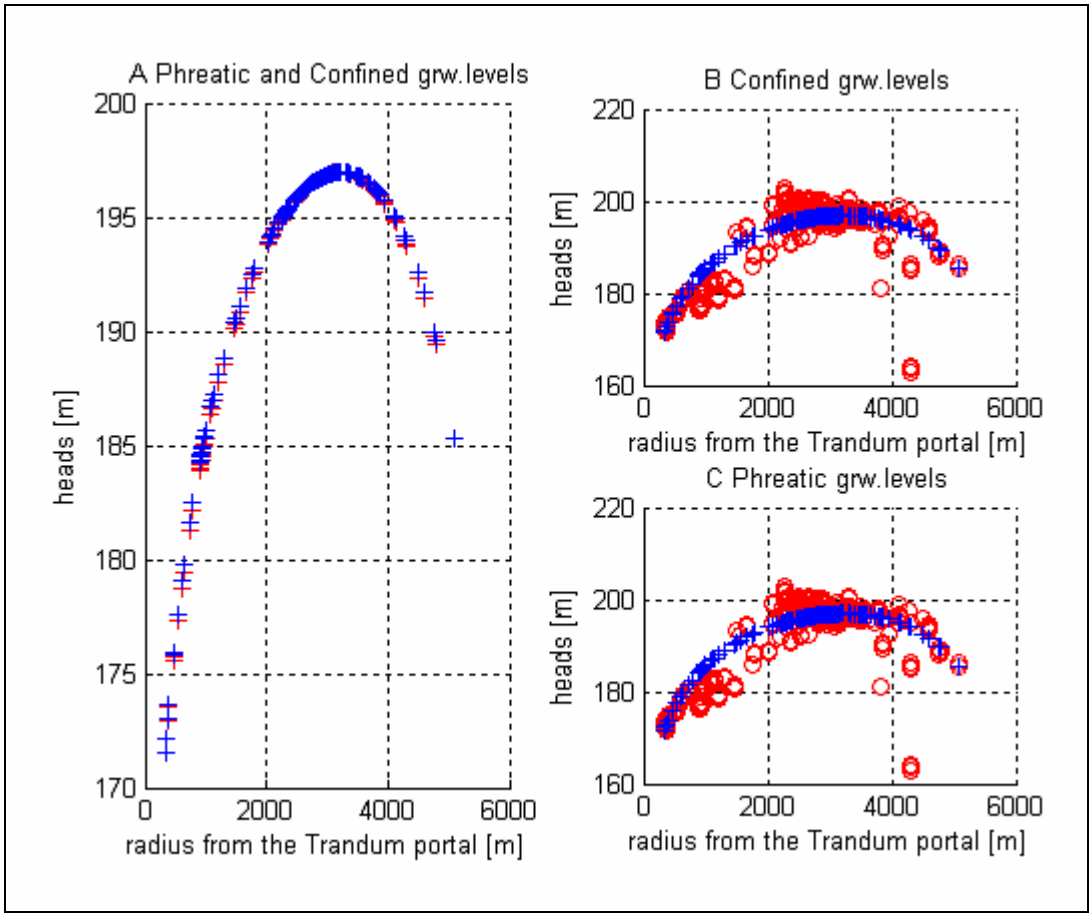

Figure 4.1.1: Heads from analytical solutions. A: The red crosses show the solution for confined aquifer and the blue crosses show the solution for phreatic aquifer. B: The blue crosses show the solution for the confined aquifer, the red rings show the field observations. C: The blue crosses show the solution for phreatic aquifer, the red rings show the field observations.

Table 4.1.2: Differences d between analytical solutions and field observations.

Calculated heads vs. field observations		
	Confined	**Phreatic**
mean(d) m	***0,2271***	***0,3023***
max(d) m	31,0826	***31,2862***
min(d) m	-8,0240	***-7,9700***
std(d) m	3,7138	***3,7700***

d = calculated heads – observed heads

The mean difference between the calculated heads and the analytical solutions constitute less than one per cent of a head of 171,50m that is the minimum head at R_1. The standard deviation (in this case: the uncertainty associated with the differences in heads) for the confined solution is ±3,7138m, and for the phreatic solution it is ±3,7700. These are small values compared to the height of the heads in the aquifer.

4.1.2 Analytical solutions considering the ravines.

The eleven different boundary conditions that were red out of the hydrogeological map by Østmo 1976a, Table 3.3, were used in the eleven different models that I made for both a phreatic aquifer and a confined aquifer. The results are illustrated in Figure 4.1.2 together with the observed heads and the heads calculated by the "doughnut"-equation.
The heads for the eleven solutions with boundary conditions from Table 3.3 have generally a lower level of the heads than the observed heads and the heads calculated by the "doughnut"-

equation. This may be due to the fact that the groundwater levels were especially low when the map was made as mentioned in chapter 1.4.

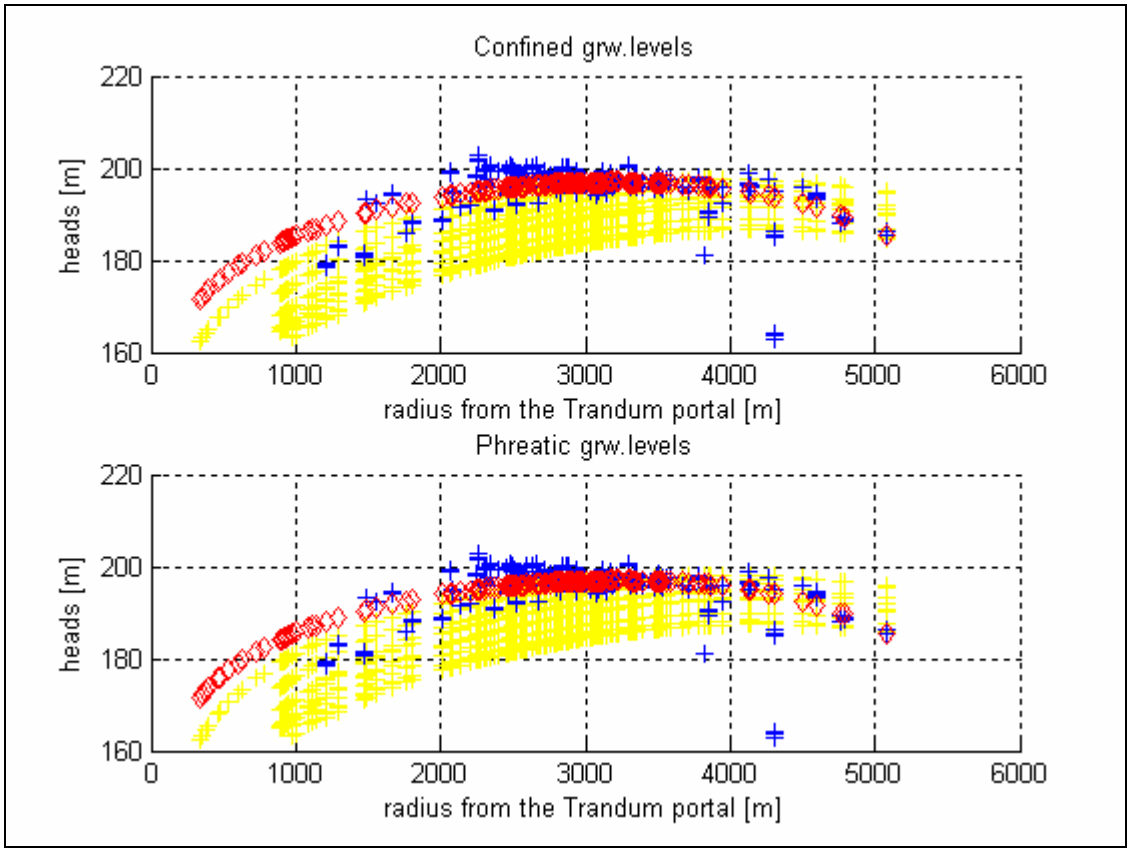

Figure 4.1.2: The analytical solutions for the eleven different boundary conditions; yellow crosses, together with the solution for the aquifer with the "doughnut"-form; red diamonds, and the field observations; blue crosses.

To find the largest and most marked differences between the models calculated with the eleven different boundary conditions from Table 3.3, the boundary conditions that differed the most from the others where picked out. Identifying the boundary conditions with R_1 and R_2 closest to the origin, and the one with R_1 and R_2 farthest away from the origin did this. For the differences in heads at the boundaries I picked out the ones with the highest head and the ones with the lowest head. The solutions are illustrated in Figure 4.1.3. The differences between the maximum conditions and the minimum conditions are listed with the maximum value of the differences and the minimum value of the differences in Table 4.1.3. When the differences are negative it means that the model that is subtracted have higher heads than the model that it is subtracted from. When the values are positive the opposite case is present. The largest differences are to be find in the case where the head at the boundaries are differing,

while the distance between the inner and outer boundary does not have the same effect on the model From Table 4.1.3 you can see that the largest difference for phreatic models is – 16,7270m (d_3), and 16,1393m (d_1) for confined model. This is when the differences in head at the border are large. In the other case where the distance between R_1 and R_2 is the subject, shown in d_5 in Table 4.1.3, you can see that the differences are quite small. The maximum difference is 4,8762m for confined model and 5,7546m for phreatic model.

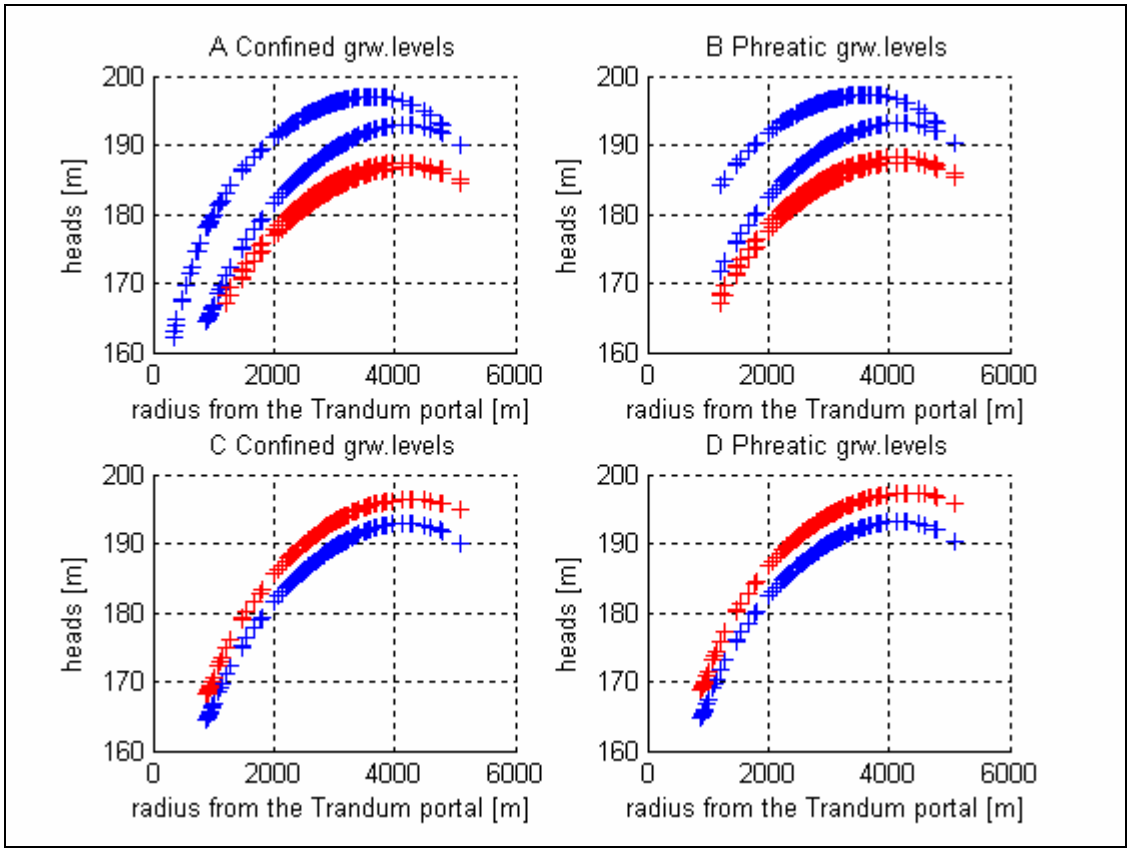

Figure 4.1.3: Heads for the boundary values that were most extreme. ***A****: Show analytical solutions for confined aquifer with the boundary conditions in Table 3.3 that have the maximum difference in head between R_1 and R_2 (nr.8 and nr.9), and for the minimum difference in head between R_1 and R_2 (nr.1 and nr.2).* ***B****: Show analytical solutions for phreatic aquifer with the same boundary conditions as for A.* ***C****: Show analytical solution for confined aquifer with the boundary conditions from Table 3.3. that has the maximum distance between R_1 and R_2 (nr.11) and the minimum distance between R_1 and R_2 (nr.2).* ***D****: Show analytical solution for phreatic aquifer with the same boundary conditions as for C. The maximum are shown as red crosses and the minimum as blue crosses.*

Table4.1.3: The differanses in head for confined and phreatic aquifer, between the boundary conditions listed in Table 3.3 with the largest and the smallest diversity with respect to head at the boundaries; d_1, d_2, d_3 and d_4, and the largest and smallest diversity with respect to the distance between the boundaries R_1 and R_2; d_5.

Differences in head; confined			**Differences in head; phreatic**	
	max m	**min m**	**max m**	**min m**
d_1	16,1393	5,4184	4,4367	-16,0119
d_2	6,2495	40,670	5,7611	4,6370
d_3	14,9034	4,9211	3,0944	-16,7270
d_4	5,5677	2,8310	5,0443	3,2947
d_5	4,8762	3,4106	5,7546	3,9259

d_1= boundary cond. nr.1- boundary condition nr 8.
d_2= boundary cond. nr.2- boundary condition nr 8.
d_3= boundary cond. nr.1- boundary condition nr 9.
d_4= boundary cond. nr.2- boundary condition nr 9.
d_5= boundary cond. nr.11-boundary condition nr 2.
The different boundary conditions are found in Table 3.3.

Table 4.1.4: Differences between calculated heads using different boundary conditions for confined and phreatic aquifer.

Differences in head; confined			**Differences in head; phreatic**	
	max m	**min m**	**max m**	**min m**
dif_1	9,2337	-4,6879	25,4714	0,0116
dif_2	16,7510	-4,6901	16,3928	-4,8083
dif_3	20,8180	0,7307	21,0298	-0,0728
dif_4	19,5820	0,2335	19,6875	-0,5860
dif_5	12,9471	-9,5663	12,1970	-10,5629

dif_1= equation(2.53) with boundary cond. from Table 3.2 - equation (2.53) with boundary cond. nr.1 from Table 3.3.
dif_2= equation(2.53) with boundary cond. from Table 3.2 - equation (2.53) with boundary cond. nr.2 from Table 3.3.
dif_3= equation(2.53) with boundary cond. from Table 3.2 - equation (2.53) with boundary cond. nr.8 from Table 3.3.
dif_4= equation(2.53) with boundary cond. from Table 3.2 - equation (2.53) with boundary cond. nr.8 from Table 3.3.
dif_5= equation(2.53) with boundary cond. from Table 3.2 - equation (2.53) with boundary cond. nr.11 from Table 3.3

Further on the different boundary conditions used in Figure 4.1.3 (the extreme boundary conditions) are compared to the analytical solutions when the boundary conditions from Table 3.2 were used. The results are given in Table 4.1.4. The differences are quite large. The maximum difference for confined is 20,8180m. For the phreatic model the differences are even larger, and the maximum value is 25,4714m. Where there are negative values the models with the extreme boundary conditions have to cross the other models, so at some point they are close to each other. Still there seems to be big variations, but the models that fit the observed heads best seems to be the ones where the nature is simplified and the boundaries are set in the middle of the ravines to a circular limit (Figure 4.1.2).

4.1.3 Analytical solutions in three dimensions

To visualize the analytical solutions, I made a grid and radiuses that are the same as the ones used in the numerical models. In this way the analytical solutions can be illustrated in 3d and it makes it easier to compare with the numerical solutions also visually. The results are shown in Figure 4.1.4 for the confined solution and in Figure 4.1.5 for the phreatic solution. These two illustrations confirm the similarity of the two models. In the 3d illustrations you can see that all of the ground water levels with the same radius are similar to each other. This is because the diagonal solutions from chapter 4.1.1 are transferred into a three dimensional grid, and for this analytical solution you will always have the same ground water levels at the same radius from the origin as mentioned in chapter 3.1.7. The blue parts in the front are the area near the inner boundary R1 and have the lowest ground water level. The ground water level then rises before it gets to the ground water divide and decreases in height before it reach the outer boundary R_2. The groundwater divide can be calculating by using equation (2.60) for the phreatic solution and equation (2.58) for the confined solution. The results for the confined model was that the ground water divide was situated at a radius of 3220,7m and for the phreatic model it was situated at a radius of 3238,1m.This seem to fit with the illustrations both in the 3d illustrations and in the illustrations of Figure 4.1.1

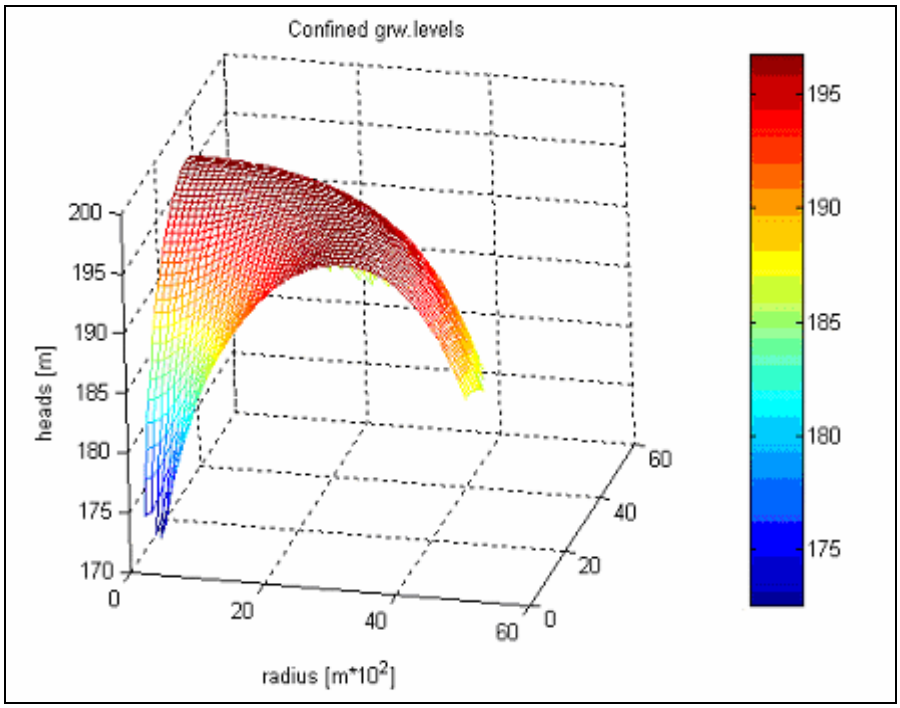

Figure 4.1.4: Analytical model with boundary conditions from Table 3.2.

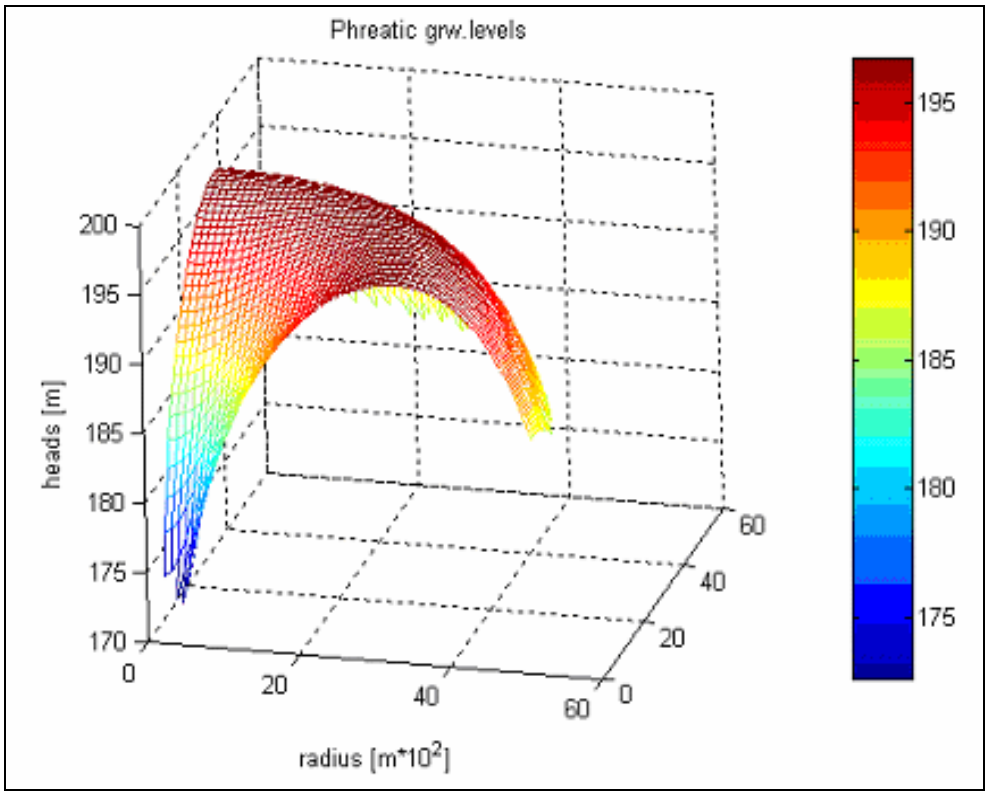

Figure 4.1.5: Analytical model with boundary condition from Table 3.2.

4.2 Numerical models

4.2.1 Confined models

The numerical model for confined ground water levels where the inner and outer boundaries have a circular shape as in the “doughnut”-equation (2.53) used in the analytical solution is shown in Figure 4.2.2. The highest head is 194,9164m (Table 4.2.2). The numerical confined model with circular boundaries is shown in Figure 4.2.2. The highest levels of the heads are lying on 194,9164m (Table 4.2.2). The numerical confined model where the ravines are considered is shown in Figure 4.2.3.The shapes of the ravines are visible at the boarders. For this model the highest level of the heads are lying on 190,4308m(Table 4.2.2). Comparing the two models the ground water divide are located closer to the outer boarder for the models including the ravines. The ground water level along the boundaries are lying lower in this model compared to the one with the circular boundaries, this is so because the constant heads at the boundaries are lower in this model. This fits to the fact that the groundwater levels in the aquifer were at its lowest when the hydrogeological map was made. Figure 4.2.3 show the presentations of the confined numerical models from PMWIN with contours that represent the ground water levels.

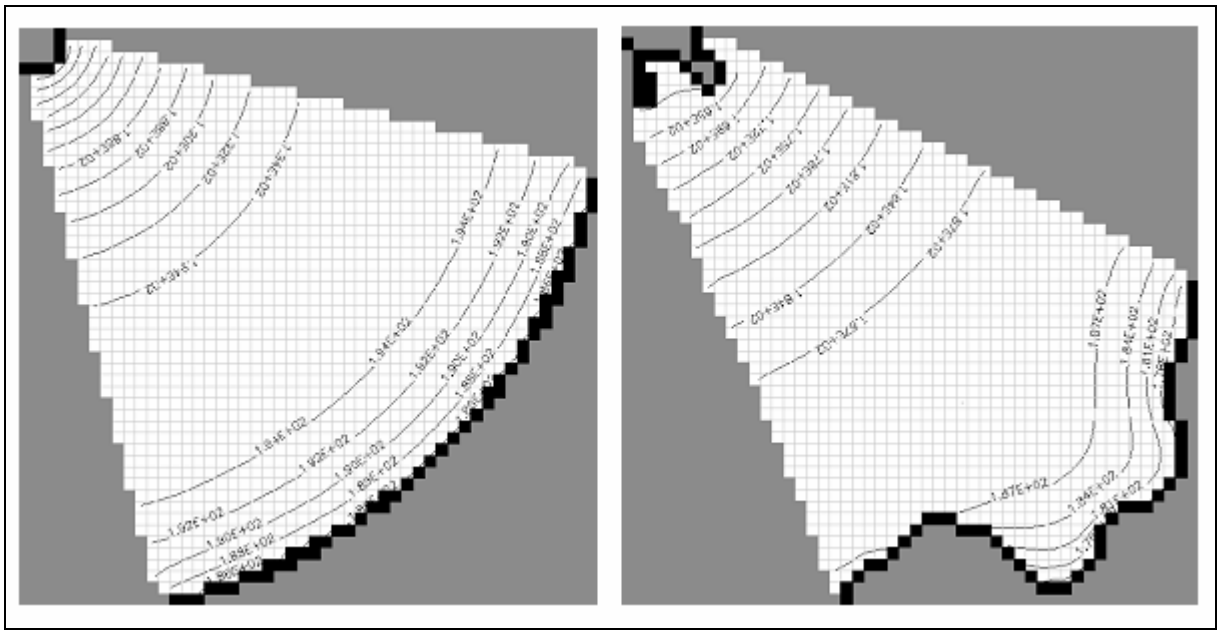

Figure 4.2.1 Numerical solution for confined groundwater levels. The contours show the ground water level.

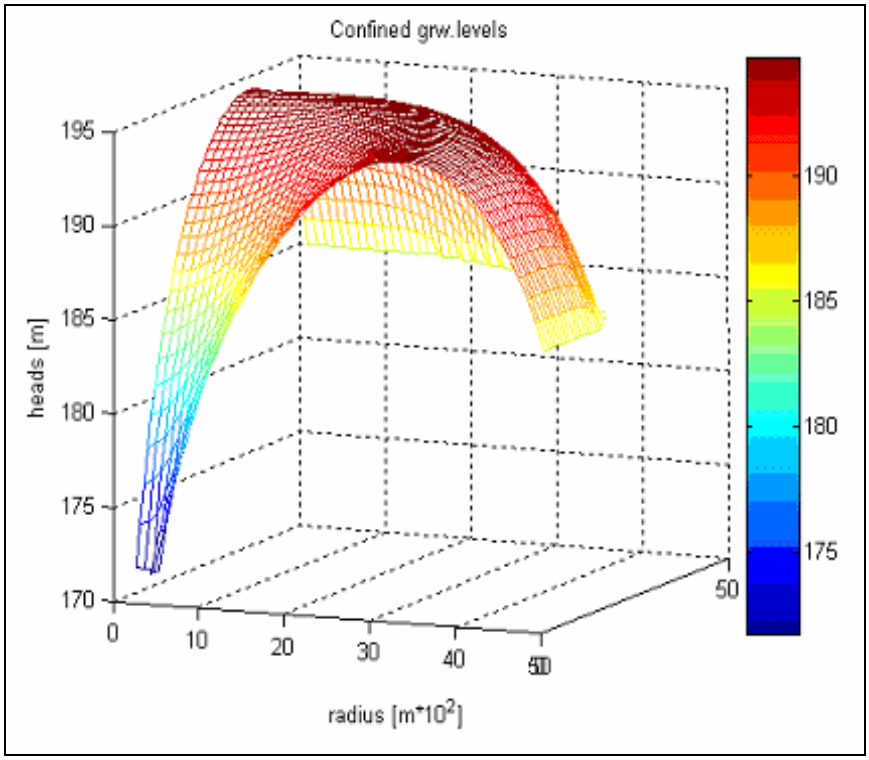

Figure 4.2.2: Numerical solution of confined ground water levels where the boundaries of the aquifer follow the circular "doughnut"-form used in the analytical solution.

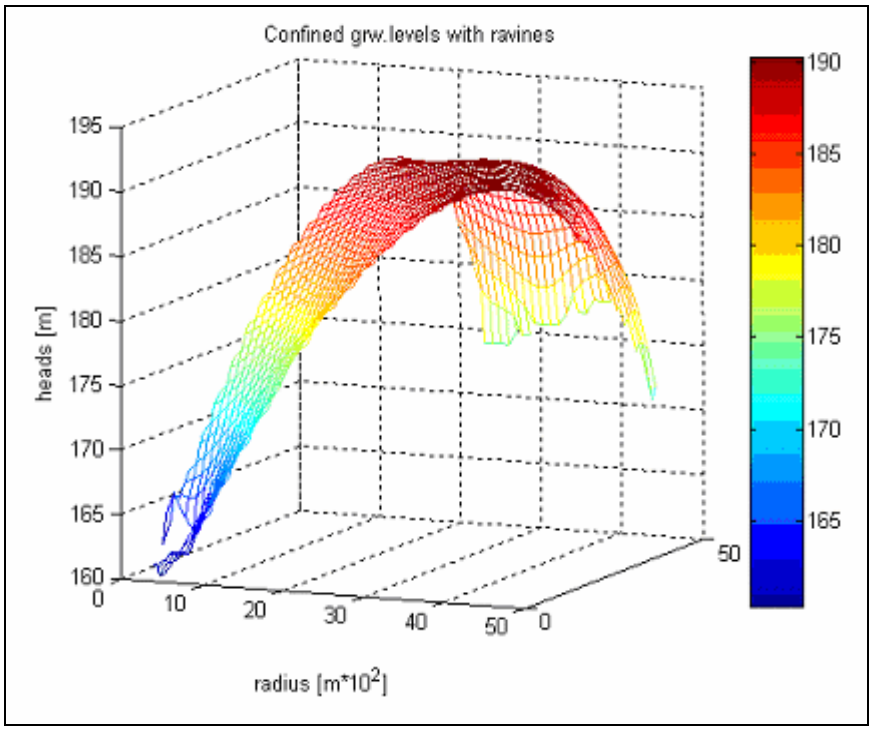

Figure 4.2.3: Numerical solution of confined ground water levels where the ravines are considered.

4.2.2 Phreatic models

The numerical model for phreatic ground water levels where the inner and outer boundaries have a circular shape as in the "doughnut"-equation (2.56) used in the analytical solution is shown in Figure 4.2.5. The highest heads are 196,0135m(Table 4.2.2). The numerical phreatic model where the ravines are considered is shown in Figure 4.2.6. Also here the shapes of the ravines are visible at the boarders. For this model the highest level of the heads are 191,9772m (Table 4.2.2). Comparing the two models the ground water divide is closer to the outer boarder in the model including the ravines as in the confined case. The ground water level along the boundaries are lying lower in this model compared to the one with the circular boundaries, this is so because the constant heads at the boundaries are lower in this model. Figure 4.2.4 show the presentations of the confined numerical models from PMWIN with contours that represent the ground water level.

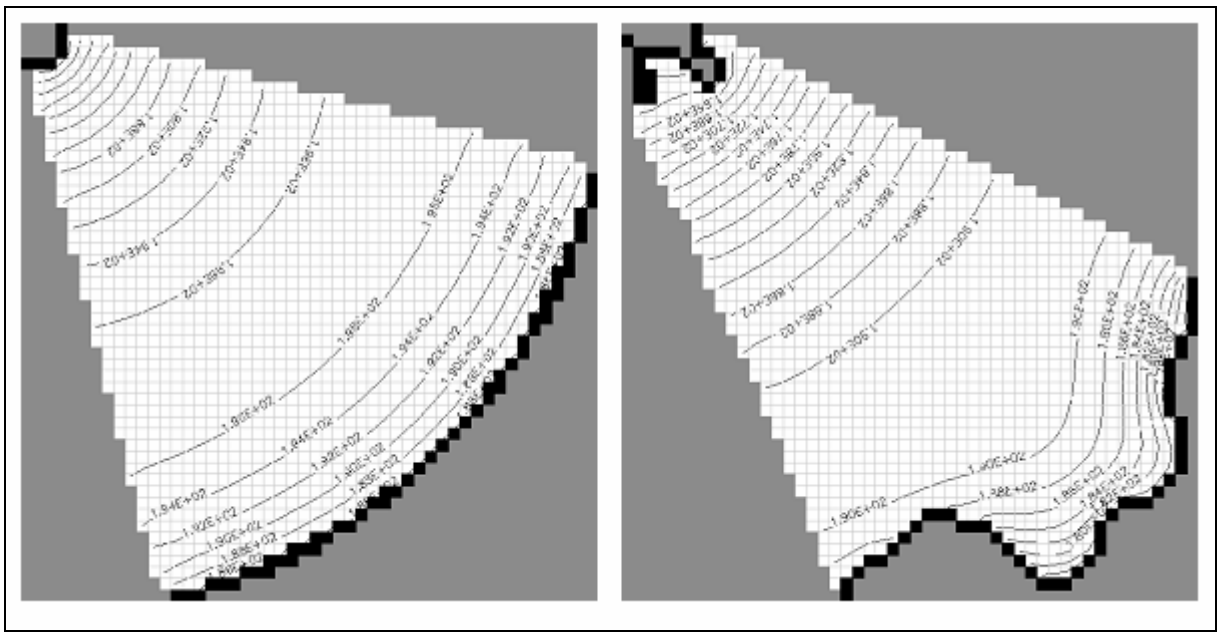

Figure 4.2.4: Numerical solution for phreatic groundwater levels. The contours show the ground water level.

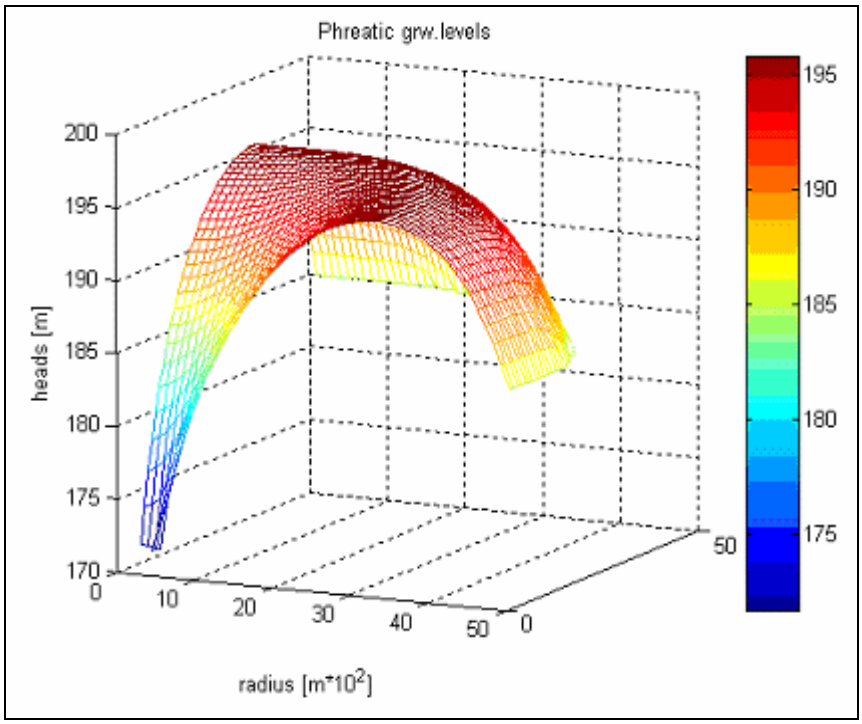

Figure 4.2.5: Numerical solution of phreatic ground water levels where the boundaries of the aquifer follow the circular "doughnut"-form used in the analytical solution.

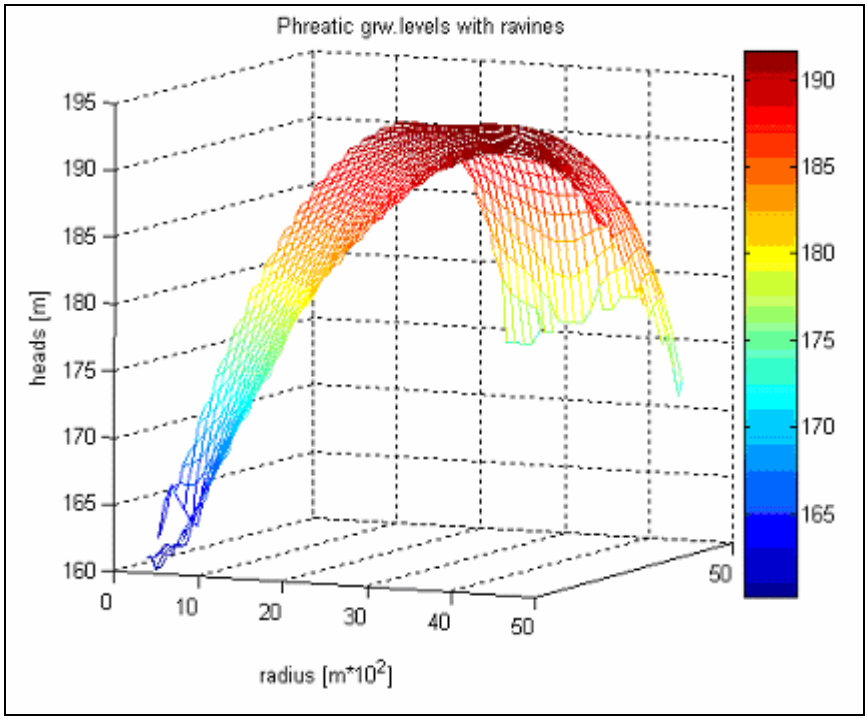

Figure 4.2.6: Numerical solution of phreatic ground water levels where the ravines are considered.

4.2.3 Comparing confined and phreatic models

To compare the numerical solutions with each other mathematically, the heads in the solution from the models with circular "doughnut"-boundaries were subtracted from the model that includes the ravines. The differences are illustrated in Figure 4.2.7 and Figure 4.2.8.The maximum- and the minimum value of the differences in heads between the models are listed in Table 4.2.1. The maximum heads of the different models are listed in Table 4.2.2. Where the differences are positive, the ground water levels of the model with circular boundaries are higher than for the models including the ravines. Where the differences are negative, the models with the circular boundaries have ground water levels lower than the models with the ravines. The area where the differences are close to zero are located close to the outer boundary, and are shown as the areas with blue colours in Figure 4.2.7 and Figure 4.2.8.

Table 4.2.1: Differences in heads between confined and phreatic numerical solutions.

Comparing numerical models		
	Confined	**Phreatic**
max(d) m	19,0370	20,1035
min(d) m	-4,0291	-5,1601

d = heads model with "doughnut"-form – heads model with ravines

Table 4.2.2: Maximum heads for confined and phreatic numerical solutions

	Confined	**Phreatic**
max head m (circular)	194,9164	196,0135
max head m (ravines)	190,4308	191,9772
difference m (circular – ravines)	4,4856	4,0363

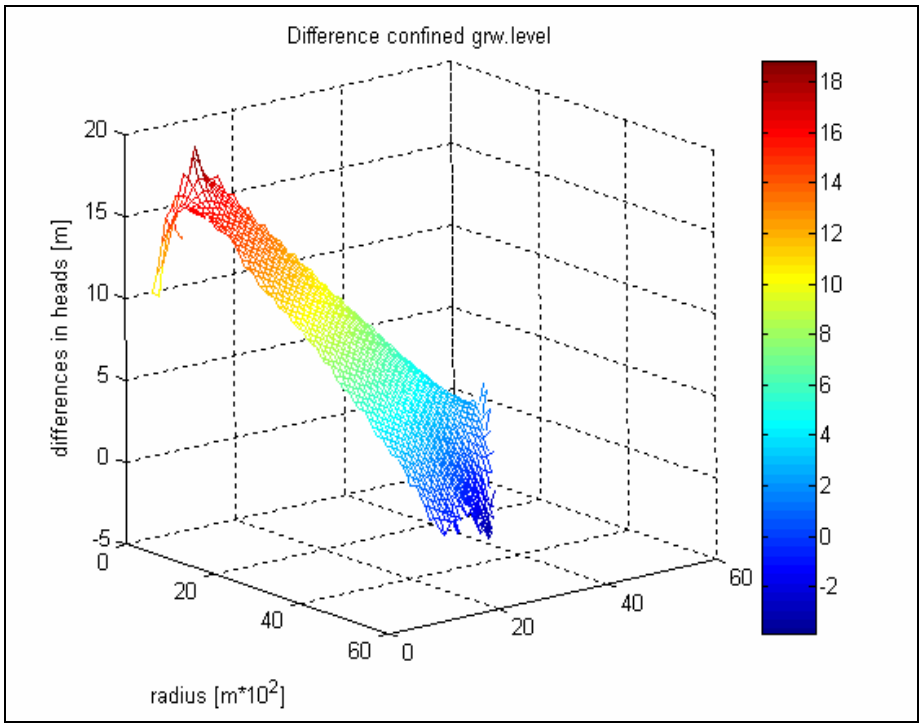

Figure 4.2.7: Differences in confined ground water levels between the model with circular boundaries and the model that consider the ravines.(model with circular boundaries - model with ravines)

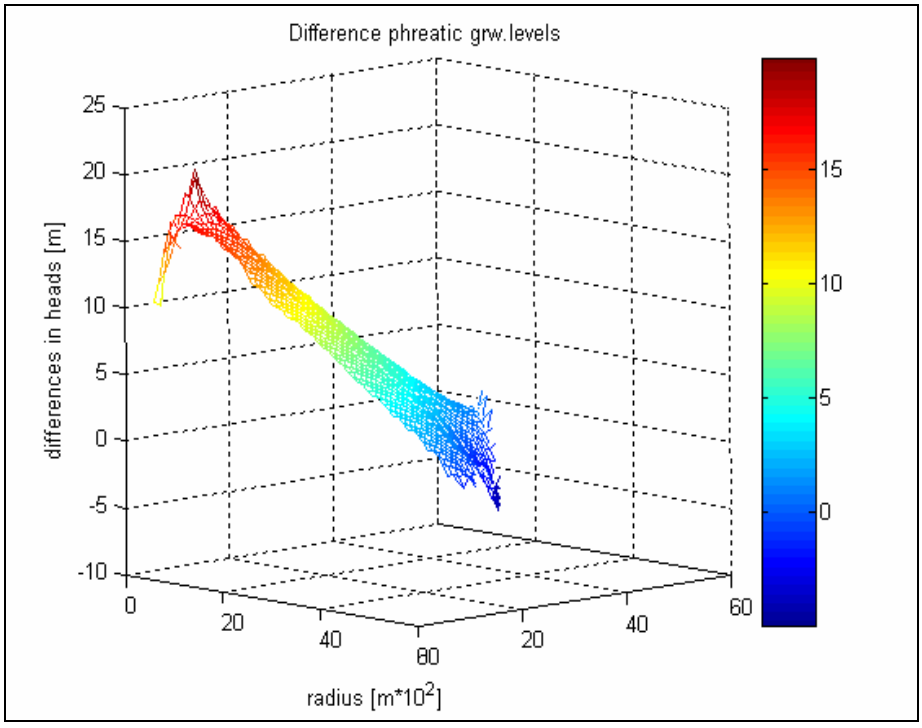

Figure 4.2.8: Differences in phreatic ground water levels between the model with circular boundaries and the model that consider the ravines (model with circular boundaries - model with ravines).

For the confined models the maximum difference is 19,2688m, while the minimum difference is –4,0291m. This is illustrated in Figure 4.2.7, and it shows that the maximum differences are close to the inner boundary, while the minimum difference is close to the outer boundary of the models. The big differences in the heads close to the inner boundary may be due to the grid in the models that may be too coarse at the inner boundary to represent the environment and fit the ravines good enough. The differences in the phreatic models are illustrated in Figure 4.2.8, and the same trends as for the differences in the confined models are present. The maximum difference is 20,1035m and the minimum difference is –5,1601m (Table 4.2.1). At the edges of the numerical models there may be some errors due to the irregular grid used in PMIN. The farther away from the boarders of the model the less error is obtained. When looking at the differences in the diagonal of the matrix that represent the output of the heads from PMWIN, illustrated in Figure 4.2.9, there is less difference between the models.

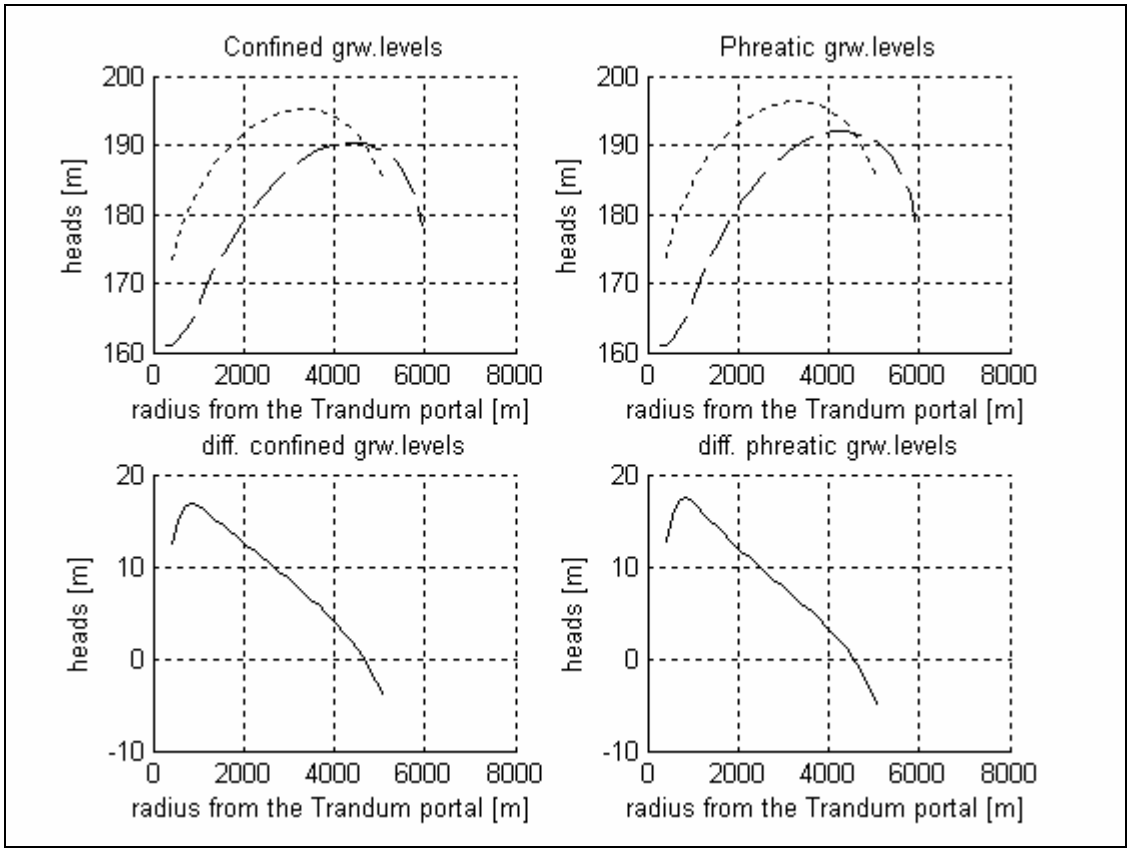

Figure 4.2.9: Comparing the numerical models with the circular boundaries with the models that consider the ravines. Dotted lines represent the diagonal of the models with circular boundaries, the dashed lines represent the diagonal of the models that consider the ravines at the boundaries. The solid lines display the difference between the two models for phreatic-and confined solutions. The graphs represent the diagonal of the output matrix from PMWIN.

The maximum for the differences between the confined solutions are 16,8583m and for the phreatic solution; 17,4869m. The minimums are still the same. Further on it seems like the ground water divide for the models that represent the ravines (dashed lines) have been displaced closer to the outer boundaries in consideration of the models with the circular boundaries (dotted lines). The shape and the level of the ground water table are quite similar, but the position differs. The greatest differences are to be found close to the inner boundary and this is concurrent with the results illustrated in Figure 4.2.7 and Figure 4.2.8. If we compare these results with the maximum of the heads for the four models listed in Table 4.2.2, you can see that the differences between the highest heads for the models with circular boundaries and for the highest heads in the model that consider the ravines, the difference is very small compared to the maximum and the minimum difference between the two models; 4,4856m for the confined models and 4,0363m for the phreatic models. This means that the groundwater levels don't differ as much in height but in position, and that is what makes the differences listed in Table 4.2.1 that large.

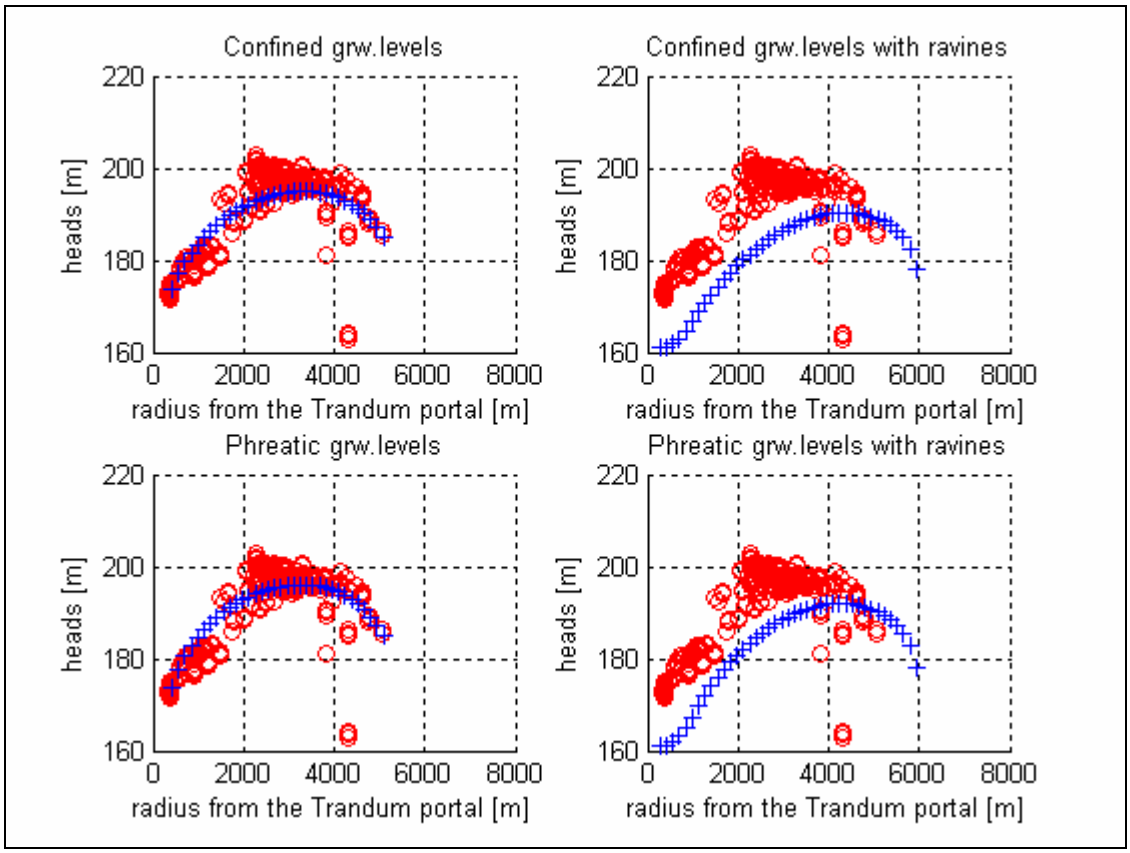

Figure 4.2.8: The numerical models compared with the observed heads. The red rings represent the observed heads and the blue crosses the numerical calculated heads (the diagonal of theoutput matrix from PMWIN).

In Figure 4.2.8, the numerical solutions of the heads are plotted together with the observed heads. For the numerical solution of confined and phreatic ground water levels with circular boundaries the calculations fits well with the observed heads, while the calculated heads for confined and phreatic numerical solutions where the ravines are considered there are lower heads than the main part of the observed heads.

4.3 Comparind numerical and analytical solutions

When comparing the numerical and the analytical models I used the numerical solutions where there is circular, "doughnut"-form of the boundaries.
To compare the two models the numerical model were subtracted from the 3d analytical model. The results are shown in Table 4.3.1 and in Figure 4.3.1 for the confined models and in Figure 4.3.2 for the phreatic models. The maximum difference for the confined models is 2,6561m and the minimum is –0,7709m. From Figure 4.3.1 you can see that the major part of the differences are positive, hence the analytical solution has higher groundwater levels through the aquifer compared to the numerical solution. The same trend is found for the phreatic models where the maximum difference is 2,0723m and the minimum is –0,9449m. In Figure 4.3.1 and in Figure 4.3.2 the differences between the models are illustrated. For the confined case, the higest differences are found from the inner boarder and out to about a radius of 3000m, illustrated by the red colour. In the confined case, the differences are lower, but they are also to be found close to the inner boarder

Table 4.3.1: Differences between numerical and analytical solutions

Differences analytical and numerical solutions		
	Confined	**Phreatic**
max(d) m	2,6561	2,0723
min(d) m	-0,7709	-0,9449

d = heads analytical – heads numerical

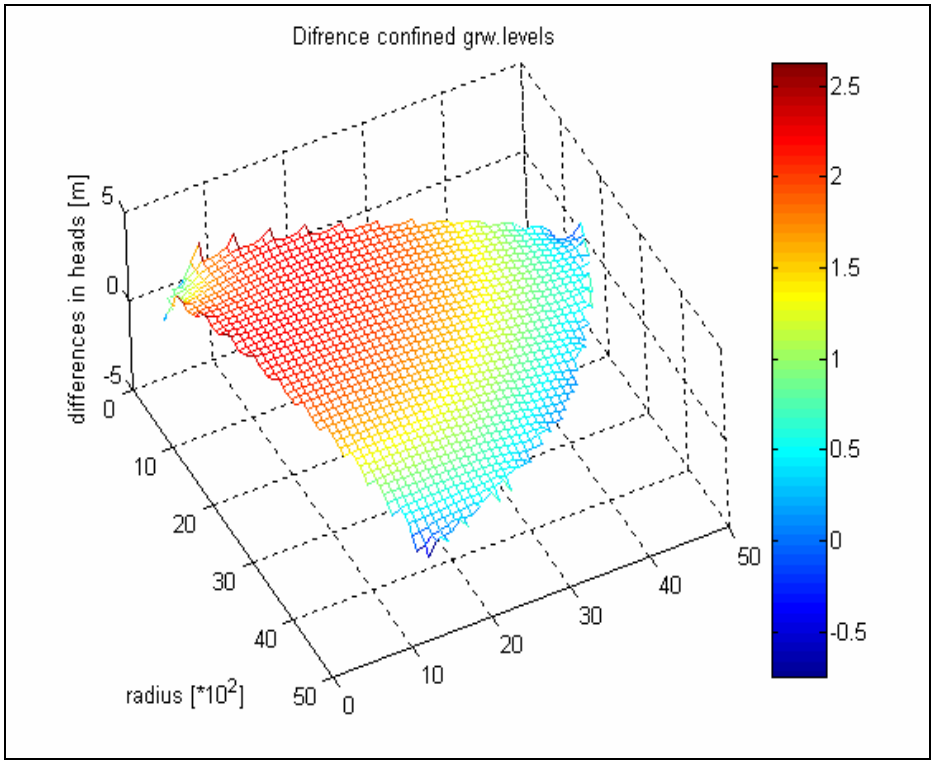

Figure 4.3.1: Difference in confined ground water level between analytical and numerical solutions (analytical solution – numerical solution).

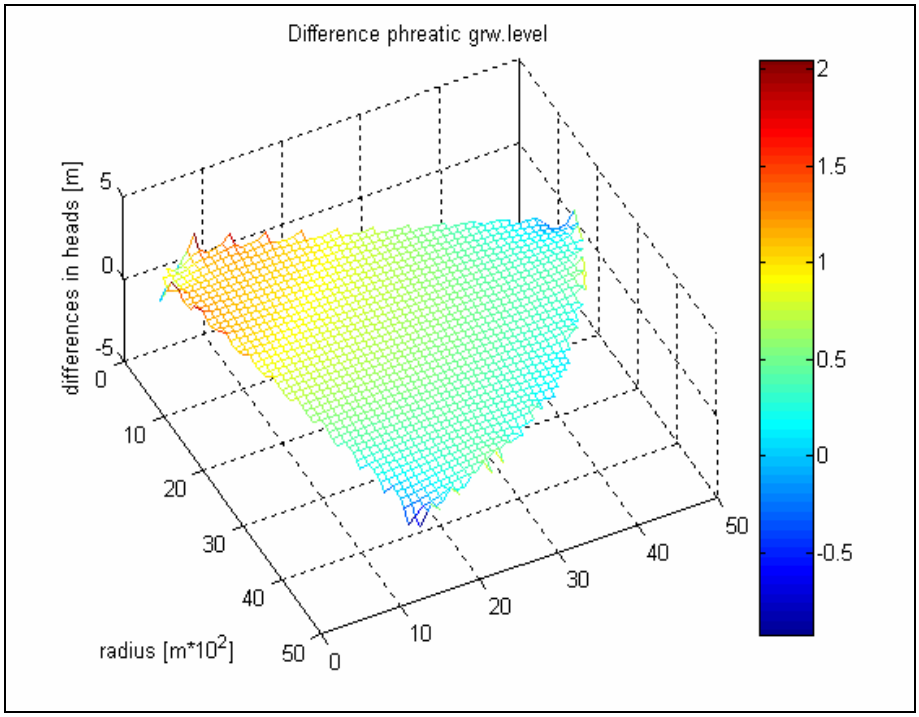

Figure 4.3.2: Difference phreatic ground water level between analytical and numerical solutions (analytical solutions – numerical solutions).

Table 4.3.2: Differences between the diagonal of the3d analytical solution and the diagonal of the PMWIN output matrix of the numerical solution.

Differences analytical and numerical solution (diagonal)		
	confined	**phreatic**
max (d)	2,1760	1,1017
min (d)	0,1492	0,1607

d = analytical solution – numerical solution

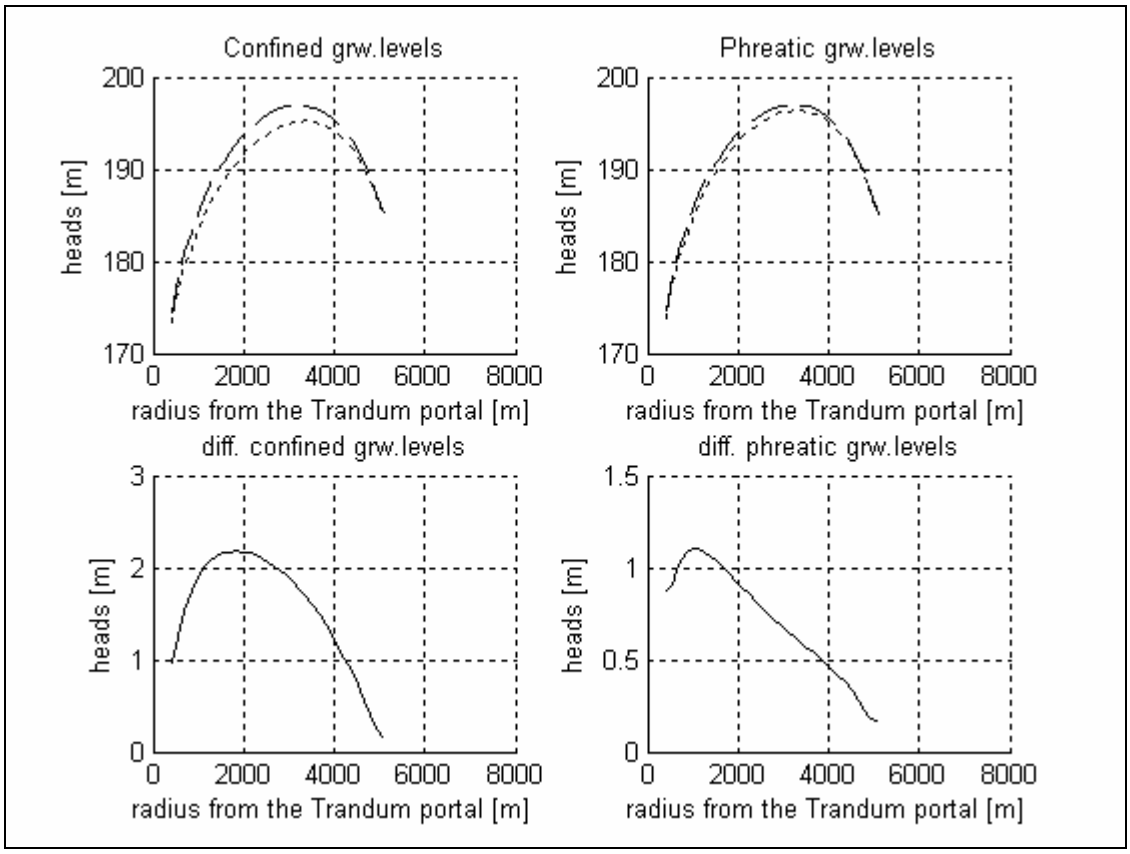

Figure 4.3.3: Comparing the numerical models with the analytical models for confined and phreatic aquifers. The dotted lined represent the numerical solutions and the ashed lines represent the analytical solutions. The solid lines are the difference in heads between the analytical and the numerical models (analytical model – numerical model). The results are the diagonal of the output from PMWIN for the numerical models, and the diagonal of the 3d numerical solution for the analytical models.

Along the boarders of the model there are some higher values, this may be because the PMWIN uses a regular grid. The farther away from the edges of the model you get the less affected the models get by this error caused by the grid. To calculate the differences in the middle of the model the diagonal of the output matrix from PMWIN and the diagonal of the 3d analytical solutions are used do calculate the differences and make 2d graphs of the differences. The results are illustrated in Figure 4.3.3. The diagonal of the analytical solutions are showed as dashed lines and the diagonal of the numerical solutions are showed as dotted lines. The differences are represented as a solid line. The analytical and the numerical models have minor differences when comparing the diagonals of the models For the confined models the differences are between 2,1760m and 0,1429m, and for the phreatic models the differences are between 1,1017m and 0,1607m (Table 4.3.2). The largest differences are found close to the inner boundaries, as in the previous models presented in 3d.

CHAPTER 5

DISCUSSION

When working with analytical models there are important to remember that analytical models and their solutions does not contain all of the details of an aquifer, but the main character of the aquifer may be produced.

The analytical models carried out using the “doughnut” equation and the optimal parameters show that there are just minor differences in ground water heads between the confined and the phreatic solution. The reason is that the two parameters involved in the equations are optimized with respect to the observed groundwater heads. Further on when comparing these two analytical solutions with the observed heads, it shows that it is possible to model the trend in the data with an analytical equation.
One of the purposes of this thesis was to evaluate the impact of the ravines. Reading out new boundary conditions corresponding to the location of the ravines from the hydrogeological map of Østmo (1976a) and calculating new analytical models gave an indication on how large the influence of the ravines may have on the ground water level in the aquifer. Still it is important to remember that hey do not represent the whole aquifer, just the radius where the boundary conditions are red out of the map. The models gave results that were lower than the observed heads and the analytical solutions made by optimal parameters. This may be due to the low ground water levels that were present when the map was deduced. It is important to take this into account when looking at the differences between the models. The calculations of heads where the boundary conditions were at its most extreme showed that the largest differences were found when there was big difference in heads between the inner and the outer boundary. The maximum difference was up to 20-30m. The length between the inner

and the outer boundary did not have the same effect. This may be due to the large distance between the inner and the outer boundary in the first place.
The analytical models using the optimal parameters were also compared with the analytical models with the most extreme boundary conditions. Calculating the differences showed that the differences were large, for some models over 30m. The different boundary conditions have a large effect on the models, but they may not have that large effect on the entire aquifer and the ground water level in it.
When comparing the extreme models with the observed heads all of the models have lower ground water levels than the observed heads, as expected. The highest mean difference was about -14m for the confined version of the model and –21,7m for the phreatic version.

The numerical models were carried out in PMWIN, and the differences between the models with circular boundaries and the models with the ravines included shows that the models with the ravines included have generally a lower ground water table than the models with the circular boundaries. When comparing the different models and calculating the differences between the models without and with ravines it shows that there are differences up to 19-20m between the models. This is about 10m lower than the most extreme differences found in the numerical models. When the differences are calculated by using the diagonal of the output matrix from PMWIN, the differences are a little less. Still they are significant. But the differences in the maximum heads in the different models are not that large, only between 4,0-4,5m. The diagonal of the output matrices from PMWIN also show that there seem to be a displacement of the ground water levels and the ground water divide toward the outer boarder when the ravines are considered. To see how the models fits compared to the observed heads it is the models with the circular boundaries that differ least, and fits well into the trend of the observed heads. Hence, the numerical models with the circular boundaries are the ones that seem to fit the field observations best.

The numerical and the analytical solutions with the circular of the boundaries were compared with each other, and the result showed that maximum difference in between the analytical and the numerical models were 2,6561m for the confined models and 2,0723m for the phreatic models. These results show that there are just a minor difference between the numerical and the analytical models where the boundaries follow the “doughnut” form.

From the foregoing it seems like the models with the circular “doughnut” form are the models that fit the observations done in the field the best, and that considering the ravines does not make the solutions any better, and may just give a lot of extra work to make the models. The analytical models gives good solutions that fits well to the field observations and are obviously a good tool to get an easy and direct insight into the physical conditions of the aquifer. In the numerical simulations, more details is included and a better reproduction of the observed heads are achieved. The numerical models are very sensitive to the boundary conditions and there is easy to make mistakes. On the other hand if you have an analytical model to support you in the work and the construction of a numerical model, such mistakes can be avoided.

CHAPTER 6

CONCLUSION

In delta structures as a Gilbert type delta, observations indicates that the flow of ground water in such structures may be simplified to a one dimensional flow due to axial symmetry of the aquifer, such as in the Trandum delta. With this assumption the ground water level can be calculated by using the "doughnut" equation (Kitterød 2004a).

The analytical solutions using the "doughnut" equation on the Trandum delta gave results that fitted well with the observations done in the field. When carrying out the numerical model with the same boundary conditions as for the analytical models over the same area, the solutions were almost similar to the analytical ones.

The eleven analytical models made with boundary conditions from the hydrogeological map did show that the differences were quite big when the ravines were considered, but it is difficult to say how much the total influence on the ground water level they have. There may be better ways to calculate their impact on the aquifer analytically.

The numerical models considering the ravines did not fit the observed heads as well as the ones where the boundaries of the aquifer were simplified to a circular boundary. The model made in this thesis did not take all of the details that may be considered in a numerical model into account and the results will probably be better if enough details are put into the model.

To use analytical modelling to obtain the general physical conditions in an aquifer may give good enough results for a start, and the models and the solutions may work as a guideline for further work in the same area, for instance for numerical modelling.

References

1. Boggs, S., *Principles og Sedimentology and Stratigraphy*, ISBN 0-02-311792-3, 1995

2. Chiang,W. - H. & Kinzelbach, W., *3D-Groundwater Modeling with PMWIN, ISBN 3-540- 67744-5, 2001*

3. Darcy, H., *Les Fountaines Publiques de la Ville de Dijon.* Victor Dalmont, Paris. 1856

4. Domenico, P.A. & Schwartz, F.W. *Physical and Chemical Hydrogeology,* ISBN 0-471-59762-7, 1990

5. Dupuit, J., *Etudes Theoriques et Practiques sur le Mouvement des Eaux dans les Canaux Decouverts et a Travers les Terrains Permeables.* Dunod, Paris. 1863

6. Engen, T., *Stochastic interpolation of groundwater levels in an ice-contact delta at Gardermoen (in Norwegian, Cand. Scient thesis, University of Oslo, department of Geophysics), 1995*

7. Forchheimer, P., *Ueber die Ergiebigkeit von Brunnen-Anlagen und Sickerschlitzen.* Architekt. Ing. Ver. Hannover 32:539-563. 1886

8. Haitjema, H.M., *Analytic element modelling of ground-water flow*, ISBN 0-120316550-4, 1995

9. Henriksen, H. & Nielsen, J.T., *Innføring i Hydrogeologi, compendium HiSF.* 1996

10. Jørgensen, P., Sørensen, R. & Haldorsen, S. *Kvartærgeologi,* ISBN 82-529-2107-8, 1997

11. Jørgensen, P. & Østmo, S.R. *Hydrogeologi in the Romerike area, southern Norway*. Nor. geol. unders. Bull. 418, 19-26. 1990

12. Jørgensen, P., Stuanes, A.O. & Østmo, S.R., *Aqueous geochemistry of the Romerike area, southern Norway*. Nor. geol. unders. Bull. 420, 57-67. 1991

13. Kitterød, N.O., *Dupuit-Forchheimer solutions for radial flow with linearly varying hydraulic conductivity or thickness of aquifer,* Water Resources Research, VOL. 40, W11507, 2004a

14. Kitterød, N.-O., Estimating runoff by analytical modeling of groundwater levels (Workshop on Groundwater and Global Change, Aas Norway) 2004b

15. Reading, H.G., *Sedimentary Environments: Processes, Facies and Stratigraphy*, ISBN 0-632-03627-3, 2002

16. Skinner, B.J. & Poerter, S.C., *The Dynamic Earth*, ISBN 0-471-59549-7, 1995

17. Tuttle, K.J., *Sedimentological and hydrological characterisation of a raised icecontact delta - the Preboreal deltacomplex at Gardermoen, southestern Norway*, Ph.D. thesis, Dept. of Geology, University of Oslo, Nov. 1997

18. US Geological Survey's Water Science for Schools site, [Viewed 05/05/05].www.usgs.gov.

19. Worsley, R., Thorsen, T. & Aagaard, P.*G250 Grunnvann – en praktisk innføring, Compendium UiO.* 2003

20. Østmo, S.R., *hydrogeologisk kart over Øvre Romerike;grunnvann i løsavsetninger mellom Jessheim og Hurdalsjøen - M. 1:20 000.* Norges geologiske undersøkelse, 1976a

21. Østmo, S.R., *Gardermoen, kvartærgeologisk kart C QR 051052-20 , M 1:20 000*. Norges geologiske undersøkelse, 1976b

22. Østmo, S.R., Kort beskrivelse til kvartærgeologisk kart, Gardermoen 1:20 000, C QR 051 052-20 og hydrogeologisk kart, Øvre Romerike 1:20 000. Int.Rapport. Norges geologiske undersøkelse, 1976c

Appendix

Table 1

Coordinates read off hydrogeological map (Østmo 1976a), Z represents the head at the points on the map. Represent the points at the outer boundary.

X	Y	Z (m)
614,68	6676,06	186
614,90	6675,72	188
614,00	6674,62	172
614,80	6674,12	178
615,04	6673,50	178
616,28	6673,08	176
616,28	6672,74	174
616,64	6672,66	174
616,68	6672,62	174
616,80	6671,82	172
617,12	6671,41	172

Table2

Coordinates read off hydrogeological map (Østmo 1976a), Z represent the head at the points on the map. Represent the points at the inner boundary.

X	Y	Z(m)
619,44	6677,84	160
619,02	6677,56	162
619,06	6677,54	162
619,26	6677,54	160
619,38	6677,60	160
619,16	6677,14	163
619,38	6677,12	163
619,14	6676,92	166
619,18	6676,98	166
619,42	6677,30	162
619,46	6677,30	162

Table 3

Coordinates for the inner and outer boundary for the models with ravines in PMWIN, together with the constant heads in the nodes.

X	Y	constant head (m)	X	Y	constant head (m)
50	23	174	7	1	162
50	24	174	4	2	162
50	25	174	7	3	164
50	26	174	8	3	166
50	27	175	9	4	164
42	28	175	9	5	163
49	29	175	8	6	163
48	30	176	7	5	162
48	31	176	6	4	161
48	32	176	5	3	160
48	33	176	4	3	160
48	34	177	3	3	161
49	35	177	2	3	161
49	36	177	2	4	161
49	37	178	3	5	162
49	38	178	2	6	162
49	39	178	3	7	162
48	40	178	2	7	162
47	41	178	2	6	162
46	42	178	2	5	162
45	42	178	1	2	160
44	42	178			
43	43	178			
42	44	178			
42	45	177			
42	46	176			
41	47	175			
40	48	174			
39	49	173			
38	49	172			
37	49	174			
36	48	176			
35	47	178			
34	46	180			
33	45	182			

32	45	184			
31	44	186			
30	44	186			
29	43	187			
28	43	188			
27	43	188			
26	44	188			
25	45	188			
24	46	187			
23	47	186			
22	47	186			
21	48	186			
20	49	186			
20	50	186			

SCRIPT 1

```
%CONFINED AQUIFER
%
% Script to solve an analytical solution of groundwater heads at the
% Trandum delta using the "Doughnut-equation", with constant heads, and
% heads as an function of radius. Precipitation is entered as an internal
% source. The thickness of the aquifer is an linear function of radius.

% Due to axis symmetry, the flow equation can be solved in 1-D. This
% corresponds to a !-D Poisson equation with Diriclet conditions on both
% sides of the doughnut.

%         A1              A2
% phi = -------{L1}  -  -------{L2}
%       A1-A2           A1-A2
%
%
% where:
%
%      L1 = (N/2ka)*(r-R2) + (N/2k)*B2 + phi_2
%      L2 = (N/2ka)*(r-R1) + (N/2k)*B1 + phi_1
%
%         A1 = {1/(H1 + a*R1)}*ln((H1*R1 - a*R1*(r - R1))/(H1*r))
%         A2 = {1/(H2 + a*R2)}*ln((H2*R2 - a*R2*(r - R2))/(H2*r))
%         B1 = {(H1+a*R1)/(a*a)}*ln[(H1-a*(r-R1))/H1]
%         B2 = {(H2+a*R2)/(a*a)}*ln[(H2-a*(r-R2))/H2]
%
%     and:
%
%      H(r) = H1 - a*(r-R1)
%
%        where
%          a = (H1 - H2)/(R2 - R1)
%
%       and H1 and H2 is the thickness of the aquifer at R1 and R2
%
%                                        H2
%        H1                             phi2
%        phi1
% -------|--------------------------------|-------> r
%        R1                               R2
%

% r = distance from origo
% R1 = distance from origo to inner boundary
% R2 = distance form origo to outer boundary
% phi1 = inner boundary condition, equal to head at inner boundary
% phi2 = outer boundary condition, equal to head at outer boundary
% N = infiltration rate
% k = average hydraulic conductivity
% H1 = aquifer thickness at R1
% H2 = aquifer thickness at R2


%Use the position of the observation wells at Trandum to find the different
%radius' that I want to use in my calculations. This makes it easy to
%compare the analytical solution with the observations done in the field.

tr = load('Trandum_corr.obs');
```

```
X = tr(:,1);
Y = tr(:,2);
heads = tr(:,3);

[n,m] = size(heads);

Trandum_origo_x = 8400.00;
Trandum_origo_y = 7150.00;

r = sqrt((X-Trandum_origo_x).^2 + (Y-Trandum_origo_y).^2);

%Use the optimal values found by calculation. N is based on the spacific
%discharge of the river Risa.

H1 = 301.86;
H2 = 66.19;
k = 1.727901e-5;
phi1 = 171.50;
phi2 = 185;
R1 = 336;
R2 = 5100;
N = 1.266730e-8;

a = (H1 - H2)/(R2 - R1);

A_1  = (1/(H1 + a*R1)) * log((H1*R1 - a*R1*(r-R1))./(H1*r));
A_2  = (1/(H2 + a*R2)) * log((H2*R2 - a*R2*(r-R2))./(H2*r));

B_1  = ((H1+a*R1)/(a^2)) * log((H1 - a*(r-R1))/H1);
B_2  = ((H2+a*R2)/(a^2)) * log((H2 - a*(r-R2))/H2);

ledd_1 =   ((N/(2*k*a)) .* (r-R2) + N/(2*k) .*B_2 + phi2) .* A_1;
ledd_2 =   ((N/(2*k*a)) .* (r-R1) + N/(2*k) .*B_1 + phi1) .* A_2;

AA = ledd_1 - ledd_2;

phi = AA./(A_1 - A_2)

% graph of the analytical head values calculated

xlabel('radius from the Trandum portal [m]'),
ylabel('heads [m]'),
title('Confined grw.levels'), grid;
hold;

plot(r,phi,'b+');

%compare with observed heads:
dif_phi= phi-heads;
mean_dif_phi=mean(dif_phi)
max_dif_phi=max(dif_phi)
min_dif_phi=min(dif_phi)
std_dif_phi=std(dif_phi)
```

SCRIPT 2

```
%UNCONFINED AQUIFER
%% Script to solve an analytical solution of groundwater heads at the
% Trandum delta using the "Doughnut-equation", with constant heads, and
```

```
% heads as an function of radius. Precipitation is entered as an internal
% source. The conductivity of the aquifer is an linear function of radius.

% Due to axis symmetry, the flow equation can be solved in 1-D. This
% corresponds to a !-D Poisson equation with Diriclet conditions on both
% sides of the doughnut.
%
% UNCONFINED:
%
%            alpha_1                    alpha_2
% h^2 = -----------------{L1}  -  -----------------{L2}
%       alpha_1-alpha_2           alpha_1-alpha_2
%
%
% where:
%
%      L1 = (N/b)*(r-R2) + (N)*beta_2 + h_2*h_2
%      L2 = (N/b)*(r-R1) + (N)*beta_1 + h_1*h_1
%
%         alpha_1 = {1/(k1 + b*R1)}*ln((k1*R1 - b*R1*(r - R1))/(k1*r))
%         alpha_2 = {1/(k2 + b*R2)}*ln((k2*R2 - b*R2*(r - R2))/(k2*r))
%
%
%         beta_1 = {(k1+b*R1)/(b*b)}*ln[(k1-b*(r-R1))/k1]
%         beta_2 = {(k2+b*R2)/(b*b)}*ln[(k2-b*(r-R2))/k2]
%
%     and:
%
%      k(r) = k1 - b*(r-R1) for an open/phreatic/unconfined aquifer
%
%        where
%          b = (k1 - k2)/(R2 - R1)
%
%       and k1 and k2 is hydr. conductivities at R1 and R2
%
%                                        k2
%        k1                              h2
%        h1
% -------|---------------------------------|-------> r
%        R1                               R2
%
% r = distance from origo
% R1 = distance from origo to inner boundary
% R2 = distance form origo to outer boundary
% h1 = inner boundary condition, equal to head at inner boundary
% h2 = outer boundary condition, equal to head at outer boundary
% k1 = hydraulic coductivity at inner boundary
% k2 = hydraulic coductivity at outer boundary


%Use the position of the observation wells at Trandum to find the different
%radius' that I want to use in my calculations. This makes it easy to
%compare the analytical solution with the observations done in the field.

tr = load('Trandum_corr.obs');

X = tr(:,1);
Y = tr(:,2);
heads = tr(:,3);

[n,m] = size(heads);
```

```
Trandum_origo_x = 8400.00;
Trandum_origo_y = 7150.00;


r = sqrt((X-Trandum_origo_x).^2 + (Y-Trandum_origo_y).^2);

%Use the optimal values found by calculation.N is based on the specific
%discharge of the river Risa.

k_1 = 2.886e-5;
k_2 = 5.693e-6;
h1 = 171.50;
h2 = 185;
R1 = 336;
R2 = 5100;
N = 1.266730e-8;


bb = (k_1 - k_2)/(R2 - R1);

alpha_1 = (1/(k_1 + bb*R1))*log((k_1*R1 - bb*R1*(r-R1))./(k_1*r));
alpha_2 = (1/(k_2 + bb*R2))*log((k_2*R2 - bb*R2*(r-R2))./(k_2*r));

beta_1  = ((k_1 +bb*R1)/(bb^2))*log((k_1  - bb*(r-R1))/k_1 );
beta_2  = ((k_2 +bb*R2)/(bb^2))*log((k_2  - bb*(r-R2))/k_2 );

L1 =   ((N/bb).*(r-R2) + (N).*beta_2 + h2*h2).*alpha_1;
L2 =   ((N/bb).*(r-R1) + (N).*beta_1 + h1*h1).*alpha_2;

AA = L1 - L2;
AA = AA./(alpha_1 - alpha_2);

h =  sqrt((AA));

% graph of the analytical head values calculated

xlabel('radius from the Trandum portal [m]'),
ylabel('heads [m]'),
title('Phreatic grw.levels'), grid;
hold;
plot(r,h,'b+');
%compare with observed heads:
dif_h= h-heads;
mean_dif_h=mean(dif_h)
max_dif_h=max(dif_h)
min_dif_h=min(dif_h)
std_dif_h=std(dif_h)
```

SCRIPT 3

```
%Script to compare the eleven different models with the eleven different
%boundary conditions with the observed heads and the models with the
%optimal parameters and circular boundaries.


%11 DIFFERENT BOUNDARY CONDITIONS: CONFINED AQUIFER
%
%Script to solve the 11 different equations with different boundary
```

```
%conditions. The bounday conditions is taken from Østmo, S.R.
%hydrogeologisk kart over Øvre Romerike, 1976. This means that R1 and R2 is
%varying together with h1 and h2. Because of the calculation I have given
%these boundary conditions new characters for the different calculations

% Compare the calculated results with the hydraulic heads found in the
% observation wells.

%CONFINED AQUIFER
%
% Script to solve an analytical solution of groundwater heads at the
% Trandum delta using the "Doughnut-equation", with constant heads, and
% heads as an function of radius. Precipitation is entered as an internal
% source. The thickness of the aquifer is an linear function of radius.

% Due to axis symmetry, the flow equation can be solved in 1-D. This
% corresponds to a !-D Poisson equation with Diriclet conditions on both
% sides of the doughnut.

%
%
%         A1              A2
% phi = -------{L1}  -  -------{L2}
%       A1-A2           A1-A2
%
%
% where:
%
%      L1 = (N/2ka)*(r-R2) + (N/2k)*B2 + phi_2
%      L2 = (N/2ka)*(r-R1) + (N/2k)*B1 + phi_1
%
%         A1 = {1/(H1 + a*R1)}*ln((H1*R1 - a*R1*(r - R1))/(H1*r))
%         A2 = {1/(H2 + a*R2)}*ln((H2*R2 - a*R2*(r - R2))/(H2*r))
%         B1 = {(H1+a*R1)/(a*a)}*ln[(H1-a*(r-R1))/H1]
%         B2 = {(H2+a*R2)/(a*a)}*ln[(H2-a*(r-R2))/H2]
%
%     and:
%
%      H(r) = H1 - a*(r-R1)
%
%        where
%          a = (H1 - H2)/(R2 - R1)
%
%       and H1 and H2 is the thickness of the aquifer at R1 and R2
%
%                                        H2
%        H1                             phi2
%        phi1
% -------|--------------------------------|-------> r
%        R1                               R2
%

% r = distance from origo
% R1 = distance from origo to inner boundary
% R2 = distance form origo to outer boundary
% phi1 = inner boundary condition, equal to head at inner boundary
% phi2 = outer boundary condition, equal to head at outer boundary
% N = infiltration rate
% k = average hydraulic conductivity
% H1 = aquifer thickness at R1
% H2 = aquifer thickness at R2
```

```
%Use the position of the observation wells at Trandum to find the different
%radius' that I want to use in my calculations. This makes it easy to
%compare the analytical solution with the observations done in the field.


tr = load('Trandum_corr.obs');

X = tr(:,1);
Y = tr(:,2);
heads = tr(:,3);

[n,m] = size(heads);

Trandum_origo_x = 8400.00;
Trandum_origo_y = 7150.00;


r = sqrt((X-Trandum_origo_x).^2 + (Y-Trandum_origo_y).^2);


%Use the optimal values found by calculation.These values are the same for
%all the 11 different calculations. N is based on the specific discharge of
%the river Risa
H1 = 301.86;
H2 = 66.19;
k = 1.727901e-5;
N = 1.266730e-8;

%setting the labels for the plots.

subplot(2,1,1),
xlabel('radius from the Trandum portal [m]'),
ylabel('heads [m]'),
title('Confined grw.levels'), grid;
hold;

% Boundary condition nr1
phi1 = 160;
phi2 = 186;
R1 = 291.2;
R2 = 5372.3;


for i=1:n;
if r(i) < R1;
    r(i) = NaN;

end
end

a = (H1 - H2)/(R2 - R1);

A_1  = (1/(H1 + a*R1)) * log((H1*R1 - a*R1*(r-R1))./(H1*r));
A_2  = (1/(H2 + a*R2)) * log((H2*R2 - a*R2*(r-R2))./(H2*r));

B_1  = ((H1+a*R1)/(a^2)) * log((H1 - a*(r-R1))/H1);
B_2  = ((H2+a*R2)/(a^2)) * log((H2 - a*(r-R2))/H2);
```

```
ledd_1 =   ((N/(2*k*a)) .* (r-R2) + N/(2*k) .*B_2 + phi2) .* A_1;
ledd_2 =   ((N/(2*k*a)) .* (r-R1) + N/(2*k) .*B_1 + phi1) .* A_2;

AA = ledd_1 - ledd_2;

phi1 = AA./(A_1 - A_2);

%Plotting calculated heads nr1
subplot(2,1,1),
plot(r,phi1, 'y+');

% Boundary condition nr2
R_1=787.1;
R_2=5298.3;
phi_1 = 162;
phi_2 = 188;


for i=1:n;
if r(i) < R_1;
    r(i) = NaN;

end
end

a = (H1 - H2)/(R_2 - R_1);

A_1  = (1/(H1 + a*R_1)) * log((H1*R_1 - a*R_1*(r-R_1))./(H1*r));
A_2  = (1/(H2 + a*R_2)) * log((H2*R_2 - a*R_2*(r-R_2))./(H2*r));

B_1  = ((H1+a*R_1)/(a^2)) * log((H1 - a*(r-R_1))/H1);
B_2  = ((H2+a*R_2)/(a^2)) * log((H2 - a*(r-R_2))/H2);

ledd_1 =   ((N/(2*k*a)) .* (r-R_2) + N/(2*k) .*B_2 + phi_2) .* A_1;
ledd_2 =   ((N/(2*k*a)) .* (r-R_1) + N/(2*k) .*B_1 + phi_1) .* A_2;

AA = ledd_1 - ledd_2;

phi2 = AA./(A_1 - A_2);

%Plotting calculated heads nr2
subplot(2,1,1),
plot(r,phi2, 'y+');

% Boundary condition nr3
C1=761.6;
C2=6603.7;
phi1C = 162;
phi2C = 172;


for i=1:n;
if r(i) < C1;
    r(i) = NaN;

end
end

a = (H1 - H2)/(C2 - C1);

A_1  = (1/(H1 + a*C1)) * log((H1*C1 - a*C1*(r-C1))./(H1*r));
```

```
A_2  = (1/(H2 + a*C2)) * log((H2*C2 - a*C2*(r-C2))./(H2*r));

B_1  = ((H1+a*C1)/(a^2)) * log((H1 - a*(r-C1))/H1);
B_2  = ((H2+a*C2)/(a^2)) * log((H2 - a*(r-C2))/H2);

ledd_1 =   ((N/(2*k*a)) .* (r-C2) + N/(2*k) .*B_2 + phi2C) .* A_1;
ledd_2 =   ((N/(2*k*a)) .* (r-C1) + N/(2*k) .*B_1 + phi1C) .* A_2;

AA = ledd_1 - ledd_2;

phi3 = AA./(A_1 - A_2);

%Plotting calculated heads nr3
subplot(2,1,1),
plot(r,phi3, 'y+');

% Boundary condition nr4

D1=596.7;
D2=6216.6;
phi1D = 160;
phi2D = 178;


for i=1:n;
if r(i) < D1;
    r(i) = NaN;

end
end

a = (H1 - H2)/(D2 - D1);

A_1  = (1/(H1 + a*D1)) * log((H1*D1 - a*D1*(r-D1))./(H1*r));
A_2  = (1/(H2 + a*D2)) * log((H2*D2 - a*D2*(r-D2))./(H2*r));

B_1  = ((H1+a*D1)/(a^2)) * log((H1 - a*(r-D1))/H1);
B_2  = ((H2+a*D2)/(a^2)) * log((H2 - a*(r-D2))/H2);

ledd_1 =   ((N/(2*k*a)) .* (r-D2) + N/(2*k) .*B_2 + phi2D) .* A_1;
ledd_2 =   ((N/(2*k*a)) .* (r-D1) + N/(2*k) .*B_1 + phi1D) .* A_2;

AA = ledd_1 - ledd_2;

phi4 = AA./(A_1 - A_2);

%Plotting calculated heads nr4
subplot(2,1,1),
plot(r,phi4, 'y+');

% Boundary condition nr5

E1=466.9;
E2=6437.3;
phi1E = 160;
phi2E = 178;


for i=1:n;
if r(i) < E1;
```

```
    r(i) = NaN;

end
end

a = (H1 - H2)/(E2 - E1);

A_1  = (1/(H1 + a*E1)) * log((H1*E1 - a*E1*(r-E1))./(H1*r));
A_2  = (1/(H2 + a*E2)) * log((H2*E2 - a*E2*(r-E2))./(H2*r));

B_1  = ((H1+a*E1)/(a^2)) * log((H1 - a*(r-E1))/H1);
B_2  = ((H2+a*E2)/(a^2)) * log((H2 - a*(r-E2))/H2);

ledd_1 =   ((N/(2*k*a)) .* (r-E2) + N/(2*k) .*B_2 + phi2E) .* A_1;
ledd_2 =   ((N/(2*k*a)) .* (r-E1) + N/(2*k) .*B_1 + phi1E) .* A_2;

AA = ledd_1 - ledd_2;

phi5 = AA./(A_1 - A_2);

%Plotting calculated heads nr5
subplot(2,1,1),
plot(r,phi5, 'y+');

% Boundary condition nr6

F1=960.2;
F2=5937.9;
phi1F = 163;
phi2F = 176;


for i=1:n;
if r(i) < F1;
    r(i) = NaN;

end
end

a = (H1 - H2)/(F2 - F1);

A_1  = (1/(H1 + a*F1)) * log((H1*F1 - a*F1*(r-F1))./(H1*r));
A_2  = (1/(H2 + a*F2)) * log((H2*F2 - a*F2*(r-F2))./(H2*r));

B_1  = ((H1+a*F1)/(a^2)) * log((H1 - a*(r-F1))/H1);
B_2  = ((H2+a*F2)/(a^2)) * log((H2 - a*(r-F2))/H2);

ledd_1 =   ((N/(2*k*a)) .* (r-F2) + N/(2*k) .*B_2 + phi2F) .* A_1;
ledd_2 =   ((N/(2*k*a)) .* (r-F1) + N/(2*k) .*B_1 + phi1F) .* A_2;

AA = ledd_1 - ledd_2;

phi6 = AA./(A_1 - A_2);

%Plotting calculated heads nr6
subplot(2,1,1),
plot(r,phi6, 'y+');

% Boundary condition nr7

G1=869.3;
```

```
G2=6218.2;
phi1G = 163;
phi2G = 174;


for i=1:n;
if r(i) < G1;
    r(i) = NaN;

end
end

a = (H1 - H2)/(G2 - G1);

A_1  = (1/(H1 + a*G1)) * log((H1*G1 - a*G1*(r-G1))./(H1*r));
A_2  = (1/(H2 + a*G2)) * log((H2*G2 - a*G2*(r-G2))./(H2*r));

B_1  = ((H1+a*G1)/(a^2)) * log((H1 - a*(r-G1))/H1);
B_2  = ((H2+a*G2)/(a^2)) * log((H2 - a*(r-G2))/H2);

ledd_1 =   ((N/(2*k*a)) .* (r-G2) + N/(2*k) .*B_2 + phi2G) .* A_1;
ledd_2 =   ((N/(2*k*a)) .* (r-G1) + N/(2*k) .*B_1 + phi1G) .* A_2;

AA = ledd_1 - ledd_2;

phi7 = AA./(A_1 - A_2);

%Plotting calculated heads nr7
subplot(2,1,1),
plot(r,phi7, 'y+');

% Boundary condition nr8

L1=1156.0;
L2=6095.4;
phi1L = 166;
phi2L = 174;


for i=1:n;
if r(i) < L1;
    r(i) = NaN;

end
end

a = (H1 - H2)/(L2 - L1);

A_1  = (1/(H1 + a*L1)) * log((H1*L1 - a*L1*(r-L1))./(H1*r));
A_2  = (1/(H2 + a*L2)) * log((H2*L2 - a*L2*(r-L2))./(H2*r));

B_1  = ((H1+a*L1)/(a^2)) * log((H1 - a*(r-L1))/H1);
B_2  = ((H2+a*L2)/(a^2)) * log((H2 - a*(r-L2))/H2);

ledd_1 =   ((N/(2*k*a)) .* (r-L2) + N/(2*k) .*B_2 + phi2L) .* A_1;
ledd_2 =   ((N/(2*k*a)) .* (r-L1) + N/(2*k) .*B_1 + phi1L) .* A_2;

AA = ledd_1 - ledd_2;

phi8 = AA./(A_1 - A_2);
```

```
%Plotting calculated heads nr8
subplot(2,1,1),
plot(r,phi8, 'y+');

% Boundary condition nr9

M1=1084.1;
M2=6110.0;
phi1M = 166;
phi2M = 174;


for i=1:n;
if r(i) < M1;
    r(i) = NaN;

end
end

a = (H1 - H2)/(M2 - M1);

A_1  = (1/(H1 + a*M1)) * log((H1*M1 - a*M1*(r-M1))./(H1*r));
A_2  = (1/(H2 + a*M2)) * log((H2*M2 - a*M2*(r-M2))./(H2*r));

B_1  = ((H1+a*M1)/(a^2)) * log((H1 - a*(r-M1))/H1);
B_2  = ((H2+a*M2)/(a^2)) * log((H2 - a*(r-M2))/H2);

ledd_1 =   ((N/(2*k*a)) .* (r-M2) + N/(2*k) .*B_2 + phi2M) .* A_1;
ledd_2 =   ((N/(2*k*a)) .* (r-M1) + N/(2*k) .*B_1 + phi1M) .* A_2;

AA = ledd_1 - ledd_2;

phi9 = AA./(A_1 - A_2);

%Plotting calculated heads nr9
subplot(2,1,1),
plot(r,phi9, 'y+');

% Boundary condition nr10

N1=688.8;
N2=6762.9;
phi1N = 162;
phi2N = 172;


for i=1:n;
if r(i) < N1;
    r(i) = NaN;

end
end

a = (H1 - H2)/(N2 - N1);

A_1  = (1/(H1 + a*N1)) * log((H1*N1 - a*N1*(r-N1))./(H1*r));
A_2  = (1/(H2 + a*N2)) * log((H2*N2 - a*N2*(r-N2))./(H2*r));

B_1  = ((H1+a*N1)/(a^2)) * log((H1 - a*(r-N1))/H1);
B_2  = ((H2+a*N2)/(a^2)) * log((H2 - a*(r-N2))/H2);
```

```
ledd_1 =   ((N/(2*k*a)) .* (r-N2) + N/(2*k) .*B_2 + phi2N) .* A_1;
ledd_2 =   ((N/(2*k*a)) .* (r-N1) + N/(2*k) .*B_1 + phi1N) .* A_2;

AA = ledd_1 - ledd_2;

phi10 = AA./(A_1 - A_2);

%Plotting calculated heads nr10
subplot(2,1,1),
plot(r,phi10, 'y+');

% Boundary condition nr11

P1=672.3;
P2=7000.7;
phi1P = 162;
phi2P = 172;


for i=1:n;
if r(i) < P1;
    r(i) = NaN;

end
end

a = (H1 - H2)/(P2 - P1);

A_1  = (1/(H1 + a*P1)) * log((H1*P1 - a*P1*(r-P1))./(H1*r));
A_2  = (1/(H2 + a*P2)) * log((H2*P2 - a*P2*(r-P2))./(H2*r));

B_1  = ((H1+a*P1)/(a^2)) * log((H1 - a*(r-P1))/H1);
B_2  = ((H2+a*P2)/(a^2)) * log((H2 - a*(r-P2))/H2);

ledd_1 =   ((N/(2*k*a)) .* (r-P2) + N/(2*k) .*B_2 + phi2P) .* A_1;
ledd_2 =   ((N/(2*k*a)) .* (r-P1) + N/(2*k) .*B_1 + phi1P) .* A_2;

AA = ledd_1 - ledd_2;

phi11 = AA./(A_1 - A_2);

%Plotting calculated heads nr11
subplot(2,1,1),
plot(r,phi11, 'y+');

%plotter observerte heads
subplot(2,1,1),
plot(r,heads, 'b+')


% optimal parameters

a = (H1 - H2)/(R2 - R1);

A_1  = (1/(H1 + a*R1)) * log((H1*R1 - a*R1*(r-R1))./(H1*r));
A_2  = (1/(H2 + a*R2)) * log((H2*R2 - a*R2*(r-R2))./(H2*r));

B_1  = ((H1+a*R1)/(a^2)) * log((H1 - a*(r-R1))/H1);
B_2  = ((H2+a*R2)/(a^2)) * log((H2 - a*(r-R2))/H2);
```

```
ledd_1 =   ((N/(2*k*a)) .* (r-R2) + N/(2*k) .*B_2 + phi2) .* A_1;
ledd_2 =   ((N/(2*k*a)) .* (r-R1) + N/(2*k) .*B_1 + phi1) .* A_2;

AA = ledd_1 - ledd_2;

phi = AA./(A_1 - A_2)

subplot(2,1,1),
plot(r,phi,'rd');

%11 DIFFERENT BOUNDARY CONDITIONS: UNCONFINED/PHREATIC AQUIFER
%
%Script to solve the 11 different equations with different boundary
%conditions. The bounday conditions is taken from Østmo, S.R.
%hydrogeologisk kart over Øvre Romerike 1976. This means that R1 and R2 is
%varying together with h1 and h2. Because of the calculation I have given
%these boundary conditions new characters, for the different calculations.

% Compare the calculated results with the hydraulic heads found in the
% observation wells.


%UNCONFINED AQUIFER
%
% Script to solve an analytical solution of groundwater heads at the
% Trandum delta using the "Doughnut-equation", with constant heads, and
% heads as an function of radius. Precipitation is entered as an internal
% source. The conductivity of the aquifer is an linear function of radius.

% Due to axis symmetry, the flow equation can be solved in 1-D. This
% corresponds to a !-D Poisson equation with Diriclet conditions on both
% sides of the doughnut.
%
%
%            alpha_1                    alpha_2
% h^2 = -----------------{L1}  -  -----------------{L2}
%        alpha_1-alpha_2            alpha_1-alpha_2
%
%
% where:
%
%      L1 = (N/b)*(r-R2) + (N)*beta_2 + h_2*h_2
%      L2 = (N/b)*(r-R1) + (N)*beta_1 + h_1*h_1
%
%         alpha_1 = {1/(k1 + b*R1)}*ln((k1*R1 - b*R1*(r - R1))/(k1*r))
%         alpha_2 = {1/(k2 + b*R2)}*ln((k2*R2 - b*R2*(r - R2))/(k2*r))
%
%
%         beta_1 = {(k1+b*R1)/(b*b)}*ln[(k1-b*(r-R1))/k1]
%         beta_2 = {(k2+b*R2)/(b*b)}*ln[(k2-b*(r-R2))/k2]
%
%     and:
%
%      k(r) = k1 - b*(r-R1) for an open/phreatic/unconfined aquifer
%
%        where
%          b = (k1 - k2)/(R2 - R1)
%
%       and k1 and k2 is hydr. conductivities at R1 and R2
%
```

```
%                                       k2
%        k1                             h2
%        h1
% -------|-------------------------------|-------> r
%        R1                             R2
%

% r = distance from origo
% R1 = distance from origo to inner boundary
% R2 = distance form origo to outer boundary
% h1 = inner boundary condition, equal to head at inner boundary
% h2 = outer boundary condition, equal to head at outer boundary
% k1 = hydraulic coductivity at inner boundary
% k2 = hydraulic coductivity at outer boundary


%Use the position of the observation wells at Trandum to find the different
%radius' that I want to use in my calculations. This makes it easy to
%compare the analytical solution with the observations done in the field.



%Use the optimal values found by calculation. These values are the same for
%all the 11 different calculations. N is based on the specific discharge of
%the river Risa.

k_1 = 2.886e-5;
k_2 = 5.693e-6;
N = 1.266730e-8;

%setting the labels for the plots.
subplot(2,1,2),
xlabel('radius from the Trandum portal [m]'),
ylabel('heads [m]'),
title('Phreatic grw.levels'), grid;
hold;

% Boundary condition nr1

h1 = 160;
h2 = 186;
R1 = 291.2;
R2 = 5372.3;

for i=1:n;
if r(i) < R1;
    r(i) = NaN;

end
end

bb = (k_1 - k_2)/(R2 - R1);

alpha_1 = (1/(k_1 + bb*R1))*log((k_1*R1 - bb*R1*(r-R1))./(k_1*r));
alpha_2 = (1/(k_2 + bb*R2))*log((k_2*R2 - bb*R2*(r-R2))./(k_2*r));

beta_1  = ((k_1 +bb*R1)/(bb^2))*log((k_1  - bb*(r-R1))/k_1 );
beta_2  = ((k_2 +bb*R2)/(bb^2))*log((k_2  - bb*(r-R2))/k_2 );
```

```
L1 =   ((N/bb).*(r-R2) + (N).*beta_2 + h2*h2).*alpha_1;
L2 =   ((N/bb).*(r-R1) + (N).*beta_1 + h1*h1).*alpha_2;

AA = L1 - L2;
AA = AA./(alpha_1 - alpha_2);

h1 =  sqrt((AA));

%Plotting calculated heads nr1
subplot(2,1,2),
plot(r,h1,'y+');


% Boundary condition nr2
R_1=787.1;
R_2=5298.3;
h_1 = 162;
h_2 = 188;

for i=1:n;
if r(i) < R_1;
    r(i) = NaN;

end
end

bb = (k_1 - k_2)/(R_2 - R_1);

alpha_1 = (1/(k_1 + bb*R_1))*log((k_1*R_1 - bb*R_1*(r-R_1))./(k_1*r));
alpha_2 = (1/(k_2 + bb*R_2))*log((k_2*R_2 - bb*R_2*(r-R_2))./(k_2*r));

beta_1  = ((k_1 +bb*R_1)/(bb^2))*log((k_1  - bb*(r-R_1))/k_1 );
beta_2  = ((k_2 +bb*R_2)/(bb^2))*log((k_2  - bb*(r-R_2))/k_2 );

L1 =   ((N/bb).*(r-R_2) + (N).*beta_2 + h_2*h_2).*alpha_1;
L2 =   ((N/bb).*(r-R_1) + (N).*beta_1 + h_1*h_1).*alpha_2;

AA = L1 - L2;
AA = AA./(alpha_1 - alpha_2);

h2 =  sqrt((AA));

%Plotting calculated heads nr2
subplot(2,1,2),
plot(r,h2, 'y+');

% Boundary condition nr3
C1=761.6;
C2=6603.7;
h1C = 162;
h2C = 172;

for i=1:n;
if r(i) < C1;
    r(i) = NaN;

end
end

bb = (k_1 - k_2)/(C2 - C1);
```

```
alpha_1 = (1/(k_1 + bb*C1))*log((k_1*C1 - bb*C1*(r-C1))./(k_1*r));
alpha_2 = (1/(k_2 + bb*C2))*log((k_2*C2 - bb*C2*(r-C2))./(k_2*r));

beta_1  = ((k_1 +bb*C1)/(bb^2))*log((k_1  - bb*(r-C1))/k_1 );
beta_2  = ((k_2 +bb*C2)/(bb^2))*log((k_2  - bb*(r-C2))/k_2 );

L1 =   ((N/bb).*(r-C2) + (N).*beta_2 + h2C*h2C).*alpha_1;
L2 =   ((N/bb).*(r-C1) + (N).*beta_1 + h1C*h1C).*alpha_2;

AA = L1 - L2;
AA = AA./(alpha_1 - alpha_2);

h3 =  sqrt((AA));

%Plotting calculated heads nr3
subplot(2,1,2),
plot(r,h3, 'y+');

% Boundary condition nr4

D1=596.7;
D2=6216.6;
h1D = 160;
h2D = 178;

for i=1:n;
if r(i) < D1;
    r(i) = NaN;

end
end

bb = (k_1 - k_2)/(D2 - D1);

alpha_1 = (1/(k_1 + bb*D1))*log((k_1*D1 - bb*D1*(r-D1))./(k_1*r));
alpha_2 = (1/(k_2 + bb*D2))*log((k_2*D2 - bb*D2*(r-D2))./(k_2*r));

beta_1  = ((k_1 +bb*D1)/(bb^2))*log((k_1  - bb*(r-D1))/k_1 );
beta_2  = ((k_2 +bb*D2)/(bb^2))*log((k_2  - bb*(r-D2))/k_2 );

L1 =   ((N/bb).*(r-D2) + (N).*beta_2 + h2D*h2D).*alpha_1;
L2 =   ((N/bb).*(r-D1) + (N).*beta_1 + h1D*h1D).*alpha_2;

AA = L1 - L2;
AA = AA./(alpha_1 - alpha_2);

h4 =  sqrt((AA));

%Plotting calculated heads nr4
subplot(2,1,2),
plot(r,h4, 'y+');


% Boundary condition nr5

E1=466.9;
E2=6437.3;
h1E = 160;
h2E = 178;
```

```
for i=1:n;
if r(i) < E1;
    r(i) = NaN;

end
end

bb = (k_1 - k_2)/(E2 - E1);

alpha_1 = (1/(k_1 + bb*E1))*log((k_1*E1 - bb*E1*(r-E1))./(k_1*r));
alpha_2 = (1/(k_2 + bb*E2))*log((k_2*E2 - bb*E2*(r-E2))./(k_2*r));

beta_1  = ((k_1 +bb*E1)/(bb^2))*log((k_1  - bb*(r-E1))/k_1 );
beta_2  = ((k_2 +bb*E2)/(bb^2))*log((k_2  - bb*(r-E2))/k_2 );

L1 =   ((N/bb).*(r-E2) + (N).*beta_2 + h2E*h2E).*alpha_1;
L2 =   ((N/bb).*(r-E1) + (N).*beta_1 + h1E*h1E).*alpha_2;

AA = L1 - L2;
AA = AA./(alpha_1 - alpha_2);

h5 =  sqrt((AA));

%Plotting calculated heads nr5
subplot(2,1,2),
plot(r,h5, 'y+');

% Boundary condition nr6

F1=960.2;
F2=5937.9;
h1F = 163;
h2F = 176;

for i=1:n;
if r(i) < F1;
    r(i) = NaN;

end
end

bb = (k_1 - k_2)/(F2 - F1);

alpha_1 = (1/(k_1 + bb*F1))*log((k_1*F1 - bb*F1*(r-F1))./(k_1*r));
alpha_2 = (1/(k_2 + bb*F2))*log((k_2*F2 - bb*F2*(r-F2))./(k_2*r));

beta_1  = ((k_1 +bb*F1)/(bb^2))*log((k_1  - bb*(r-F1))/k_1 );
beta_2  = ((k_2 +bb*F2)/(bb^2))*log((k_2  - bb*(r-F2))/k_2 );

L1 =   ((N/bb).*(r-F2) + (N).*beta_2 + h2F*h2F).*alpha_1;
L2 =   ((N/bb).*(r-F1) + (N).*beta_1 + h1F*h1F).*alpha_2;

AA = L1 - L2;
AA = AA./(alpha_1 - alpha_2);

h6 =  sqrt((AA));

%Plotting calculated heads nr6
subplot(2,1,2),
plot(r,h6, 'y+');
```

```
% Boundary condition nr7

G1=869.3;
G2=6218.2;
h1G = 163;
h2G = 174;

for i=1:n;
if r(i) < G1;
    r(i) = NaN;

end
end

bb = (k_1 - k_2)/(G2 - G1);

alpha_1 = (1/(k_1 + bb*G1))*log((k_1*G1 - bb*G1*(r-G1))./(k_1*r));
alpha_2 = (1/(k_2 + bb*G2))*log((k_2*G2 - bb*G2*(r-G2))./(k_2*r));

beta_1  = ((k_1 +bb*G1)/(bb^2))*log((k_1  - bb*(r-G1))/k_1 );
beta_2  = ((k_2 +bb*G2)/(bb^2))*log((k_2  - bb*(r-G2))/k_2 );

L1 =   ((N/bb).*(r-G2) + (N).*beta_2 + h2G*h2G).*alpha_1;
L2 =   ((N/bb).*(r-G1) + (N).*beta_1 + h1G*h1G).*alpha_2;

AA = L1 - L2;
AA = AA./(alpha_1 - alpha_2);

h7 =  sqrt((AA));

%Plotting calculated heads nr7
subplot(2,1,2),
plot(r,h7, 'y+');

% Boundary condition nr8

S1=1156.0;
S2=6095.4;
h1S = 166;
h2S = 174;

for i=1:n;
if r(i) < S1;
    r(i) = NaN;

end
end

bb = (k_1 - k_2)/(S2 - S1);

alpha_1 = (1/(k_1 + bb*S1))*log((k_1*S1 - bb*S1*(r-S1))./(k_1*r));
alpha_2 = (1/(k_2 + bb*S2))*log((k_2*S2 - bb*S2*(r-S2))./(k_2*r));

beta_1  = ((k_1 +bb*S1)/(bb^2))*log((k_1  - bb*(r-S1))/k_1 );
beta_2  = ((k_2 +bb*S2)/(bb^2))*log((k_2  - bb*(r-S2))/k_2 );

L1 =   ((N/bb).*(r-S2) + (N).*beta_2 + h2S*h2S).*alpha_1;
L2 =   ((N/bb).*(r-S1) + (N).*beta_1 + h1S*h1S).*alpha_2;

AA = L1 - L2;
```

```
AA = AA./(alpha_1 - alpha_2);

h8 =  sqrt((AA));

%Plotting calculated heads nr8
subplot(2,1,2),
plot(r,h8, 'y+');

% Boundary condition nr9

M1=1084.1;
M2=6110.0;
h1M = 166;
h2M = 174;

for i=1:n;
if r(i) < M1;
    r(i) = NaN;

end
end

bb = (k_1 - k_2)/(M2 - M1);

alpha_1 = (1/(k_1 + bb*M1))*log((k_1*M1 - bb*M1*(r-M1))./(k_1*r));
alpha_2 = (1/(k_2 + bb*M2))*log((k_2*M2 - bb*M2*(r-M2))./(k_2*r));

beta_1  = ((k_1 +bb*M1)/(bb^2))*log((k_1  - bb*(r-M1))/k_1 );
beta_2  = ((k_2 +bb*M2)/(bb^2))*log((k_2  - bb*(r-M2))/k_2 );

L1 =   ((N/bb).*(r-M2) + (N).*beta_2 + h2M*h2M).*alpha_1;
L2 =   ((N/bb).*(r-M1) + (N).*beta_1 + h1M*h1M).*alpha_2;

AA = L1 - L2;
AA = AA./(alpha_1 - alpha_2);

h9 =  sqrt((AA));

%Plotting calculated heads nr9
subplot(2,1,2),
plot(r,h9, 'y+');

% Boundary condition nr10

N1=688.8;
N2=6762.9;
h1N = 162;
h2N = 172;

for i=1:n;
if r(i) < N1;
    r(i) = NaN;

end
end

bb = (k_1 - k_2)/(N2 - N1);

alpha_1 = (1/(k_1 + bb*N1))*log((k_1*N1 - bb*N1*(r-N1))./(k_1*r));
alpha_2 = (1/(k_2 + bb*N2))*log((k_2*N2 - bb*N2*(r-N2))./(k_2*r));
```

```
beta_1  = ((k_1 +bb*N1)/(bb^2))*log((k_1  - bb*(r-N1))/k_1 );
beta_2  = ((k_2 +bb*N2)/(bb^2))*log((k_2  - bb*(r-N2))/k_2 );

L1 =   ((N/bb).*(r-N2) + (N).*beta_2 + h2N*h2N).*alpha_1;
L2 =   ((N/bb).*(r-N1) + (N).*beta_1 + h1N*h1N).*alpha_2;

AA = L1 - L2;
AA = AA./(alpha_1 - alpha_2);

h10 =  sqrt((AA));

%Plotting calculated heads nr10
subplot(2,1,2),
plot(r,h10, 'y+');

% Boundary condition nr11

P1=672.3;
P2=7000.7;
h1P = 162;
h2P = 172;


for i=1:n;
if r(i) < P1;
    r(i) = NaN;

end
end

bb = (k_1 - k_2)/(P2 - P1);

alpha_1 = (1/(k_1 + bb*P1))*log((k_1*P1 - bb*P1*(r-P1))./(k_1*r));
alpha_2 = (1/(k_2 + bb*P2))*log((k_2*P2 - bb*P2*(r-P2))./(k_2*r));

beta_1  = ((k_1 +bb*P1)/(bb^2))*log((k_1  - bb*(r-P1))/k_1 );
beta_2  = ((k_2 +bb*P2)/(bb^2))*log((k_2  - bb*(r-P2))/k_2 );

L1 =   ((N/bb).*(r-P2) + (N).*beta_2 + h2P*h2P).*alpha_1;
L2 =   ((N/bb).*(r-P1) + (N).*beta_1 + h1P*h1P).*alpha_2;

AA = L1 - L2;
AA = AA./(alpha_1 - alpha_2);

h11 =  sqrt((AA));

%Plotting calculated heads nr11
subplot(2,1,2),
plot(r,h11, 'y+');

%plotting observerte heads
subplot(2,1,2),
plot(r,heads, 'b+');


% optimal parameters


bb = (k_1 - k_2)/(R2 - R1);
```

```
alpha_1 = (1/(k_1 + bb*R1))*log((k_1*R1 - bb*R1*(r-R1))./(k_1*r));
alpha_2 = (1/(k_2 + bb*R2))*log((k_2*R2 - bb*R2*(r-R2))./(k_2*r));

beta_1  = ((k_1 +bb*R1)/(bb^2))*log((k_1  - bb*(r-R1))/k_1 );
beta_2  = ((k_2 +bb*R2)/(bb^2))*log((k_2  - bb*(r-R2))/k_2 );

L1 =   ((N/bb).*(r-R2) + (N).*beta_2 + h2*h2).*alpha_1;
L2 =   ((N/bb).*(r-R1) + (N).*beta_1 + h1*h1).*alpha_2;

AA = L1 - L2;
AA = AA./(alpha_1 - alpha_2);

h =  sqrt((AA));

subplot(2,1,2),
plot(r,h,'rd');
```

SCRIPT 4

```
%Script to find the differences between the extreme of the eleven models
%and the simplified models.

tr = load('Trandum_corr.obs');

X = tr(:,1);
Y = tr(:,2);
heads = tr(:,3);

[n,m] = size(heads);

Trandum_origo_x = 8400.00;
Trandum_origo_y = 7150.00;

r = sqrt((X-Trandum_origo_x).^2 + (Y-Trandum_origo_y).^2);

%CONFINED

%Use the optimal values found by calculation. N is based on the spacific
%discharge of the river Risa.

H1 = 301.86;
H2 = 66.19;
k = 1.727901e-5;
phi1 = 171.50;
phi2 = 185;
R1 = 336;
R2 = 5100;
N = 1.266730e-8;

a = (H1 - H2)/(R2 - R1);

A_1  = (1/(H1 + a*R1)) * log((H1*R1 - a*R1*(r-R1))./(H1*r));
A_2  = (1/(H2 + a*R2)) * log((H2*R2 - a*R2*(r-R2))./(H2*r));

B_1  = ((H1+a*R1)/(a^2)) * log((H1 - a*(r-R1))/H1);
B_2  = ((H2+a*R2)/(a^2)) * log((H2 - a*(r-R2))/H2);

ledd_1 =   ((N/(2*k*a)) .* (r-R2) + N/(2*k) .*B_2 + phi2) .* A_1;
ledd_2 =   ((N/(2*k*a)) .* (r-R1) + N/(2*k) .*B_1 + phi1) .* A_2;

AA = ledd_1 - ledd_2;
```

```
phi = AA./(A_1 - A_2)

%PHREATIC

%Use the optimal values found by calculation.N is based on the specific
%discharge of the river Risa.

k_1 = 2.886e-5;
k_2 = 5.693e-6;
h1 = 171.50;
h2 = 185;
R1 = 336;
R2 = 5100;
N = 1.266730e-8;


bb = (k_1 - k_2)/(R2 - R1);

alpha_1 = (1/(k_1 + bb*R1))*log((k_1*R1 - bb*R1*(r-R1))./(k_1*r));
alpha_2 = (1/(k_2 + bb*R2))*log((k_2*R2 - bb*R2*(r-R2))./(k_2*r));

beta_1  = ((k_1 +bb*R1)/(bb^2))*log((k_1  - bb*(r-R1))/k_1 );
beta_2  = ((k_2 +bb*R2)/(bb^2))*log((k_2  - bb*(r-R2))/k_2 );

L1 =   ((N/bb).*(r-R2) + (N).*beta_2 + h2*h2).*alpha_1;
L2 =   ((N/bb).*(r-R1) + (N).*beta_1 + h1*h1).*alpha_2;

AA = L1 - L2;
AA = AA./(alpha_1 - alpha_2);

h =  sqrt((AA));


%CONFINED

% Boundary condition nr1
phi1 = 160;
phi2 = 186;
R1 = 291.2;
R2 = 5372.3;


for i=1:n;
if r(i) < R1;
    r(i) = NaN;

end
end

a = (H1 - H2)/(R2 - R1);

A_1  = (1/(H1 + a*R1)) * log((H1*R1 - a*R1*(r-R1))./(H1*r));
A_2  = (1/(H2 + a*R2)) * log((H2*R2 - a*R2*(r-R2))./(H2*r));

B_1  = ((H1+a*R1)/(a^2)) * log((H1 - a*(r-R1))/H1);
B_2  = ((H2+a*R2)/(a^2)) * log((H2 - a*(r-R2))/H2);

ledd_1 =   ((N/(2*k*a)) .* (r-R2) + N/(2*k) .*B_2 + phi2) .* A_1;
ledd_2 =   ((N/(2*k*a)) .* (r-R1) + N/(2*k) .*B_1 + phi1) .* A_2;
```

```
AA = ledd_1 - ledd_2;

phi1 = AA./(A_1 - A_2);


% Boundary condition nr2
R_1=787.1;
R_2=5298.3;
phi_1 = 162;
phi_2 = 188;


for i=1:n;
if r(i) < R_1;
    r(i) = NaN;

end
end

a = (H1 - H2)/(R_2 - R_1);

A_1  = (1/(H1 + a*R_1)) * log((H1*R_1 - a*R_1*(r-R_1))./(H1*r));
A_2  = (1/(H2 + a*R_2)) * log((H2*R_2 - a*R_2*(r-R_2))./(H2*r));

B_1  = ((H1+a*R_1)/(a^2)) * log((H1 - a*(r-R_1))/H1);
B_2  = ((H2+a*R_2)/(a^2)) * log((H2 - a*(r-R_2))/H2);

ledd_1 =   ((N/(2*k*a)) .* (r-R_2) + N/(2*k) .*B_2 + phi_2) .* A_1;
ledd_2 =   ((N/(2*k*a)) .* (r-R_1) + N/(2*k) .*B_1 + phi_1) .* A_2;

AA = ledd_1 - ledd_2;

phi2 = AA./(A_1 - A_2);

% Boundary condition nr8

L1=1156.0;
L2=6095.4;
phi1L = 166;
phi2L = 174;


for i=1:n;
if r(i) < L1;
    r(i) = NaN;

end
end

a = (H1 - H2)/(L2 - L1);

A_1  = (1/(H1 + a*L1)) * log((H1*L1 - a*L1*(r-L1))./(H1*r));
A_2  = (1/(H2 + a*L2)) * log((H2*L2 - a*L2*(r-L2))./(H2*r));

B_1  = ((H1+a*L1)/(a^2)) * log((H1 - a*(r-L1))/H1);
B_2  = ((H2+a*L2)/(a^2)) * log((H2 - a*(r-L2))/H2);

ledd_1 =   ((N/(2*k*a)) .* (r-L2) + N/(2*k) .*B_2 + phi2L) .* A_1;
ledd_2 =   ((N/(2*k*a)) .* (r-L1) + N/(2*k) .*B_1 + phi1L) .* A_2;
```

```
AA = ledd_1 - ledd_2;

phi8 = AA./(A_1 - A_2);

% Boundary condition nr9

M1=1084.1;
M2=6110.0;
phi1M = 166;
phi2M = 174;


for i=1:n;
if r(i) < M1;
    r(i) = NaN;

end
end

a = (H1 - H2)/(M2 - M1);

A_1  = (1/(H1 + a*M1)) * log((H1*M1 - a*M1*(r-M1))./(H1*r));
A_2  = (1/(H2 + a*M2)) * log((H2*M2 - a*M2*(r-M2))./(H2*r));

B_1  = ((H1+a*M1)/(a^2)) * log((H1 - a*(r-M1))/H1);
B_2  = ((H2+a*M2)/(a^2)) * log((H2 - a*(r-M2))/H2);

ledd_1 =   ((N/(2*k*a)) .* (r-M2) + N/(2*k) .*B_2 + phi2M) .* A_1;
ledd_2 =   ((N/(2*k*a)) .* (r-M1) + N/(2*k) .*B_1 + phi1M) .* A_2;

AA = ledd_1 - ledd_2;

phi9 = AA./(A_1 - A_2);

%PHREATIC

% Boundary condition nr1

h1 = 160;
h2 = 186;
R1 = 291.2;
R2 = 5372.3;


for i=1:n;
if r(i) < R1;
    r(i) = NaN;

end
end

bb = (k_1 - k_2)/(R2 - R1);

alpha_1 = (1/(k_1 + bb*R1))*log((k_1*R1 - bb*R1*(r-R1))./(k_1*r));
alpha_2 = (1/(k_2 + bb*R2))*log((k_2*R2 - bb*R2*(r-R2))./(k_2*r));

beta_1  = ((k_1 +bb*R1)/(bb^2))*log((k_1  - bb*(r-R1))/k_1 );
beta_2  = ((k_2 +bb*R2)/(bb^2))*log((k_2  - bb*(r-R2))/k_2 );

L1 =   ((N/bb).*(r-R2) + (N).*beta_2 + h2*h2).*alpha_1;
```

```
L2 =   ((N/bb).*(r-R1) + (N).*beta_1 + h1*h1).*alpha_2;

AA = L1 - L2;
AA = AA./(alpha_1 - alpha_2);

h1 =  sqrt((AA));

% Boundary condition nr2
R_1=787.1;
R_2=5298.3;
h_1 = 162;
h_2 = 188;


for i=1:n;
if r(i) < R_1;
    r(i) = NaN;

end
end

bb = (k_1 - k_2)/(R_2 - R_1);

alpha_1 = (1/(k_1 + bb*R_1))*log((k_1*R_1 - bb*R_1*(r-R_1))./(k_1*r));
alpha_2 = (1/(k_2 + bb*R_2))*log((k_2*R_2 - bb*R_2*(r-R_2))./(k_2*r));

beta_1  = ((k_1 +bb*R_1)/(bb^2))*log((k_1  - bb*(r-R_1))/k_1 );
beta_2  = ((k_2 +bb*R_2)/(bb^2))*log((k_2  - bb*(r-R_2))/k_2 );

L1 =   ((N/bb).*(r-R_2) + (N).*beta_2 + h_2*h_2).*alpha_1;
L2 =   ((N/bb).*(r-R_1) + (N).*beta_1 + h_1*h_1).*alpha_2;

AA = L1 - L2;
AA = AA./(alpha_1 - alpha_2);

h2 =  sqrt((AA));

% Boundary condition nr8

S1=1156.0;
S2=6095.4;
h1S = 166;
h2S = 174;


for i=1:n;
if r(i) < S1;
    r(i) = NaN;

end
end

bb = (k_1 - k_2)/(S2 - S1);

alpha_1 = (1/(k_1 + bb*S1))*log((k_1*S1 - bb*S1*(r-S1))./(k_1*r));
alpha_2 = (1/(k_2 + bb*S2))*log((k_2*S2 - bb*S2*(r-S2))./(k_2*r));

beta_1  = ((k_1 +bb*S1)/(bb^2))*log((k_1  - bb*(r-S1))/k_1 );
beta_2  = ((k_2 +bb*S2)/(bb^2))*log((k_2  - bb*(r-S2))/k_2 );

L1 =   ((N/bb).*(r-S2) + (N).*beta_2 + h2S*h2S).*alpha_1;
```

```
L2 =   ((N/bb).*(r-S1) + (N).*beta_1 + h1S*h1S).*alpha_2;

AA = L1 - L2;
AA = AA./(alpha_1 - alpha_2);

h8 =  sqrt((AA));

% Boundary condition nr9

M1=1084.1;
M2=6110.0;
h1M = 166;
h2M = 174;


for i=1:n;
if r(i) < M1;
    r(i) = NaN;

end
end

bb = (k_1 - k_2)/(M2 - M1);

alpha_1 = (1/(k_1 + bb*M1))*log((k_1*M1 - bb*M1*(r-M1))./(k_1*r));
alpha_2 = (1/(k_2 + bb*M2))*log((k_2*M2 - bb*M2*(r-M2))./(k_2*r));

beta_1  = ((k_1 +bb*M1)/(bb^2))*log((k_1  - bb*(r-M1))/k_1 );
beta_2  = ((k_2 +bb*M2)/(bb^2))*log((k_2  - bb*(r-M2))/k_2 );

L1 =   ((N/bb).*(r-M2) + (N).*beta_2 + h2M*h2M).*alpha_1;
L2 =   ((N/bb).*(r-M1) + (N).*beta_1 + h1M*h1M).*alpha_2;

AA = L1 - L2;
AA = AA./(alpha_1 - alpha_2);

h9 =  sqrt((AA));

%CONFINED

H1 = 301.86;
H2 = 66.19;
k = 1.727901e-5;
N = 1.266730e-8;

% Boundary condition nr2

R_1=787.1;
R_2=5298.3;
phi_1 = 162;
phi_2 = 188;


for i=1:n;
if r(i) < R_1;
    r(i) = NaN;

end
end
```

```
a = (H1 - H2)/(R_2 - R_1);

A_1  = (1/(H1 + a*R_1)) * log((H1*R_1 - a*R_1*(r-R_1))./(H1*r));
A_2  = (1/(H2 + a*R_2)) * log((H2*R_2 - a*R_2*(r-R_2))./(H2*r));

B_1  = ((H1+a*R_1)/(a^2)) * log((H1 - a*(r-R_1))/H1);
B_2  = ((H2+a*R_2)/(a^2)) * log((H2 - a*(r-R_2))/H2);

ledd_1 =   ((N/(2*k*a)) .* (r-R_2) + N/(2*k) .*B_2 + phi_2) .* A_1;
ledd_2 =   ((N/(2*k*a)) .* (r-R_1) + N/(2*k) .*B_1 + phi_1) .* A_2;

AA = ledd_1 - ledd_2;

phi2 = AA./(A_1 - A_2);

% Boundary condition nr11

P1=672.3;
P2=7000.7;
phi1P = 162;
phi2P = 172;


for i=1:n;
if r(i) < P1;
    r(i) = NaN;

end
end

a = (H1 - H2)/(P2 - P1);

A_1  = (1/(H1 + a*P1)) * log((H1*P1 - a*P1*(r-P1))./(H1*r));
A_2  = (1/(H2 + a*P2)) * log((H2*P2 - a*P2*(r-P2))./(H2*r));

B_1  = ((H1+a*P1)/(a^2)) * log((H1 - a*(r-P1))/H1);
B_2  = ((H2+a*P2)/(a^2)) * log((H2 - a*(r-P2))/H2);

ledd_1 =   ((N/(2*k*a)) .* (r-P2) + N/(2*k) .*B_2 + phi2P) .* A_1;
ledd_2 =   ((N/(2*k*a)) .* (r-P1) + N/(2*k) .*B_1 + phi1P) .* A_2;

AA = ledd_1 - ledd_2;

phi11 = AA./(A_1 - A_2);

%PHREATIC

h1 = 171.50;
h2 = 185;
N = 1.266730e-8;

% Boundary condition nr2
R_1=787.1;
R_2=5298.3;
h_1 = 162;
h_2 = 188;


for i=1:n;
if r(i) < R_1;
    r(i) = NaN;
```

```
end
end

bb = (k_1 - k_2)/(R_2 - R_1);

alpha_1 = (1/(k_1 + bb*R_1))*log((k_1*R_1 - bb*R_1*(r-R_1))./(k_1*r));
alpha_2 = (1/(k_2 + bb*R_2))*log((k_2*R_2 - bb*R_2*(r-R_2))./(k_2*r));

beta_1  = ((k_1 +bb*R_1)/(bb^2))*log((k_1  - bb*(r-R_1))/k_1 );
beta_2  = ((k_2 +bb*R_2)/(bb^2))*log((k_2  - bb*(r-R_2))/k_2 );

L1 =   ((N/bb).*(r-R_2) + (N).*beta_2 + h_2*h_2).*alpha_1;
L2 =   ((N/bb).*(r-R_1) + (N).*beta_1 + h_1*h_1).*alpha_2;

AA = L1 - L2;
AA = AA./(alpha_1 - alpha_2);

h2 =  sqrt((AA));

% Boundary condition nr11

P1=672.3;
P2=7000.7;
h1P = 162;
h2P = 172;


for i=1:n;
if r(i) < P1;
    r(i) = NaN;

end
end

bb = (k_1 - k_2)/(P2 - P1);

alpha_1 = (1/(k_1 + bb*P1))*log((k_1*P1 - bb*P1*(r-P1))./(k_1*r));
alpha_2 = (1/(k_2 + bb*P2))*log((k_2*P2 - bb*P2*(r-P2))./(k_2*r));

beta_1  = ((k_1 +bb*P1)/(bb^2))*log((k_1  - bb*(r-P1))/k_1 );
beta_2  = ((k_2 +bb*P2)/(bb^2))*log((k_2  - bb*(r-P2))/k_2 );

L1 =   ((N/bb).*(r-P2) + (N).*beta_2 + h2P*h2P).*alpha_1;
L2 =   ((N/bb).*(r-P1) + (N).*beta_1 + h1P*h1P).*alpha_2;

AA = L1 - L2;
AA = AA./(alpha_1 - alpha_2);

h11 =  sqrt((AA));


%confined

dif1=phi-phi1;
dif2=phi-phi2;
dif3=phi-phi8;
dif4=phi-phi9;
dif5=phi-phi11;
max_dif1=max(dif1)
```

```
min_dif1=min(dif1)
max_dif2=max(dif2)
min_dif2=min(dif2)
max_dif3=max(dif3)
min_dif3=min(dif3)
max_dif4=max(dif4)
min_dif4=min(dif4)
max_dif5=max(dif5)
min_dif5=min(dif5)


%phreatic

dif6=h-h1;
dif7=h-h2;
dif8=h-h8;
dif9=h-h9;
dif10=h-h11;

max_dif6=max(dif6)
min_dif6=min(dif6)
max_dif7=max(dif7)
min_dif7=min(dif7)
max_dif8=max(dif8)
min_dif8=min(dif8)
max_dif9=max(dif9)
min_dif9=min(dif9)
max_dif10=max(dif10)
min_dif10=min(dif10)
```

SCRIPT 5

```
%Script to visualize the maximum and the minimum differenses in head from
%the eleven measurements analytical solutions. The maximums are for
%boundary condition nr eight and nine, and the minimum values are for
%boundary condition one and two.
%(see script for the eleven different boundary conditions)

%Script to visualize the maximum and the minimum differenses in distance
%between R1 and R2 from the eleven measurements analytical solutions. The
maximum is for
%boundary condition nr eleven, and the minimum value is for boundary
condition two.
%(see script for the eleven different boundary conditions.


%The script contains equations both for confined and phreatic aquifer.


tr = load('Trandum_corr.obs');

X = tr(:,1);
Y = tr(:,2);
heads = tr(:,3);

[n,m] = size(heads);

Trandum_origo_x = 8400.00;
Trandum_origo_y = 7150.00;

%Use the position of the observation wells at Trandum to find the different
%radius' that I want to use in my calculations. This makes it easy to
```

```
%compare the analytical solution with the observations done in the field.

r = sqrt((X-Trandum_origo_x).^2 + (Y-Trandum_origo_y).^2);

%Use the optimal values found by calculation. N is based on the spacific
%discharge of the river Risa.

H1 = 301.86;
H2 = 66.19;
k = 1.727901e-5;
N = 1.266730e-8;

subplot(2,2,1)
xlabel('radius from the Trandum portal [m]'),
ylabel('heads [m]'),
title('A Confined grw.levels'), grid;
hold;

%CONFINED

% Boundary condition nr1
phi1 = 160;
phi2 = 186;
R1 = 291.2;
R2 = 5372.3;

for i=1:n;
if r(i) < R1;
    r(i) = NaN;

end
end

a = (H1 - H2)/(R2 - R1);

A_1  = (1/(H1 + a*R1)) * log((H1*R1 - a*R1*(r-R1))./(H1*r));
A_2  = (1/(H2 + a*R2)) * log((H2*R2 - a*R2*(r-R2))./(H2*r));

B_1  = ((H1+a*R1)/(a^2)) * log((H1 - a*(r-R1))/H1);
B_2  = ((H2+a*R2)/(a^2)) * log((H2 - a*(r-R2))/H2);

ledd_1 =   ((N/(2*k*a)) .* (r-R2) + N/(2*k) .*B_2 + phi2) .* A_1;
ledd_2 =   ((N/(2*k*a)) .* (r-R1) + N/(2*k) .*B_1 + phi1) .* A_2;

AA = ledd_1 - ledd_2;

phi1 = AA./(A_1 - A_2);

subplot(2,2,1)
plot(r,phi1, 'b+');


% Boundary condition nr2
R_1=787.1;
R_2=5298.3;
phi_1 = 162;
phi_2 = 188;

for i=1:n;
if r(i) < R_1;
```

```
    r(i) = NaN;

end
end

a = (H1 - H2)/(R_2 - R_1);

A_1  = (1/(H1 + a*R_1)) * log((H1*R_1 - a*R_1*(r-R_1))./(H1*r));
A_2  = (1/(H2 + a*R_2)) * log((H2*R_2 - a*R_2*(r-R_2))./(H2*r));

B_1  = ((H1+a*R_1)/(a^2)) * log((H1 - a*(r-R_1))/H1);
B_2  = ((H2+a*R_2)/(a^2)) * log((H2 - a*(r-R_2))/H2);

ledd_1 =   ((N/(2*k*a)) .* (r-R_2) + N/(2*k) .*B_2 + phi_2) .* A_1;
ledd_2 =   ((N/(2*k*a)) .* (r-R_1) + N/(2*k) .*B_1 + phi_1) .* A_2;

AA = ledd_1 - ledd_2;

phi2 = AA./(A_1 - A_2);

subplot(2,2,1)
plot(r,phi2, 'b+');

% Boundary condition nr8

L1=1156.0;
L2=6095.4;
phi1L = 166;
phi2L = 174;


for i=1:n;
if r(i) < L1;
    r(i) = NaN;

end
end

a = (H1 - H2)/(L2 - L1);

A_1  = (1/(H1 + a*L1)) * log((H1*L1 - a*L1*(r-L1))./(H1*r));
A_2  = (1/(H2 + a*L2)) * log((H2*L2 - a*L2*(r-L2))./(H2*r));

B_1  = ((H1+a*L1)/(a^2)) * log((H1 - a*(r-L1))/H1);
B_2  = ((H2+a*L2)/(a^2)) * log((H2 - a*(r-L2))/H2);

ledd_1 =   ((N/(2*k*a)) .* (r-L2) + N/(2*k) .*B_2 + phi2L) .* A_1;
ledd_2 =   ((N/(2*k*a)) .* (r-L1) + N/(2*k) .*B_1 + phi1L) .* A_2;

AA = ledd_1 - ledd_2;

phi8 = AA./(A_1 - A_2);

subplot(2,2,1)
plot(r,phi8, 'r+');

% Boundary condition nr9

M1=1084.1;
M2=6110.0;
phi1M = 166;
```

```
phi2M = 174;


for i=1:n;
if r(i) < M1;
    r(i) = NaN;

end
end

a = (H1 - H2)/(M2 - M1);

A_1  = (1/(H1 + a*M1)) * log((H1*M1 - a*M1*(r-M1))./(H1*r));
A_2  = (1/(H2 + a*M2)) * log((H2*M2 - a*M2*(r-M2))./(H2*r));

B_1  = ((H1+a*M1)/(a^2)) * log((H1 - a*(r-M1))/H1);
B_2  = ((H2+a*M2)/(a^2)) * log((H2 - a*(r-M2))/H2);

ledd_1 =   ((N/(2*k*a)) .* (r-M2) + N/(2*k) .*B_2 + phi2M) .* A_1;
ledd_2 =   ((N/(2*k*a)) .* (r-M1) + N/(2*k) .*B_1 + phi1M) .* A_2;

AA = ledd_1 - ledd_2;

phi9 = AA./(A_1 - A_2);

subplot(2,2,1)
plot(r,phi9, 'r+');


%UNCONFINED/PHREATIC

%Use the optimal values found by calculation. N is based on the spacific
%discharge of the river Risa.
k_1 = 2.886e-5;
k_2 = 5.693e-6;
N = 1.266730e-8;


subplot(2,2,2)
xlabel('radius from the Trandum portal [m]'),
ylabel('heads [m]'),
title('B Phreatic grw.levels'), grid;
hold;

% Boundary condition nr1

h1 = 160;
h2 = 186;
R1 = 291.2;
R2 = 5372.3;

for i=1:n;
if r(i) < R1;
    r(i) = NaN;

end
end

bb = (k_1 - k_2)/(R2 - R11);
```

```
alpha_1 = (1/(k_1 + bb*R1))*log((k_1*R1 - bb*R1*(r-R1))./(k_1*r));
alpha_2 = (1/(k_2 + bb*R2))*log((k_2*R2 - bb*R2*(r-R2))./(k_2*r));

beta_1  = ((k_1 +bb*R1)/(bb^2))*log((k_1  - bb*(r-R1))/k_1 );
beta_2  = ((k_2 +bb*R2)/(bb^2))*log((k_2  - bb*(r-R2))/k_2 );

L1 =   ((N/bb).*(r-R2) + (N).*beta_2 + h2*h2).*alpha_1;
L2 =   ((N/bb).*(r-R1) + (N).*beta_1 + h1*h1).*alpha_2;

AA = L1 - L2;
AA = AA./(alpha_1 - alpha_2);

h1 =  sqrt((AA));

subplot(2,2,2)
plot(r,h1,'b+');

% Boundary condition nr2
R_1=787.1;
R_2=5298.3;
h_1 = 162;
h_2 = 188;

for i=1:n;
if r(i) < R_1;
    r(i) = NaN;

end
end

bb = (k_1 - k_2)/(R_2 - R_1);

alpha_1 = (1/(k_1 + bb*R_1))*log((k_1*R_1 - bb*R_1*(r-R_1))./(k_1*r));
alpha_2 = (1/(k_2 + bb*R_2))*log((k_2*R_2 - bb*R_2*(r-R_2))./(k_2*r));

beta_1  = ((k_1 +bb*R_1)/(bb^2))*log((k_1  - bb*(r-R_1))/k_1 );
beta_2  = ((k_2 +bb*R_2)/(bb^2))*log((k_2  - bb*(r-R_2))/k_2 );

L1 =   ((N/bb).*(r-R_2) + (N).*beta_2 + h_2*h_2).*alpha_1;
L2 =   ((N/bb).*(r-R_1) + (N).*beta_1 + h_1*h_1).*alpha_2;

AA = L1 - L2;
AA = AA./(alpha_1 - alpha_2);

h2 =  sqrt((AA));

subplot(2,2,2)
plot(r,h2, 'b+');

% Boundary condition nr8

S1=1156.0;
S2=6095.4;
h1S = 166;
h2S = 174;

for i=1:n;
if r(i) < S1;
    r(i) = NaN;

end
```

```
end

bb = (k_1 - k_2)/(S2 - S1);

alpha_1 = (1/(k_1 + bb*S1))*log((k_1*S1 - bb*S1*(r-S1))./(k_1*r));
alpha_2 = (1/(k_2 + bb*S2))*log((k_2*S2 - bb*S2*(r-S2))./(k_2*r));

beta_1  = ((k_1 +bb*S1)/(bb^2))*log((k_1  - bb*(r-S1))/k_1 );
beta_2  = ((k_2 +bb*S2)/(bb^2))*log((k_2  - bb*(r-S2))/k_2 );

L1 =   ((N/bb).*(r-S2) + (N).*beta_2 + h2S*h2S).*alpha_1;
L2 =   ((N/bb).*(r-S1) + (N).*beta_1 + h1S*h1S).*alpha_2;

AA = L1 - L2;
AA = AA./(alpha_1 - alpha_2);

h8 =  sqrt((AA));

subplot(2,2,2)
plot(r,h8, 'r+');

% Boundary condition nr9

M1=1084.1;
M2=6110.0;
h1M = 166;
h2M = 174;

for i=1:n;
if r(i) < M1;
    r(i) = NaN;

end
end

bb = (k_1 - k_2)/(M2 - M1);

alpha_1 = (1/(k_1 + bb*M1))*log((k_1*M1 - bb*M1*(r-M1))./(k_1*r));
alpha_2 = (1/(k_2 + bb*M2))*log((k_2*M2 - bb*M2*(r-M2))./(k_2*r));

beta_1  = ((k_1 +bb*M1)/(bb^2))*log((k_1  - bb*(r-M1))/k_1 );
beta_2  = ((k_2 +bb*M2)/(bb^2))*log((k_2  - bb*(r-M2))/k_2 );

L1 =   ((N/bb).*(r-M2) + (N).*beta_2 + h2M*h2M).*alpha_1;
L2 =   ((N/bb).*(r-M1) + (N).*beta_1 + h1M*h1M).*alpha_2;

AA = L1 - L2;
AA = AA./(alpha_1 - alpha_2);

h9 =  sqrt((AA));

subplot(2,2,2)
plot(r,h9, 'r+');


% largest and smallest distance between R1 and R2


subplot(2,2,3);
xlabel('radius from the Trandum portal [m]'),
```

```
ylabel('heads [m]'),
title('C Confined grw.levels'), grid;
hold;

%CONFINED AQUIFER

%Use the optimal values found by calculation. N is based on the spacific
%discharge of the river Risa.

H1 = 301.86;
H2 = 66.19;
k = 1.727901e-5;
N = 1.266730e-8;

% Boundary condition nr2

R_1=787.1;
R_2=5298.3;
phi_1 = 162;
phi_2 = 188;


for i=1:n;
if r(i) < R_1;
    r(i) = NaN;

end
end

a = (H1 - H2)/(R_2 - R_1);

A_1  = (1/(H1 + a*R_1)) * log((H1*R_1 - a*R_1*(r-R_1))./(H1*r));
A_2  = (1/(H2 + a*R_2)) * log((H2*R_2 - a*R_2*(r-R_2))./(H2*r));

B_1  = ((H1+a*R_1)/(a^2)) * log((H1 - a*(r-R_1))/H1);
B_2  = ((H2+a*R_2)/(a^2)) * log((H2 - a*(r-R_2))/H2);

ledd_1 =   ((N/(2*k*a)) .* (r-R_2) + N/(2*k) .*B_2 + phi_2) .* A_1;
ledd_2 =   ((N/(2*k*a)) .* (r-R_1) + N/(2*k) .*B_1 + phi_1) .* A_2;

AA = ledd_1 - ledd_2;

phi2 = AA./(A_1 - A_2);

%plotting heads nr2

subplot(2,2,3)
plot(r,phi2, 'b+');

% Boundary condition nr11

P1=672.3;
P2=7000.7;
phi1P = 162;
phi2P = 172;


for i=1:n;
if r(i) < P1;
    r(i) = NaN;
```

```
end
end

a = (H1 - H2)/(P2 - P1);

A_1  = (1/(H1 + a*P1)) * log((H1*P1 - a*P1*(r-P1))./(H1*r));
A_2  = (1/(H2 + a*P2)) * log((H2*P2 - a*P2*(r-P2))./(H2*r));

B_1  = ((H1+a*P1)/(a^2)) * log((H1 - a*(r-P1))/H1);
B_2  = ((H2+a*P2)/(a^2)) * log((H2 - a*(r-P2))/H2);

ledd_1 =   ((N/(2*k*a)) .* (r-P2) + N/(2*k) .*B_2 + phi2P) .* A_1;
ledd_2 =   ((N/(2*k*a)) .* (r-P1) + N/(2*k) .*B_1 + phi1P) .* A_2;

AA = ledd_1 - ledd_2;

phi11 = AA./(A_1 - A_2);

%plotting heads nr 11

subplot(2,2,3)
plot(r,phi11, 'r+');

%OPEN/PHREATIC AQUIFER

%Use the optimal values found by calculation. N is based on the spacific
%discharge of the river Risa.

h1 = 171.50;
h2 = 185;
N = 1.266730e-8;


subplot(2,2,4);
xlabel('radius from the Trandum portal [m]'),
ylabel('heads [m]'),
title('D Phreatic grw.levels'), grid;
hold;



% Boundary condition nr2
R_1=787.1;
R_2=5298.3;
h_1 = 162;
h_2 = 188;


for i=1:n;
if r(i) < R_1;
    r(i) = NaN;

end
end

bb = (k_1 - k_2)/(R_2 - R_1);

alpha_1 = (1/(k_1 + bb*R_1))*log((k_1*R_1 - bb*R_1*(r-R_1))./(k_1*r));
alpha_2 = (1/(k_2 + bb*R_2))*log((k_2*R_2 - bb*R_2*(r-R_2))./(k_2*r));
```

```
beta_1  = ((k_1 +bb*R_1)/(bb^2))*log((k_1  - bb*(r-R_1))/k_1 );
beta_2  = ((k_2 +bb*R_2)/(bb^2))*log((k_2  - bb*(r-R_2))/k_2 );

L1 =   ((N/bb).*(r-R_2) + (N).*beta_2 + h_2*h_2).*alpha_1;
L2 =   ((N/bb).*(r-R_1) + (N).*beta_1 + h_1*h_1).*alpha_2;

AA = L1 - L2;
AA = AA./(alpha_1 - alpha_2);

h2 =  sqrt((AA));

%plotting heads nr2

subplot(2,2,4)
plot(r,h2, 'b+');

% Boundary condition nr11

P1=672.3;
P2=7000.7;
h1P = 162;
h2P = 172;


for i=1:n;
if r(i) < P1;
    r(i) = NaN;

end
end

bb = (k_1 - k_2)/(P2 - P1);

alpha_1 = (1/(k_1 + bb*P1))*log((k_1*P1 - bb*P1*(r-P1))./(k_1*r));
alpha_2 = (1/(k_2 + bb*P2))*log((k_2*P2 - bb*P2*(r-P2))./(k_2*r));

beta_1  = ((k_1 +bb*P1)/(bb^2))*log((k_1  - bb*(r-P1))/k_1 );
beta_2  = ((k_2 +bb*P2)/(bb^2))*log((k_2  - bb*(r-P2))/k_2 );

L1 =   ((N/bb).*(r-P2) + (N).*beta_2 + h2P*h2P).*alpha_1;
L2 =   ((N/bb).*(r-P1) + (N).*beta_1 + h1P*h1P).*alpha_2;

AA = L1 - L2;
AA = AA./(alpha_1 - alpha_2);

h11 =  sqrt((AA));

%plotting heads nr11

subplot(2,2,4)
plot(r,h11, 'r+');


%confined

d1 = phi1 - phi8;
d2 = phi2 - phi8;
d3 = phi1 - phi9;
d4 = phi2 - phi9;
d5 = phi11 - phi2;
```

```
max_d1=max(d1)
min_d1=min(d1)
max_d2=max(d2)
min_d2=min(d2)
max_d3=max(d3)
min_d3=min(d3)
max_d4=max(d4)
min_d4=min(d4)
max_d5=max(d5)
min_d5=min(d5)


%phreatic

d6 = h1 - h8;
d7 = h2 - h8;
d8 = h1 - h9;
d9 = h2 - h9;
d10 = h11 - h2;

max_d6=max(d6)
min_d6=min(d6
max_d7=max(d7)
min_d7=min(d7)
max_d8=max(d8)
min_d8=min(d8)
max_d9=max(d9)
min_d9=min(d9)
max_d10=max(d10)
min_d10=min(d10)
```

SCRIPT 6

```
%Compare calculated head for an confined aquifer and the heads observed in
the
%field.Analytical solution.
%Compare the analytical solutions between open/phreatic and closed aquifer

tr = load('Trandum_corr.obs');

X = tr(:,1);
Y = tr(:,2);
heads = tr(:,3);


Trandum_origo_x = 8400.00;
Trandum_origo_y = 7150.00;

%Use the position of the observation wells at Trandum to find the different
%radius' that I want to use in my calculations. This makes it easy to
%compare the analytical solution with the observations done in the field.

r = sqrt((X-Trandum_origo_x).^2 + (Y-Trandum_origo_y).^2);



%CONFINED AQUIFER
```

```
%Use the optimal values found by calculation. N is based on the spacific
%discharge of the river Risa.

H1 = 301.86;
H2 = 66.19;
k = 1.727901e-5;
phi1 = 171.50;
phi2 = 185;
R1 = 336;
R2 = 5100;
N = 1.266730e-8;

subplot(2,2,[1 3])
xlabel('radius from the Trandum portal [m]'),
ylabel('heads [m]'),
title(' A Phreatic and Confined grw.levels'), grid;
hold;

a = (H1 - H2)/(R2 - R1);

A_1  = (1/(H1 + a*R1)) * log((H1*R1 - a*R1*(r-R1))./(H1*r));
A_2  = (1/(H2 + a*R2)) * log((H2*R2 - a*R2*(r-R2))./(H2*r));

B_1  = ((H1+a*R1)/(a^2)) * log((H1 - a*(r-R1))/H1);
B_2  = ((H2+a*R2)/(a^2)) * log((H2 - a*(r-R2))/H2);

ledd_1 =   ((N/(2*k*a)) .* (r-R2) + N/(2*k) .*B_2 + phi2) .* A_1;
ledd_2 =   ((N/(2*k*a)) .* (r-R1) + N/(2*k) .*B_1 + phi1) .* A_2;

AA = ledd_1 - ledd_2;

phi = AA./(A_1 - A_2);

subplot(2,2,[1 3])
plot(r,phi,'r+')

%OPEN/PHREATIC AQUIFER

%Use the optimal values found by calculation. N is based on the spacific
%discharge of the river Risa.

k_1 = 2.886e-5;
k_2 = 5.693e-6
h1 = 171.50;
h2 = 185;
R1 = 336;
R2 = 5100;
N = 1.266730e-8;


bb = (k_1 - k_2)/(R2 - R1);

alpha_1 = (1/(k_1 + bb*R1))*log((k_1*R1 - bb*R1*(r-R1))./(k_1*r));
alpha_2 = (1/(k_2 + bb*R2))*log((k_2*R2 - bb*R2*(r-R2))./(k_2*r));

beta_1  = ((k_1 +bb*R1)/(bb^2))*log((k_1  - bb*(r-R1))/k_1 );
beta_2  = ((k_2 +bb*R2)/(bb^2))*log((k_2  - bb*(r-R2))/k_2 );

L1 =   ((N/bb).*(r-R2) + (N).*beta_2 + h2*h2).*alpha_1;
L2 =   ((N/bb).*(r-R1) + (N).*beta_1 + h1*h1).*alpha_2;
```

```
AA = L1 - L2;
AA = AA./(alpha_1 - alpha_2);

h =  sqrt((AA));

subplot(2,2,[1 3])
plot(r,h,'b+');

% observed heads

tr = load('Trandum_corr.obs');

X = tr(:,1);
Y = tr(:,2);
heads = tr(:,3);

%calculated heads

Trandum_origo_x = 8400.00;
Trandum_origo_y = 7150.00;

%Use the position of the observation wells at Trandum to find the different
%radius' that I want to use in my calculations. This makes it easy to
%compare the analytical solution with the observations done in the field.

r = sqrt((X-Trandum_origo_x).^2 + (Y-Trandum_origo_y).^2);

%Use the optimal values found by calculation. N is based on the spacific
%discharge of the river Risa.

H1 = 301.86;
H2 = 66.19;
k = 1.727901e-5;
phi1 = 171.50;
phi2 = 185;
R1 = 336;
R2 = 5100;
N = 1.266730e-8;

subplot(2,2,2),
xlabel('radius from the Trandum portal [m]'),
ylabel('heads [m]'),
title('B Confined grw.levels'), grid;
hold;


a = (H1 - H2)/(R2 - R1);

A_1  = (1/(H1 + a*R1)) * log((H1*R1 - a*R1*(r-R1))./(H1*r));
A_2  = (1/(H2 + a*R2)) * log((H2*R2 - a*R2*(r-R2))./(H2*r));

B_1  = ((H1+a*R1)/(a^2)) * log((H1 - a*(r-R1))/H1);
B_2  = ((H2+a*R2)/(a^2)) * log((H2 - a*(r-R2))/H2);

ledd_1 =   ((N/(2*k*a)) .* (r-R2) + N/(2*k) .*B_2 + phi2) .* A_1;
ledd_2 =   ((N/(2*k*a)) .* (r-R1) + N/(2*k) .*B_1 + phi1) .* A_2;

AA = ledd_1 - ledd_2;

phi = AA./(A_1 - A_2);
```

```
%plotting observed heads
subplot(2,2,2),
plot(r,heads,'ro');

%plotting calculated heads
subplot(2,2,2),
plot(r,phi,'b+');

%Compare calculated head for an open/phreatic aquifer and the heads
observed in the
%field.Analytical solution.



%observed heads
tr = load('Trandum_corr.obs');

X = tr(:,1);
Y = tr(:,2);
heads = tr(:,3);

[n,m] = size(heads);

Trandum_origo_x = 8400.00;
Trandum_origo_y = 7150.00;

%Use the position of the observation wells at Trandum to find the different
%radius' that I want to use in my calculations. This makes it easy to
%compare the analytical solution with the observations done in the field.

r = sqrt((X-Trandum_origo_x).^2 + (Y-Trandum_origo_y).^2);

%Use the optimal values found by calculation. N is based on the spacific
%discharge of the river Risa.

k_1 = 2.886e-5;
k_2 = 5.693e-6;
h1 = 171.50;
h2 = 185;
R1 = 336;
R2 = 5100;
N = 1.266730e-8;

subplot(2,2,4),
xlabel('radius from the Trandum portal [m]'),
ylabel('heads [m]'),
title('C Phreatic grw.levels'), grid;
hold;

bb = (k_1 - k_2)/(R2 - R1);

alpha_1 = (1/(k_1 + bb*R1))*log((k_1*R1 - bb*R1*(r-R1))./(k_1*r));
alpha_2 = (1/(k_2 + bb*R2))*log((k_2*R2 - bb*R2*(r-R2))./(k_2*r));

beta_1  = ((k_1 +bb*R1)/(bb^2))*log((k_1  - bb*(r-R1))/k_1 );
beta_2  = ((k_2 +bb*R2)/(bb^2))*log((k_2  - bb*(r-R2))/k_2 );

L1 =   ((N/bb).*(r-R2) + (N).*beta_2 + h2*h2).*alpha_1;
L2 =   ((N/bb).*(r-R1) + (N).*beta_1 + h1*h1).*alpha_2;
```

```
AA = L1 - L2;
AA = AA./(alpha_1 - alpha_2);

h =  sqrt((AA));

%plotting the observed heads
subplot(2,2,4),
plot(r,heads,'ro')

%plotting the calculated heads
subplot(2,2,4),
plot(r,h,'b+');


%compare phreatic and confined
dif_phi_h= phi-h;
mean_dif_phi_h=mean(dif_phi_h)
max_dif_phi_h=max(dif_phi_h)
min_dif_phi_h=min(dif_phi_h)
```
std_dif_phi_h=std(dif_phi_h

SCRIPT 7

```
%Script to make 3-d model of the analytical solution for a confined
%aquifer.

R1=336;              % inner radius
R2=5100;             % outer radius
dx=100;              % grid spacing in x
dy=100;              % grid spacing in y
H1 = 301.86;
H2 = 66.19;
R1 = 336;
R2 = 5100;
N = 1.266730e-8;
phi1 = 171.50;
phi2 = 185;
k = 1.727901e-5;
origo_x = dx/2;         % x-origo
origo_y = dy/2;      % y-origo
x=origo_x:dx:R2+dx;        % x-array
y=origo_y:dy:R2+dy;        % y-array
xcol=(R2+dx)/dx;  % no of columns in x
ycol=(R2+dy)/dy;  % no of rows in y

for i = 1:xcol
  for j = 1:ycol

    r(i,j) = (sqrt((x(i)-origo_x)^2 + (y(j)-origo_y)^2));

    if (r(i,j) >= R1 && r(i,j) <= R2);

a = (H1 - H2)/(R2 - R1);

A_1  = (1/(H1 + a*R1)) * log((H1*R1 - a*R1*(r(i,j)-R1))./(H1*r(i,j)));
A_2  = (1/(H2 + a*R2)) * log((H2*R2 - a*R2*(r(i,j)-R2))./(H2*r(i,j)));

B_1  = ((H1+a*R1)/(a^2)) * log((H1 - a*(r(i,j)-R1))/H1);
```

```
B_2  = ((H2+a*R2)/(a^2)) * log((H2 - a*(r(i,j)-R2))/H2);

ledd_1 =   ((N/(2*k*a)) .* (r(i,j)-R2) + N/(2*k) .*B_2 + phi2) .* A_1;
ledd_2 =   ((N/(2*k*a)) .* (r(i,j)-R1) + N/(2*k) .*B_1 + phi1) .* A_2;

AA = ledd_1 - ledd_2;
phi(i,j) = AA./(A_1 - A_2);

      else

      h(i,j) = NaN;
      phi(i,j) = NaN;

    end;

  end;
end;

mesh(phi)
```

SCRIPT 8

```
%Script to make 3-d model of the analytical solution for a phreatic
%aquifer.
R1=336;              % inner radius
R2=5100;             % outher radius
dx=100;              % grid spacing in x
dy=100;              % grid spacing in y
k_1 = 2.886e-5;
k_2 = 5.693e-6;
h1 = 171.50;
h2 = 185;
R1 = 336;
R2 = 5100;
N = 1.266730e-8;
origo_x = dx/2;         % x-origo
origo_y = dy/2;      % y-origo
x=origo_x:dx:R2+dx;        % x-array
y=origo_y:dy:R2+dy;        % y-array
xcol=(R2+dx)/dx;  % no of columns in x
ycol=(R2+dy)/dy;  % no of rows in y

for i = 1:xcol
  for j = 1:ycol

    r(i,j) = (sqrt((x(i)-origo_x)^2 + (y(j)-origo_y)^2));

    if (r(i,j) >= R1 && r(i,j) <= R2);


bb = (k_1 - k_2)/(R2 - R1);
alpha_1 = (1/(k_1 + bb*R1))*log((k_1*R1 - bb*R1*(r(i,j)-
R1))./(k_1*r(i,j)));
alpha_2 = (1/(k_2 + bb*R2))*log((k_2*R2 - bb*R2*(r(i,j)-
R2))./(k_2*r(i,j)));
beta_1  = ((k_1 +bb*R1)/(bb^2))*log((k_1  - bb*(r(i,j)-R1))/k_1 );
beta_2  = ((k_2 +bb*R2)/(bb^2))*log((k_2  - bb*(r(i,j)-R2))/k_2 );
L1 =   ((N/bb).*(r(i,j)-R2) + (N).*beta_2 + h2*h2).*alpha_1;
L2 =   ((N/bb).*(r(i,j)-R1) + (N).*beta_1 + h1*h1).*alpha_2;
AA = L1 - L2;
AA = AA./(alpha_1 - alpha_2);
```

```
h(i,j) =  sqrt((AA));

    else

      h(i,j) = NaN;

    end;

  end;
end;

mesh(h)
```

SCRIPT 9

```
% make inputfiles to PWMIN

R1=336.0;              % inner radius
R2=5100.0;             % outher radius
dx=100;              % grid spacing in x
dy=100;              % grid spacing in y

h1=100.0;            % initial head  at R1
h2=100.0;            % initial head  at R2

xcol=(R2+dx)/dx;  % no of columns in x
ycol=(R2+dy)/dy;  % no of rows in y

origo_x = dx/2;      % x-origo
origo_y = dy/2;      % y-origo

x=origo_x:dx:R2+dx;        % x-array
y=origo_y:dy:R2+dx;        % y-array

N  = 1.266730e-8;

H1 = 301.86;
H2 = 66.19;
k1 = 1.727901e-5;
k2 = 1.727901e-5;
k  = 1.727901e-5;

a = (H1-H2)/(R2-R1); % H(r) = H1 - a*(r-R1)

kc = 1.727901e-5;


top = 0;


fh = fopen('ihead.DAT','w');  % file with initial heads
fk = fopen('khead.DAT','w');  % file with constant heads, and
                              % inactive cells
fhyd = fopen('hydc.DAT','w');  % file with hydraluclic
                              % conductivities
fpre = fopen('prec.DAT','w'); % file precipitation
```

```
ftop = fopen('aqtop.DAT','w');% top of aquifer
fbot = fopen('aqbot.DAT','w');% bottom of aquifer

fprintf(fh,' %d            %d\n',xcol,ycol);
fprintf(fk,' %d            %d\n',xcol,ycol);
fprintf(fhyd,' %d            %d\n',xcol,ycol);
fprintf(fpre,' %d            %d\n',xcol,ycol);
fprintf(ftop,' %d            %d\n',xcol,ycol);
fprintf(fbot,' %d            %d\n',xcol,ycol);
hsmesh = ones(xcol,ycol);
ihead  = ones(xcol,ycol);
ik     = ones(xcol,ycol);
itop   = ones(xcol,ycol);
ibot   = ones(xcol,ycol);
```

SCRIPT 10

```
%make inputfiles to PWMIN

clear;

R1=336.0;             % inner radius
R2=5100.0;            % outher radius
dx=100;              % grid spacing in x
dy=100;              % grid spacing in y

h1=171.50;           % initial head  at R1
h2=185.00;           % initial head  at R2

xcol=(R2+dx)/dx;  % no of columns in x
ycol=(R2+dy)/dy;  % no of rows in y

origo_x = dx/2;     % x-origo
origo_y = dy/2;     % y-origo

x=origo_x:dx:R2+dx;       % x-array
y=origo_y:dy:R2+dx;       % y-array
N  = 1.266730e-8
H1 = 301.86;
H2 = 66.19;          % for phreatic bot = -0.1 m is OK
k1 = 2.886e-05;
k2 = 5.693e-06;
k  = 1.727901e-5;

b = (k1-k2)/(R2-R1); % H(r) = H1 - a*(r-R1)

kc = 1.727901e-5;

top = 0;


fh = fopen('ihead2.DAT','w');  % file with initial heads
fk = fopen('khead2.DAT','w');  % file with constant heads, and
                              % inactive cells
fhyd = fopen('hydc2.DAT','w');  % file with hydraluclic
                              % conductivities
fpre = fopen('prec2.DAT','w'); % file precipitation

ftop = fopen('aqtop2.DAT','w');% top of aquifer
fcond = fopen('cond2.DAT','w');% bottom of aquifer
```

```
fprintf(fh,' %d            %d\n',xcol,ycol);
fprintf(fk,' %d            %d\n',xcol,ycol);
fprintf(fhyd,' %d            %d\n',xcol,ycol);
fprintf(fpre,' %d            %d\n',xcol,ycol);
fprintf(ftop,' %d            %d\n',xcol,ycol);
fprintf(fcond,' %d            %d\n',xcol,ycol);

hsmesh = ones(xcol,ycol);
ihead  = ones(xcol,ycol);
ik     = ones(xcol,ycol);
itop   = ones(xcol,ycol);
icond   = ones(xcol,ycol);
```

SCRIPT 11

```
%Script to calculate the differences between the numerical solutions with
%circular boundaries and ravines. Phreatic

R1=336;             % inner radius
R2=5100;            % outher radius
dx=100;             % grid spacing in x
dy=100;             % grid spacing in y

origo_x = dx/2;        % x-origo
origo_y = dy/2;     % y-origo
x=origo_x:dx:R2+dx;       % x-array
y=origo_y:dy:R2+dy;       % y-array
xcol=(R2-dx)/dx;  % no of columns in x
ycol=(R2-dy)/dy;  % no of rows in y

for i = 1:xcol
  for j = 1:ycol

    r(i,j) = (sqrt((x(i)-origo_x)^2 + (y(j)-origo_y)^2));

    if (r(i,j) >= R1 && r(i,j) <= R2);
    else
      phipmw3(i,j) = NaN;
      phipmw4(i,j) = NaN;
    end;

  end;
end;

hif=fopen('modell_3_h','r');
 col = fscanf(hif,'%d',[1 1]);
rad = fscanf(hif,'%d',[1 1]);
 phipmw3 = fscanf(hif,'%f', [col rad]);
 for i=1:col;
  for j=1:rad;
    if phipmw3(i,j)== -999.9900;
      phipmw3(i,j) = NaN;
    end;
  end;
end;
hif=fopen('modell_4_h','r');
col = fscanf(hif,'%d',[1 1]);
rad = fscanf(hif,'%d',[1 1]);
```

```
phipmw4 = fscanf(hif,'%f', [col rad]);

for i=1:col;
  for j=1:rad;
    if phipmw4(i,j)== -999.9900;
      phipmw4(i,j) = NaN;
    end;
  end;
end;
dif_m3_m4 =phipmw3-phipmw4;
mesh(dif_m3_m4);
max_dif_m3_m4=max(dif_m3_m4);
```

SCRIPT 12

```
%Script to calculate the differences between the numerical solutions with
%circular boundaries and ravines. Confined

R1=336;             % inner radius
R2=5100;            % outher radius
dx=100;             % grid spacing in x
dy=100;             % grid spacing in y

origo_x = dx/2;        % x-origo
origo_y = dy/2;     % y-origo
x=origo_x:dx:R2+dx;       % x-array
y=origo_y:dy:R2+dy;       % y-array
xcol=(R2-dx)/dx;  % no of columns in x
ycol=(R2-dy)/dy;  % no of rows in y

for i = 1:xcol
  for j = 1:ycol

    r(i,j) = (sqrt((x(i)-origo_x)^2 + (y(j)-origo_y)^2));

    if (r(i,j) >= R1 && r(i,j) <= R2);
 else

      phipmw1(i,j) = NaN;
      phipmw2(i,j) = NaN;
      phipmw3(i,j) = NaN;
      phipmw4(i,j) = NaN;
    end;

  end;
end;
hif=fopen('modell_1_h','r');
col = fscanf(hif,'%d',[1 1]);
rad = fscanf(hif,'%d',[1 1]);
phipmw1 = fscanf(hif,'%f', [col rad]);
for i=1:col;
  for j=1:rad;
    if phipmw1(i,j)== -999.9900;
      phipmw1(i,j) = NaN;
    end;
  end;
end;
hif=fopen('modell_2_h','r');
col = fscanf(hif,'%d',[1 1]);
rad = fscanf(hif,'%d',[1 1]);
phipmw2 = fscanf(hif,'%f', [col rad]);
```

```
for i=1:col;
  for j=1:rad;
    if phipmw2(i,j)== -999.9900;
      phipmw2(i,j) = NaN;
    end;
  end;
end;
dif_m1_m2 =phipmw1-phipmw2;
mesh(dif_m1_m2);
max_dif_m1_m2=max(dif_m1_m2);
```

SCRIPT 13

```
% script to compare analytical and numerical models. Confined

R1=336;             % inner radius
R2=5100;            % outher radius
dx=100;             % grid spacing in x
dy=100;             % grid spacing in y

H1 = 301.86;
H2 = 66.19;
k_1 = 2.886e-5;
k_2 = 5.693e-6;
h1 = 171.50;
h2 = 185;
R1 = 336;
R2 = 5100;
N = 1.266730e-8;
phi1 = 171.50;
phi2 = 185;
k = 1.727901e-5;

origo_x = dx/2;        % x-origo
origo_y = dy/2;     % y-origo

x=origo_x:dx:R2+dx;       % x-array
y=origo_y:dy:R2+dy;       % y-array

xcol=(R2-dx)/dx;  % no of columns in x
ycol=(R2-dy)/dy;  % no of rows in y

for i = 1:xcol
  for j = 1:ycol

    r(i,j) = (sqrt((x(i)-origo_x)^2 + (y(j)-origo_y)^2));

    if (r(i,j) >= R1 && r(i,j) <= R2);

a = (H1 - H2)/(R2 - R1);

A_1  = (1/(H1 + a*R1)) * log((H1*R1 - a*R1*(r(i,j)-R1))./(H1*r(i,j)));
A_2  = (1/(H2 + a*R2)) * log((H2*R2 - a*R2*(r(i,j)-R2))./(H2*r(i,j)));

B_1  = ((H1+a*R1)/(a^2)) * log((H1 - a*(r(i,j)-R1))/H1);
B_2  = ((H2+a*R2)/(a^2)) * log((H2 - a*(r(i,j)-R2))/H2);

ledd_1 =   ((N/(2*k*a)) .* (r(i,j)-R2) + N/(2*k) .*B_2 + phi2) .* A_1;
ledd_2 =   ((N/(2*k*a)) .* (r(i,j)-R1) + N/(2*k) .*B_1 + phi1) .* A_2;
```

```
AA = ledd_1 - ledd_2;

phi(i,j) = AA./(A_1 - A_2);
      else
       phi(i,j) = NaN;
     end;

  end;
end;

% model 1 from pmwin: confined
hif=fopen('modell_1_h','r');

col = fscanf(hif,'%d',[1 1]);
rad = fscanf(hif,'%d',[1 1]);

phipmw1 = fscanf(hif,'%f', [col rad]);

for i=1:col;
  for j=1:rad;
    if phipmw1(i,j)== -999.9900;
      phipmw1(i,j) = NaN;
    end;
  end;
end;
dif_phi_pmw1=phi-phipmw1;
mesh(dif_phi_pmw1);
```

SCRIPT 14

```
% script to compare analytical and numerical models. Phreatic

R1=336;             % inner radius
R2=5100;            % outher radius
dx=100;             % grid spacing in x
dy=100;             % grid spacing in y

H1 = 301.86;
H2 = 66.19;
k_1 = 2.886e-5;
k_2 = 5.693e-6;
h1 = 171.50;
h2 = 185;
R1 = 336;
R2 = 5100;
N = 1.266730e-8;
phi1 = 171.50;
phi2 = 185;
k = 1.727901e-5;

origo_x = dx/2;        % x-origo
origo_y = dy/2;     % y-origo

x=origo_x:dx:R2+dx;       % x-array
y=origo_y:dy:R2+dy;       % y-array

xcol=(R2-dx)/dx;  % no of columns in x
ycol=(R2-dy)/dy;  % no of rows in y

for i = 1:xcol
```

```
  for j = 1:ycol

    r(i,j) = (sqrt((x(i)-origo_x)^2 + (y(j)-origo_y)^2));

    if (r(i,j) >= R1 && r(i,j) <= R2);


bb = (k_1 - k_2)/(R2 - R1);

alpha_1 = (1/(k_1 + bb*R1))*log((k_1*R1 - bb*R1*(r(i,j)-
R1))./(k_1*r(i,j)));
alpha_2 = (1/(k_2 + bb*R2))*log((k_2*R2 - bb*R2*(r(i,j)-
R2))./(k_2*r(i,j)));

beta_1  = ((k_1 +bb*R1)/(bb^2))*log((k_1  - bb*(r(i,j)-R1))/k_1 );
beta_2  = ((k_2 +bb*R2)/(bb^2))*log((k_2  - bb*(r(i,j)-R2))/k_2 );

L1 =   ((N/bb).*(r(i,j)-R2) + (N).*beta_2 + h2*h2).*alpha_1;
L2 =   ((N/bb).*(r(i,j)-R1) + (N).*beta_1 + h1*h1).*alpha_2;

AA = L1 - L2;
AA = AA./(alpha_1 - alpha_2);

h(i,j) =  sqrt((AA));
            else

      h(i,j) = NaN;

      end;

  end;
end;
%% read heads from PMWIN output
hif=fopen('modell_3_h','r');

col = fscanf(hif,'%d',[1 1]);
rad = fscanf(hif,'%d',[1 1]);

phipmw3 = fscanf(hif,'%f', [col rad]);

for i=1:col;
  for j=1:rad;
    if phipmw3(i,j)== -999.9900;
      phipmw3(i,j) = NaN;
    end;
  end;
end;

dif_h_pmw2=h-phipmw3;
mesh(dif_h_pmw2);
```

SCRIPT 15

```
%confined model with circular boundaries from PMWIN.

hif=fopen('modell_1_h','r');

col = fscanf(hif,'%d',[1 1]);
rad = fscanf(hif,'%d',[1 1]);
```

```
phipmw1 = fscanf(hif,'%f', [col rad]);

for i=1:col;
  for j=1:rad;
    if phipmw1(i,j)== -999.9900;
      phipmw1(i,j) = NaN;
    end;
  end;
end;
mesh(phipmw1);
```

SCRIPT 16

```
%Confined model with ravines from PMWIN.
hif=fopen('modell_2_h','r');

col = fscanf(hif,'%d',[1 1]);
rad = fscanf(hif,'%d',[1 1]);

phipmw2 = fscanf(hif,'%f', [col rad]);

for i=1:col;
  for j=1:rad;
    if phipmw2(i,j)== -999.9900;
      phipmw2(i,j) = NaN;
    end;
  end;
end;
mesh(phipmw2)
```

SCRIPT 17

```
% Phreatic model with circular boundaries from PMWIN.
hif=fopen('modell_3_h','r');

col = fscanf(hif,'%d',[1 1]);
rad = fscanf(hif,'%d',[1 1]);

phipmw3 = fscanf(hif,'%f', [col rad]);

for i=1:col;
  for j=1:rad;
    if phipmw3(i,j)== -999.9900;
      phipmw3(i,j) = NaN;
    end;
  end;
end;
mesh(phipmw3)
```

SCRIPT 18

```
% Phreatic model with ravines from PMWIN.
hif=fopen('modell_4_h','r');

col = fscanf(hif,'%d',[1 1]);
rad = fscanf(hif,'%d',[1 1]);

phipmw4 = fscanf(hif,'%f', [col rad]);

for i=1:col;
```

```
  for j=1:rad;
    if phipmw4(i,j)== -999.9900;
      phipmw4(i,j) = NaN;
    end;
  end;
end;
mesh(phipmw4)
```

SCRIPT 19

```
% script to compare analytical and numerical models

R1=336;             % inner radius
R2=5100;            % outher radius
dx=100;             % grid spacing in x
dy=100;             % grid spacing in y

H1 = 301.86;
H2 = 66.19;
k_1 = 2.886e-5;
k_2 = 5.693e-6;
h1 = 171.50;
h2 = 185;
R1 = 336;
R2 = 5100;
N = 1.266730e-8;
phi1 = 171.50;
phi2 = 185;
k = 1.727901e-5;

origo_x = dx/2;        % x-origo
origo_y = dy/2;     % y-origo

x=origo_x:dx:R2+dx;       % x-array
y=origo_y:dy:R2+dy;       % y-array

xcol=(R2-dx)/dx;  % no of columns in x
ycol=(R2-dy)/dy;  % no of rows in y

for i = 1:xcol
  for j = 1:ycol

    r(i,j) = (sqrt((x(i)-origo_x)^2 + (y(j)-origo_y)^2));

    if (r(i,j) >= R1 && r(i,j) <= R2);


bb = (k_1 - k_2)/(R2 - R1);

alpha_1 = (1/(k_1 + bb*R1))*log((k_1*R1 - bb*R1*(r(i,j)-
R1))./(k_1*r(i,j)));
alpha_2 = (1/(k_2 + bb*R2))*log((k_2*R2 - bb*R2*(r(i,j)-
R2))./(k_2*r(i,j)));

beta_1  = ((k_1 +bb*R1)/(bb^2))*log((k_1  - bb*(r(i,j)-R1))/k_1 );
beta_2  = ((k_2 +bb*R2)/(bb^2))*log((k_2  - bb*(r(i,j)-R2))/k_2 );

L1 =   ((N/bb).*(r(i,j)-R2) + (N).*beta_2 + h2*h2).*alpha_1;
L2 =   ((N/bb).*(r(i,j)-R1) + (N).*beta_1 + h1*h1).*alpha_2;
```

```
AA = L1 - L2;
AA = AA./(alpha_1 - alpha_2);

h(i,j) =  sqrt((AA));



a = (H1 - H2)/(R2 - R1);

A_1  = (1/(H1 + a*R1)) * log((H1*R1 - a*R1*(r(i,j)-R1))./(H1*r(i,j)));
A_2  = (1/(H2 + a*R2)) * log((H2*R2 - a*R2*(r(i,j)-R2))./(H2*r(i,j)));

B_1  = ((H1+a*R1)/(a^2)) * log((H1 - a*(r(i,j)-R1))/H1);
B_2  = ((H2+a*R2)/(a^2)) * log((H2 - a*(r(i,j)-R2))/H2);

ledd_1 =   ((N/(2*k*a)) .* (r(i,j)-R2) + N/(2*k) .*B_2 + phi2) .* A_1;
ledd_2 =   ((N/(2*k*a)) .* (r(i,j)-R1) + N/(2*k) .*B_1 + phi1) .* A_2;

AA = ledd_1 - ledd_2;

phi(i,j) = AA./(A_1 - A_2);


    else

      h(i,j) = NaN;
      phi(i,j) = NaN;

    end;

  end;
end;
%% read heads from PMWIN output
hif=fopen('modell_1_h','r');

col = fscanf(hif,'%d',[1 1]);
rad = fscanf(hif,'%d',[1 1]);

phipmw1 = fscanf(hif,'%f', [col rad]);

for i=1:col;
  for j=1:rad;
    if phipmw1(i,j)== -999.9900;
      phipmw1(i,j) = NaN;
    end;
  end;
end;


% model 1 from pmwin: confined
hif=fopen('modell_1_h','r');

col = fscanf(hif,'%d',[1 1]);
rad = fscanf(hif,'%d',[1 1]);

phipmw1 = fscanf(hif,'%f', [col rad]);

for i=1:col;
  for j=1:rad;
    if phipmw1(i,j)== -999.9900;
```

```
      phipmw1(i,j) = NaN;
    end;
  end;
end;


% model 1 from pmwin: confined
hif=fopen('modell_3_h','r');

col = fscanf(hif,'%d',[1 1]);
rad = fscanf(hif,'%d',[1 1]);

phipmw3 = fscanf(hif,'%f', [col rad]);

for i=1:col;
  for j=1:rad;
    if phipmw3(i,j)== -999.9900;
      phipmw3(i,j) = NaN;
    end;
  end;
end;


diff3=phi-phipmw1;
max_diff3=max(diff3)
min_diff3=min(diff3)

diff4=h-phipmw3;
max_diff4=max(diff4)
min_diff4=min(diff4)

diff_diag_phi=diag(phi)-diag(phipmw1)
diff_diag_h=diag(h)-diag(phipmw3)

maxdiff_diag_phi=max(diff_diag_phi)
maxdiff_diag_h=max(diff_diag_h)
mindiff_diag_phi=min(diff_diag_phi)
mindiff_diag_h=min(diff_diag_h)

subplot(2,2,1)
xlabel('radius from the Trandum portal [m]'),
ylabel('heads [m]'),
title('Confined grw.levels'), grid;
hold;
plot(diag(r),diag(phipmw1),'black:',diag(r),diag(phi),'black--');

subplot(2,2,2)
xlabel('radius from the Trandum portal [m]'),
ylabel('heads [m]'),
title('Phreatic grw.levels'), grid;
hold;
plot(diag(r),diag(phipmw3),'black: ',diag(r),diag(h),'black--');

subplot(2,2,3)
xlabel('radius from the Trandum portal [m]'),
ylabel('heads [m]'),
title('diff. confined grw.levels'), grid;
hold;
plot(diag(r),diag(diff3),'black')
```

```
subplot(2,2,4)
xlabel('radius from the Trandum portal [m]'),
ylabel('heads [m]'),
title('diff. phreatic grw.levels'), grid;
hold;
plot(diag(r),diag(diff4),'black')
```

SCRIPT 20

```
% Script to compare the numerical model with each other.

R1=336;             % inner radius
R2=5100;            % outher radius
dx=100;             % grid spacing in x
dy=100;             % grid spacing in y

origo_x = dx/2;        % x-origo
origo_y = dy/2;     % y-origo

x=origo_x:dx:R2+dx;       % x-array
y=origo_y:dy:R2+dy;       % y-array

xcol=(R2-dx)/dx;  % no of columns in x
ycol=(R2-dy)/dy;  % no of rows in y

for i = 1:xcol
  for j = 1:ycol

    r(i,j) = (sqrt((x(i)-origo_x)^2 + (y(j)-origo_y)^2));

    if (r(i,j) >= R1 && r(i,j) <= R2);
 else

      phipmw1(i,j) = NaN;
      phipmw2(i,j) = NaN;
      phipmw3(i,j) = NaN;
      phipmw4(i,j) = NaN;
    end;

  end;
end;


%modell 1: Confined
%% read heads from PMWIN output
hif=fopen('modell_1_h','r');

col = fscanf(hif,'%d',[1 1]);
rad = fscanf(hif,'%d',[1 1]);

phipmw1 = fscanf(hif,'%f', [col rad]);

for i=1:col;
  for j=1:rad;
    if phipmw1(i,j)== -999.9900;
      phipmw1(i,j) = NaN;
    end;
  end;
end;

%Modell 2: Confined with ravines
% read heads from pmwin output
```

```
hif=fopen('modell_2_h','r');

col = fscanf(hif,'%d',[1 1]);
rad = fscanf(hif,'%d',[1 1]);

phipmw2 = fscanf(hif,'%f', [col rad]);

for i=1:col;
  for j=1:rad;
    if phipmw2(i,j)== -999.9900;
      phipmw2(i,j) = NaN;
    end;
  end;
end;

% Modell 3: Phreatic
% read heads from pmwin output
hif=fopen('modell_3_h','r');

col = fscanf(hif,'%d',[1 1]);
rad = fscanf(hif,'%d',[1 1]);

phipmw3 = fscanf(hif,'%f', [col rad]);

for i=1:col;
  for j=1:rad;
    if phipmw3(i,j)== -999.9900;
      phipmw3(i,j) = NaN;
    end;
  end;
end;

%Modell 4: Phreatic, with ravines
%read heads from pmwin output
hif=fopen('modell_4_h','r');

col = fscanf(hif,'%d',[1 1]);
rad = fscanf(hif,'%d',[1 1]);

phipmw4 = fscanf(hif,'%f', [col rad]);

for i=1:col;
  for j=1:rad;
    if phipmw4(i,j)== -999.9900;
      phipmw4(i,j) = NaN;
    end;
  end;
end;




diff1=phipmw1-phipmw2;
max_diff1=max(diff1);
min_diff1=min(diff1);

diff2=phipmw3-phipmw4;
max_diff2=max(diff2);
min_diff2=min(diff2);
```

```
max1=max(phipmw1);
max2=max(phipmw2);
max3=max(phipmw3);
max4=max(phipmw4);

dif_diag_1_2=diag(phipmw1)-diag(phipmw2);
dif_diag_3_4=diag(phipmw3)-diag(phipmw4);
maxdif_diag_1_2=max(dif_diag_1_2)
mindif_diag_1_2=min(dif_diag_1_2)
maxdif_diag_3_4=max(dif_diag_3_4)
mindif_diag_3_4=min(dif_diag_3_4)

subplot(2,2,1)
xlabel('radius from the Trandum portal [m]'),
ylabel('heads [m]'),
title('Confined grw.levels'), grid;
hold;
plot(diag(r),diag(phipmw1),'black:',diag(r),diag(phipmw2),'black--');

subplot(2,2,2)
xlabel('radius from the Trandum portal [m]'),
ylabel('heads [m]'),
title('Phreatic grw.levels'), grid;
hold;
plot(diag(r),diag(phipmw3),'black:',diag(r),diag(phipmw4),'black--');

subplot(2,2,3)
xlabel('radius from the Trandum portal [m]'),
ylabel('heads [m]'),
title('diff. confined grw.levels'), grid;
hold;
plot(diag(r),diag(diff1),'black');

subplot(2,2,4)
xlabel('radius from the Trandum portal [m]'),
ylabel('heads [m]'),
title('diff. phreatic grw.levels'), grid;
hold;
plot(diag(r),diag(diff2),'black');
```

SCRIPT 21

```
%Compare numerical models with observed heads.

R1=336;             % inner radius
R2=5100;            % outher radius
dx=100;             % grid spacing in x
dy=100;             % grid spacing in y

origo_x = dx/2;        % x-origo
origo_y = dy/2;     % y-origo

x=origo_x:dx:R2+dx;       % x-array
y=origo_y:dy:R2+dy;       % y-array

xcol=(R2-dx)/dx;  % no of columns in x
ycol=(R2-dy)/dy;  % no of rows in y

for i = 1:xcol
  for j = 1:ycol

    r(i,j) = (sqrt((x(i)-origo_x)^2 + (y(j)-origo_y)^2));
```

```
    if (r(i,j) >= R1 && r(i,j) <= R2);
 else

      phipmw1(i,j) = NaN;
      phipmw2(i,j) = NaN;
      phipmw3(i,j) = NaN;
      phipmw4(i,j) = NaN;

    end;

  end;
end;


%modell 1: Confined
%% read heads from PMWIN output
hif=fopen('modell_1_h','r');

col = fscanf(hif,'%d',[1 1]);
rad = fscanf(hif,'%d',[1 1]);

phipmw1 = fscanf(hif,'%f', [col rad]);

for i=1:col;
  for j=1:rad;
    if phipmw1(i,j)== -999.9900;
      phipmw1(i,j) = NaN;
    end;
  end;
end;

%Modell 2: Confined with ravines
% read heads from pmwin output
hif=fopen('modell_2_h','r');

col = fscanf(hif,'%d',[1 1]);
rad = fscanf(hif,'%d',[1 1]);

phipmw2 = fscanf(hif,'%f', [col rad]);

for i=1:col;
  for j=1:rad;
    if phipmw2(i,j)== -999.9900;
      phipmw2(i,j) = NaN;
    end;
  end;
end;

% Modell 3: Phreatic
% read heads from pmwin output
hif=fopen('modell_3_h','r');

col = fscanf(hif,'%d',[1 1]);
rad = fscanf(hif,'%d',[1 1]);

phipmw3 = fscanf(hif,'%f', [col rad]);

for i=1:col;
  for j=1:rad;
```

```
    if phipmw3(i,j)== -999.9900;
      phipmw3(i,j) = NaN;
    end;
  end;
end;

%Modell 4: Phreatic, with ravines
%read heads from pmwin output
hif=fopen('modell_4_h','r');

col = fscanf(hif,'%d',[1 1]);
rad = fscanf(hif,'%d',[1 1]);

phipmw4 = fscanf(hif,'%f', [col rad]);

for i=1:col;
  for j=1:rad;
    if phipmw4(i,j)== -999.9900;
      phipmw4(i,j) = NaN;
    end;
  end;
end;

%observerte heads

tr = load('Trandum_corr.obs');

X = tr(:,1);
Y = tr(:,2);
heads = tr(:,3);


Trandum_origo_x = 8400.00;
Trandum_origo_y = 7150.00;

%Use the position of the observation wells at Trandum to find the different
%radius' that I want to use in my calculations. This makes it easy to
%compare the analytical solution with the observations done in the field.

r2 = sqrt((X-Trandum_origo_x).^2 + (Y-Trandum_origo_y).^2);

%sammenligner

subplot(2,2,1)
xlabel('radius from the Trandum portal [m]'),
ylabel('heads [m]'),
title('Confined grw.levels'), grid;
hold;

subplot(2,2,1)
plot(r2,heads,'ro')


subplot(2,2,1)
plot(diag(r),diag(phipmw1),'b+');




subplot(2,2,2)
xlabel('radius from the Trandum portal [m]'),
```

```
ylabel('heads [m]'),
title('Confined grw.levels with ravines'), grid;
hold;

subplot(2,2,2)
plot(r2,heads,'ro')


subplot(2,2,2)
plot(diag(r),diag(phipmw2),'b+');



subplot(2,2,3)
xlabel('radius from the Trandum portal [m]'),
ylabel('heads [m]'),
title('Phreatic grw.levels'), grid;
hold;

subplot(2,2,3)
plot(r2,heads,'ro')


subplot(2,2,3)
plot(diag(r),diag(phipmw3),'b+');


subplot(2,2,4)
xlabel('radius from the Trandum portal [m]'),
ylabel('heads [m]'),
title('Phreatic grw.levels with ravines'), grid;
hold;

subplot(2,2,4)
plot(r2,heads,'ro')


subplot(2,2,4)
plot(diag(r),diag(phipmw4),'b+');
```

SCRIPT 22

```
%Find the groundwater divide for a confined aquifer where H is a
%linear function of r.

%           H(r) = Ho - ar
% where:    a = (H1 - H2)/(R2 - R1)

%       dh^2/dr = 0 is the groundwater divide.

%   l^2 = Ho * M2/N2
% where:    M2 = ((R2-R1)/a)+((Ho/a^2)ln(H2/H1))+((2k/N)*(phi1^2-phi2^2))
%           P2 = ln(H2/H1)+ln(R1/R2)


%Use the optimal values found by calculation. These values are the same for
%all the 11 different calculations. N is based on the specific discharge of
%the river Risa.
```

```
H1 = 301.86;
H2 = 66.19;
k = 1.727901e-5;
phi1 = 171.50;
phi2 = 185;
R1 = 336;
R2 = 5100;
N = 1.266730e-8;


a = (H1  - H2) / (R2- R1);

Ho = a*R1 + H1;

M2 =(R2-R1)/a+(Ho/(a^2))*log(H2/H1)+ (2*k/N)*(phi1-phi2);

P2 = log(H2/H1) + log(R1/R2);

ll = Ho*((M2)/(P2));

l = sqrt(ll)

if l>R2
     l=R2;
end;

if l<R1
     l=R1;
end;
```

SCRIPT 23

```
%Find the groundwater divide for an open/phreatic aquifer where k is a
%linear function of r.

%           k(r) = ko - br
% where:    b = (k1 - k2)/(R2 - R1)

%       dh^2/dr = 0 is the groundwater divide.

%   l^2 = ko * M1/N1
% where:    M1 = ((R2-R1)/b)+((ko/b^2)ln(k2/k1))+((1/N)*(h1^2-h2^2))
%           P1 = ln(k2/k1)+ln(R1/R2)



%Use the optimal values found by calculation. These values are the same for
%all the 11 different calculations. N is based on the specific discharge of
%the river Risa.

k1 = 2.886e-5;
k2 = 5.693e-6;
h1 = 171.50;
h2 = 185;
R1 = 336;
R2 = 5100;
N = 1.266730e-8;
```

```
b = (k1  - k2) / (R2- R1);  % gradient i k

ko = b*R1 + k1;

M1 =(R2-R1)/b+(ko/(b^2))*log(k2/k1)+ (1/N)*(h1^2-h2^2);

P1 = log(k2/k1) + log(R1/R2);

ll = ko*((M1)/(P1));

l = sqrt(ll)

if l>R2
     l=R2;
end;

if l<R1
     l=R1;
end;
```